COBALT AND CHROMIUM SALEN COMPLEXES CATALYZED COPOLYMERIZATION OF CO_2 AND EPOXIDES: THE SCOPE OF EPOXIDES

A Dissertation

by

WAN-CHUN CHUNG

Submitted to the Office of Graduate and Professional Studies of
Texas A&M University
in partial fulfillment of the requirements for the degree of

DOCTOR OF PHILOSOPHY

Chair of Committee,	Donald J. Darensbourg
Committee Members,	François P. Gabbaï
	Timothy R. Hughbanks
	Hong Liang
Head of Department,	François P. Gabbaï

December 2015

Major Subject: Chemistry

ABSTRACT

The copolymerization of epoxide and carbon dioxide catalyzed by metal complexes provides an efficient method for synthesizing polycarbonates. Compared to industrial polycarbonate production, which involves toxic phosgene reagent, this is a cleaner and greener way which uses a renewable, abundant and non-toxic gas CO_2, and has 100 % atom economy. This dissertation focuses on the investigation of epoxide reactivities in the copolymerization with CO_2 and the properties of the resulting polycarbonates.

First of all, the electronics of the epoxide monomers were studied. Herein, we determined the epoxide coordinating ability, or basicity, by infrared spectroscopy, based on the O-D vibration shifts of CH_3OD in epoxides *versus* that observed in benzene. As expected, epoxides with electron-donating alkyl groups were found to be more basic compared to those with electron-withdrawing substituents. The relative basicities of epoxides were shown to greatly influence the interpretation of reactivity ratios of two epoxides in their terpolymerization with CO_2. On the other hand, steric effects of epoxides were also studied by investigating copolymerization of CO_2 with a series of butene oxides with methyl substituent groups in different positions. Among these butene oxides, only *cis*-2-butene oxide when coupled with CO_2 was able to produce polycarbonate.

Copolymerizations of different cyclic epoxides with CO_2 were discussed regarding their ring sizes and functionalities. Cyclopentene oxide was shown to have

distinct reactivity and polymer selectivity over cyclic carbonate compared to widely studied cyclohexene oxide. Postpolymeization functionalization of the polycarbonate from cyclohexadiene oxide *via* the thiol-ene reaction was applied to provide totally water-soluble polycarbonate. Besides, the olefin positions in cyclohexadiene oxides affected their reactivities. That is, 1,3-cyclohexadiene oxide, which has the olefin group adjacent to epoxide group, was more active than the 1,4-isomer.

In the last part of this dissertation, the application of metal-organic frameworks (MOF) in CO_2 sequestration was investigated. CO_2 collected at atmospheric pressure over MOF was thermally released and utilized in copolymerization with propylene oxide to synthesize poly(propylene carbonate). Comparative studies using CO_2 provided directly from a compressed gas source gave similar propylene oxide conversion and molecular weight. This study showed the feasibility of utilizing MOF for CO_2 storage.

DEDICATION

I would like to dedicate my dissertation to my beloved parents, brother and sister for their endless love and support.

ACKNOWLEDGEMENTS

The first and biggest thank you goes to my fantastic advisor, Prof. Donald J. Darensbourg, for bringing me to A&M and recruiting me to his lab. You are the best advisor a graduate student can ask for. I appreciate the guidance and training you provided in these five years, as well as the freedom you gave us on our research topics and directions and your patience. The ways you think, you present research, you interact with students, and you care about the energy and environment issues all affected me. And of course your sense of humor and generosity are of the best things I've learned from you. There is only one word to describe the time I spent in your group: SUPER! You are also a wonderful teacher, your chalk talks in the summer group meetings and Green Chemistry classes are unforgettable. Special thanks go to Prof. Marcetta Darensbourg for her support and guidance during this course. Thank you for taking care of us either in research, in class or in life, and also taking care of Don's health. Your passion for teaching inspired me.

I would like to thank my committee members Prof. François P. Gabbaï, Prof. Timothy R. Hughbanks and Prof. Hong Liang for their guidance and comments, as well as the classes they taught. The five years' education in the Chemistry graduate program is solid, thank Chemistry Department for providing useful courses and trainings which helped me build up the skills I need.

Thank you Ethel, our superwoman secretary, for everything you did, I could not have finished this without your help. Thank you to the old Darensbourg group members

Drs. Osit Karroonnirun, Ross Poland, Sheng-Hsuan Wei, Stephanie Wilson and Andrew Yeung for their effort to help me setup everything in lab and to provide me ideas. I would also like to thank the current Darensbourg group members Dr. Fu-Te Tsai, Dr. Hamid Samouei, Dr. Sam Kyran, Yanyan Wang and Mong Lo for discussing research with me and helping me solve my problems.

Thanks Drs. Andrew Yeung, Sam Kyran and Randara Pulukkody for your friendship from the very beginning of our graduate lives, we have been through all of this together. Thanks also go to my friends from “Taiwanese Mafia”. I know I am not alone when I need to face the stress, thank you for your support and company.

Finally, I would like to express my gratitude to my family for their inspiration, encouragement and understanding. You are my best support and strength, I was made much stronger with your love.

NOMENCLATURE

1,3-CHDO	1,2-epoxy-3-cyclohexene
1,4-CHDO	1,2-epoxy-4-cyclohexene
AGE	Allyl Glycidyl Ether
AIBN	Azobisisobutyronitrile
Anal. Cal.	Analysis Calculation
br	(NMR) broad
BC	Butene Carbonate
BGE	Benzyl Glycidyl Ether
BO	1-Butene Oxide
Cat	Catalyst
CHO	Cyclohexene oxide
Co	Cobalt
CO_2	Carbon Dioxide
Conv	Conversion
COPO	3,4-Epoxytetrahydrofuran
CPO	Cyclopentene Oxide
Cr	Chromium
CXO	3,5,8-Trioxa-bicyclo[5.1.0]octane
D	(NMR) Doublet
Da	Dalton

DHNO	Dihydronaphthalene Oxide
DMF	Dimethylformamide
DNP	Dinitrophenoxide
DSC	Differential Scanning Calorimetry
ECH	Epichlorohydrin
eq.	Equation
F	Monomer Feed Ratio
f	Mole Fraction of Monomer 1 in the Copolymer
FGE	Furfuryl Glycidyl Ether
FTIR	Fourier Transform Infrared Spectroscopy
GME	Glycidyl Methyl Ether
GPC	Gel Permeation Chromatography
h	Hour
HO	1-Hexene Oxide
IO	Indene Oxide
IR	Infrared Spectroscopy
LCST	Lower Critical Solution Temperature
m	(NMR) Multiplet
mCPBA	*m*-Chloroperoxybenzoic Acid
ME_3MO	2-((2-(2-(2-Methxyethoxy)ethoxy)ethoxy)methyl)oxirane
M_n	Number Average Molecular Weight
MS	Mass Spectroscopy

MPa	Mega Pascal
M_w	Weight Average Molecular Weight
NMR	Nuclear Magnetic Resonance
OAc	Acetate
ONBGE	*o*-Nitrobenzyl Glycidyl Ether
PCHC	Poly(cyclohexene carbonate)
PDI	Polydispersity index, M_n/M_w
PGE	Phenyl Glycidyl Ether
PO	Propylene oxide
Polym. Selec.	Polymer Selectivity
PPC	Poly(propylene carbonate)
PPNCl	Bis(triphenylphosphine)iminium Chloride
PPNDNP	Bis(triphenylphosphine)iminium Dinitrophenoxide
$PPNN_3$	Bis(triphenylphosphine)iminium Azide
r	Reactivity Ration
rt	Room Temprature
s	(NMR) Singlet
Salen	N,N'-Bis(3,5-di-tert-butylsalicylidene)-1,2-cyclohexanediamine
SO	Styrene Oxide
^{t}Bu	*tert*-Butyl
TBD	1,5,7-Triazabicyclo[4,4,0]dec-5-ene
T_d	Decomposition Temperature

Temp	Temperature
T_g	Glass Transition Temperature
TGA	Thermogravimetric Analysis
THF	Tetrahydrofuran
TMSO	(2-(3,4-Epoxycyclohexyl)ethyl)trimethoxysilane
TOF	Turnover Frequency
VCHO	Vinylcyclohexene Oxide
VIO	Vinyloxirane
W_1	Weight Fraction of Monomer 1 in the Copolymer

TABLE OF CONTENTS

Page

LIST OF FIGURES

Page

LIST OF TABLES

Page

CHAPTER I

INTRODUCTION AND LITERATURE REVIEW

Chemical Utilization of Carbon Dioxide in Polycarbonate Production

Carbon dioxide utilization is one of the many technologies available for alleviating the rising CO_2 level in the atmosphere. In addition to its wide industrial application as a solvent in extraction and purification, there are a variety of chemical reactions that convert CO_2 to useful materials such as methanol, urea, carboxylic acids and carbonates.[1] Being cheap, abundant, renewable and nontoxic, CO_2 is a good C1 feed stock candidate for chemical synthesis. However, strategies are needed to address its high thermodynamic stability. The following are some methods that can be employed: (1) reaction of CO_2 with molecules of high energy such as small membered rings, dihydrogen or unsaturated compounds, (2) driving an unfavorable reaction with CO_2 forward by product removal as the reaction progresses, (3) synthesis of products in the oxidized form, and (4) the use of energy from renewable source. Productions of high oxidation state compounds(carboxylates, carbonates and carbamates) which incorporate the entire CO_2 molecule, have low energy content and may occur at room temperature. Reactions where CO_2 is reduced require energy input.[1] An epoxide, a strained three-membered ring molecule, is a relatively high-energy molecule, representing a good candidate to react with CO_2. In the presence of a suitable catalyst, CO_2 can couple with epoxides to generate polycarbonates or cyclic carbonates (eq. 1).[2] The catalyst can be either an organic compound or a metal complex for the cyclic carbonate formation, but

only metal complexes, sometimes with cocatalysts, can help in polycarbonate formation. This kind of reaction has 100 % atom economy and does not need additional solvent as the epoxide can act as the solvent. This dissertation will focus on the coupling of epoxides and CO_2 to generate polycarbonates.

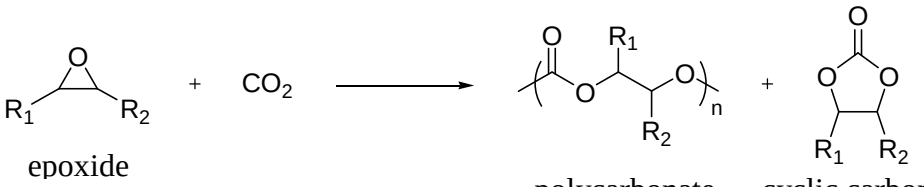

epoxide polycarbonate cyclic carbonate (eq. 1)

Polycarbonates are engineering thermoplastics and are widely used in industries, such as construction and automobile materials, electronic devices, data storage and lenses owing to their excellent mechanical properties like toughness, transparency, lightness, high impact resistance and non-electrical conductivity. The most common polycarbonate in industry is the bisphenol A polycarbonate. Bearing two rigid phenyl rings on the backbone, bisphenol A polycarbonate is very tough and has a high glass transition temperature (T_g) of 150 ^oC. It is made by the polycondensation of the bisphenol A diol and phosgene (eq. 2).

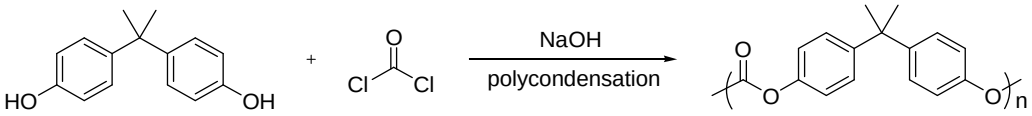

bisphenol A bisphenol A polycarbonate (eq. 2)

As phosgene being toxic, there are safer substitutes for it, diphosgene or triphosgene, which are derivatives of phosgene thus still not very safe. Later Asahi Kasei, a chemical company, developed a greener reagent, diphenyl carbonate, to replace phosgene. It is made by the transesterification of phenol and dimethyl carbonate, which can be derived from CO_2 and ethylene oxide (Scheme 1).[3]

Scheme 1

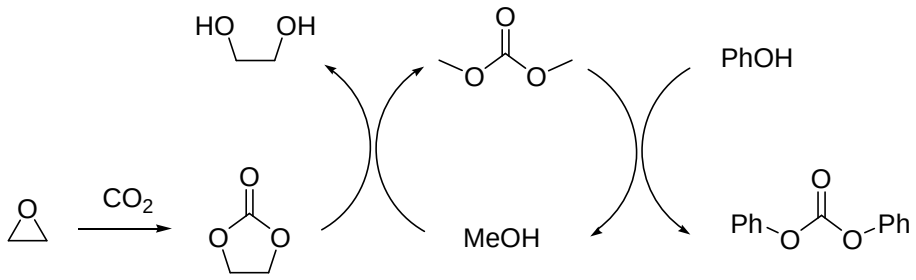

Copolymerization of CO_2 and epoxides provide an alternate method to produce polycarbonates. The polycarbonates made by this method have different mechanical properties than bisphenol A polycarbonate, they are softer and have lower glass transition temperatures, so they are applied in different areas like ceramic binders or lubricants, coating, surfactants and polyurethane precursor. This copolymerization method was first developed by Inoue in 1969. They achieved it using a heterogeneous catalyst system obtained from diethylzinc and water to copolymerize propylene oxide (PO) and CO_2.[4]

Catalyst Development

After the first heterogeneous catalytic system, a variety of homogeneous zinc catalysts, as well as other organometallic complexes with different metals and ligand scaffolds were developed for this copolymerization. This section will focus on metal salen catalysts, with the metal being mainly cobalt.

Inspired by Jacobsen's research of epoxide hydrolysis with salen chromium catalyst, Darensbourg and coworkers used metal salen complex in the epoxide/CO_2 copolymerization.[5] Air and moisture stable chromium salen catalyst (**1**) was shown to be active for cyclohexene oxide (CHO)/CO_2 copolymerization, producing poly(cyclohexene carbonate) (PCHC) with narrow molecular weight distribution. The turnover frequency (TOF) (10-30 h^{-1}) at 80 ^{o}C with 58.5 bar CO_2 for 24 h was moderate and positively related to amount of Lewis base cocatalyst. This catalyst was shown to be active towards CO_2/PO copolymerization with more temperature-dependent polymer selectivity.

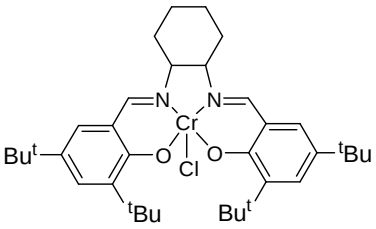

1

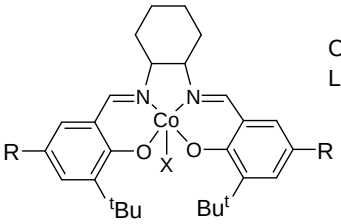

2

Coates: R= Br, X=OAc
Lu: R=^{t}Bu, X=dinitrophenoxide

Later on, Coates's group utilized cobalt salen complexes (**2**) for copolymerization of CO_2 and propylene oxide.[6] The cobalt catalyst was active alone without any cocatalyst at relatively low temperature, showing good turnover frequency

of 81 h^{-1} at 25 ^{o}C at 55.2 bar CO_2 for 3 h. Compared to Cr salen catalyst working at 75 ^{o}C, Co salen was less activity but more selective for polymer over cyclic carbonate. Soon after this work, Lu's group published their results on similar copolymerization in the presence of Co salen catalyst and ammonium salt cocatalyst.[7] In this work, 100 % carbonate linkage was obtained at lower (20 bar) CO_2 pressure along with excellent turnover frequency (> 200 h^{-1} for 3h at 25 ^{o}C). It is noteworthy that the polycarbonate selectivity over cyclic carbonate was heavily dependent on the fifth ligand on the cobalt catalyst. In the presence of a tetrabutylammonium bromide cocatalyst, the polymer selectivity was low when the ligand was acetate, but reached 99 % when the ligand is nitrophenoxide. In contrast, Coates reported polymer selectivity is > 99 % with the acetate ligand without cocatalyst. Furthermore, with the R configuration on the chiral centers of the cyclohexyl backbone, the catalyst showed unprecedented stereoselectivity in PO ring-opening. From this point, ammonium or iminium salt cocatalysts started to have a large role in CO_2/epoxide copolymerization. This combination was named binary catalyst system, involving (1) metal center for epoxide activation and (2) anion or Lewis base from the cocatalyst for epoxide ring-opening.

Afterwards, researchers developed various superior catalyst achieving higher activity and polymer selectivity by building functionalities on salen ligand framework. With attached functional groups bearing positive charge, these second generation catalysts have built-in initiators, the counter anions. They are able to serve as catalysts for epoxide binding and activation and cocatalysts for epoxide ring-opening at the same time, making them bifunctional catalysts. They have been successful in reducing cyclic

carbonate formation and stabilizing cobalt complexes at relatively high temperature. Nozaki's group in 2006 revealed their Co salen catalyst with two axial acetate ligands.[8] This complex had two piperidinyl substituent groups on the salen's phenol rings, where one of them is protonated. The proton can be used to cap the dissociated polymer chain to prevent backbiting, which results in undesired cyclic carbonate formation (Scheme 2). The catalyst provided high polymer selectivity, 90 %, at raised temperature of 60 ^{o}C and gave the high turnover frequency of 602 h^{-1}. Given longer reaction time with higher monomer/catalyst ratio, molecular weight of the resulting poly(propylene carbonate) (PPC) can be greater than 80 kDa.

Scheme 2

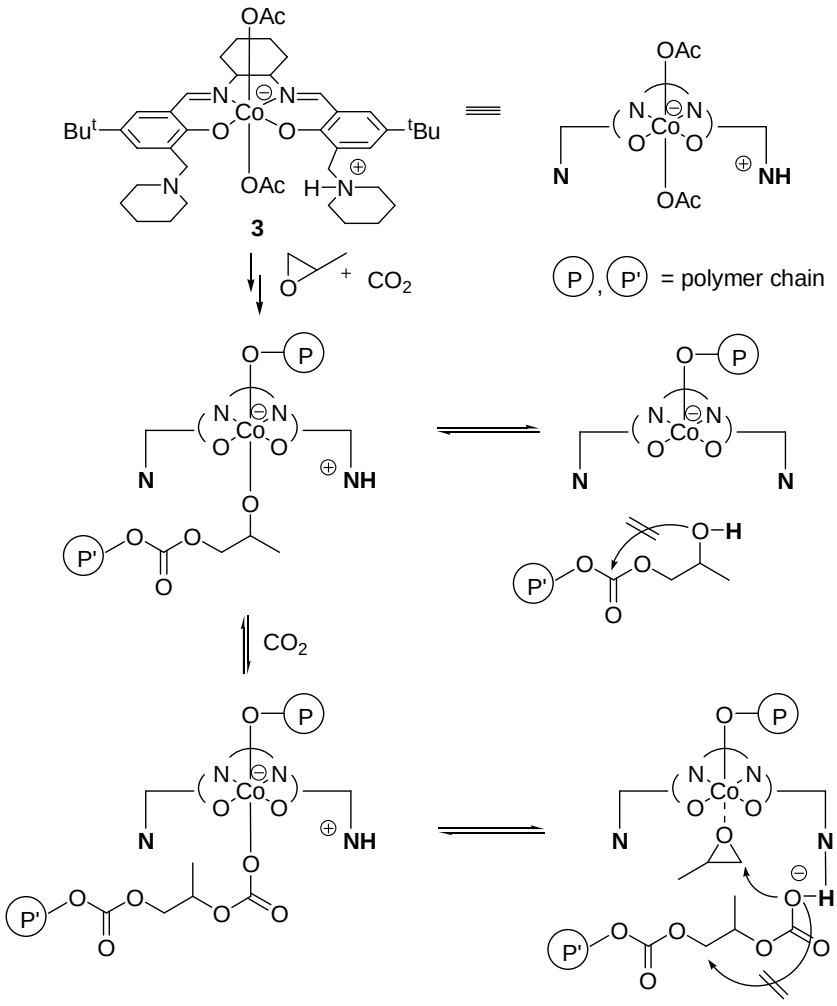

Following this work, the other kind of bifunctional cobalt salen catalyst was developed by Lee's group.[9] Equipped with two side arms with ammonium groups and nitrophenoxide counter anions (**4**, Figure 1, left), this catalyst gave superior turnover frequency (>1000 h^{-1}) in the copolymerization of CO_2 and propylene oxide, at very low catalyst loading (0.004 mol %) at temperatures higher than 70 ^{o}C. At this high

temperature, catalyst **4** retained excellent polymer selectivity, where the previously mentioned binary Co salen catalyst system only gave cyclic propylene carbonate.

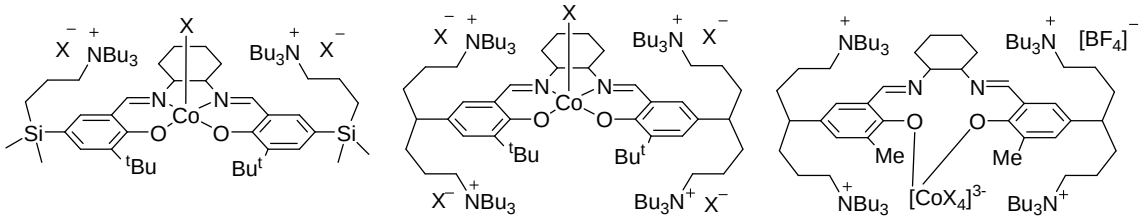

4 **5** **6**

Figure 1 Bifunctional catalysts developed by Lee.[9-11]

Later in 2008, the same group published results of catalyst with four ammonium side arms (**5**, Figure 1, middle).[10] This catalyst achieved even higher turnover frequency, higher than 10000 h^{-1}at 80 ^{o}C for less than 3h. With low catalyst loading (0.001 mole %) the molecular weight of the resulting PPC was as high as 285 kDa. These are the highest turnover frequency and molecular weight reported so far in this kind of copolymerization. Moreover, this catalyst is recyclable due to its increased affinity with silica gel resulted from four ammonium groups. When passing the reaction solution through a silica gel pad, the catalyst stayed on the silica gel and polymer was eluted out, and the catalyst was recovered later by $NaBF_4$ methanol solution. After treated with nitrophenoxide, the recovered catalyst showed similar activity in subsequent copolymerization. In a later report, the structure of this catalyst was investigated by NMR spectroscopy and unusual coordination structures were elucidated.[11] Imine nitrogens were observed to not coordinate to the Co center, instead, nitrophenoxides and

solvents took its place (Figure 1, right). This only happened with less bulkier methyl groups on the 3-position of the salicylaldehyde, and catalysts with this kind of structure had higher activity than those of normal structure having four coordinating salen ligand (13000 vs. 1300 h^{-1}). The extraordinarily high activity was ascribed by the authors to the scrambling of labile nitrophenoxide anion initiators with epoxide and propagating chains. In 2009, Lu's group developed another kind of bifunctional Co salen catalyst with only one TBD (1,5,7-Triazabicyclo[4,4,0]dec-5-ene) or ammonium side arm (**7** and **8**, Figure 2, upper left and middle) which as well showed superb activity and polymer selectivity.[12]

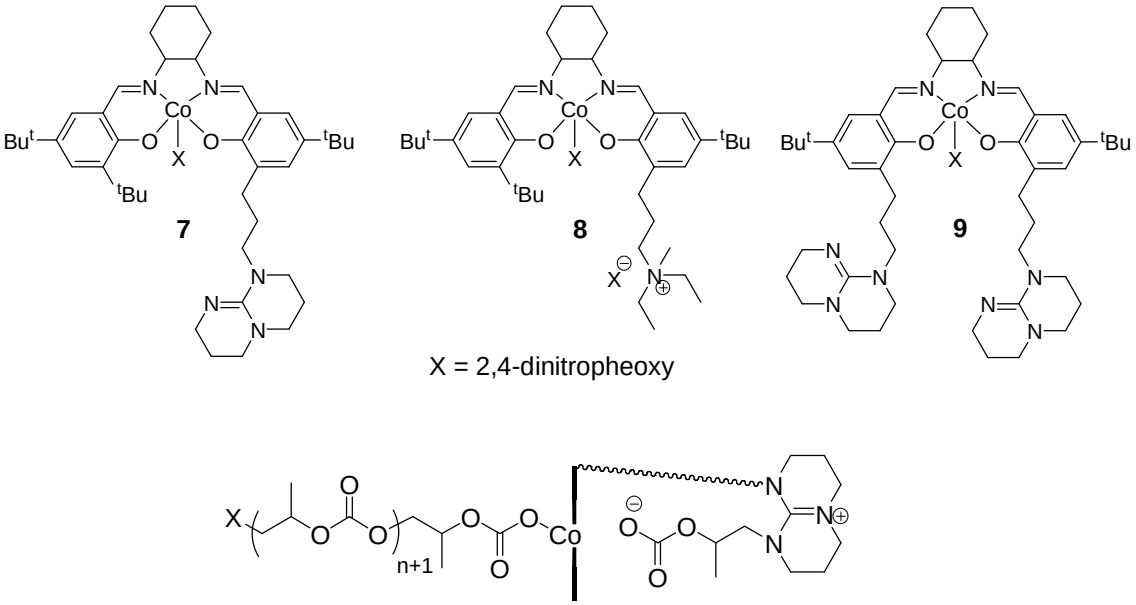

Figure 2 Bifunctional catalysts developed by Lu.[12]

In the mechanism study, they suggested that in the initiation, the anchored TBD reacted with one PO and CO_2 to form a carbonate (Figure 2, bottom), and coordination

of this carbonate to metal helped stabilize the Co(III) against decomposition to Co(II) and also activated the epoxide or anions on the trans position. Thus the Co catalyst was stable at temperatures over 100 ^{o}C. Interestingly, the symmetric bifunctional catalyst **9** of this kind (Figure 2, upper right), bearing two TBD showed much lower activity and polymer selectivity than the ones with only one TBD (TOF 41 and 410 h^{-1}, polymer selectivity 85 and > 99 %). Later the same group conducted the kinetic study of CO_2/PO couplings with both binary and bifunctional Co catalysts.[13] Unlike binary catalyst system, coupling reaction by bifunctional catalyst did not have induction period and the reaction rate had first order dependence on catalyst concentration, where in binary system it was order of 1.61. The activation energy for cyclic propylene carbonate formation was determined to be 77.0 kJ/mol, which was higher than that of binary system (50.1 kJ/mol). The activation energy for poly(propylene carbonate) formation was 29.5 kJ/mol, lower than 33.8 kJ/mol from binary catalyst. The bigger energy difference between cyclic carbonate and polycarbonate formation from bifunctional catalyst reflects the higher polymer selectivity.

Epoxide Scope

The most widely studied epoxides are propylene oxide and cyclohexene oxide. These two epoxides have good reactivity in their copolymerization with CO_2. Propylene oxide, a linear epoxide, can couple with CO_2 at low temperature while cyclohexene oxide, an alicyclic epoxide, needs higher temperature. Interestingly, in the coupling with propylene oxide, cyclic carbonate is often observed concomitantly with polycarbonate,

but with cyclohexene oxide, the product is mostly polycarbonate due to the difficulty for it to backbite with the rigid cyclohexyl backbone. In this section different epoxides copolymerization with CO_2 will be discussed in terms of reactivity, polymer selectivity and resultant polycarbonate property.

Linear epoxides with different length

While propylene oxide is widely studied, other aliphatic linear epoxides with longer chain do not draw too much attention. When Lu first published their binary Co catalyst in 2004, for PO/CO_2 copolymerization, 1-butene oxide (BO) and 1-hexene oxide (HO) were also studied.[7] While having identical polymer selectivity, HO was shown to be less reactive than BO, and both were much less reactive than PO.

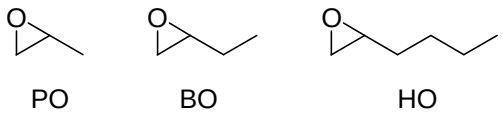

Same trend but higher reactivity with PPNCl (Bis(triphenylphosphine)iminium chloride) cocatalyst was conveyed in their 2006 publication.[14] Also with Lu's enantio-selective catalyst (**10**), epoxide with longer chain showed lower reactivity and enantio-selectivity.[15] With Nozaki's bifunctional catalyst, copolymerization of PO/CO_2 in a solvent completed for two days while BO and HO showed only 89 % conversion.[8]

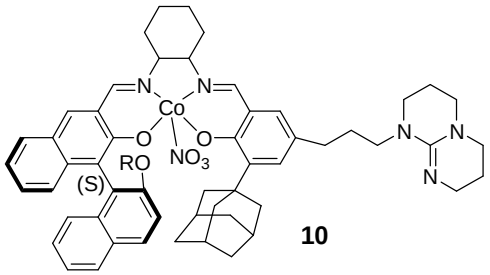

10

The trend was also observed in Lee's terpolymerization of CO_2 and PO with either BO or HO, using quaternary ammonium tethered Co catalyst (**5**).[16] The resulting polycarbonates' T_g varies with the epoxide length, longer chains gave lower T_g. They are 40 ^oC, 9 ^oC and -15 ^oC for poly(propylene carbonate), poly(butene carbonate) and poly(hexene carbonate), respectively. In Lu's another research of CHO/CO_2/long chain epoxide terpolymerization by bifunctional catalyst **8**, longer chain epoxide resulted in lower reactivity as expected and higher cyclohexene carbonate component in the terpolymer.[17]

Linear epoxides with electron-withdrawing groups

Linear epoxides with electron-withdrawing groups are of another kind. Styrene oxide (SO) and epichlorohydrin (ECH) are two examples. Electron-withdrawing group plays a role in three perspectives: (1) it makes the epoxide less basic thus less easily coordinate to metal, (2) it makes the epoxide carbon more electrophilic thus more easily be ring-opened and (3) it facilitates back-biting for cyclic carbonate formation.

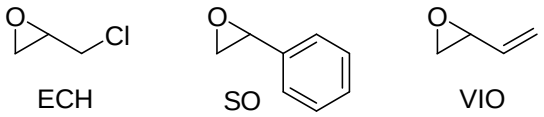

In 2011 Lu and Darensbourg first published the investigation of CO_2/ECH copolymerization.[18] The result showed that ECH has slightly lower reactivity but much lower polymer selectivity than PO. ECH had higher activation energies for both polycarbonate (53.1 vs. 34.5 kJ/mol) and cyclic carbonate formation (98.5 vs. 88.0 kJ/mol) than PO, and smaller difference between the two activation energies (45.4 vs.53.5 kJ/mol). This smaller energy difference between polymer and cyclic carbonate formation reflects the lower polymer selectivity of ECH. The T_g of poly(epichlorohydrin carbonate)s were around 30 ^oC, slightly lower than PPC. Furthermore, highly stereospecific poly(epichlorohydrin carbonate) was prepared by utilizing chiral bifunctional catalyst.[19] These catalysts also provided regioselectivity in epoxide ring-opening, where the methylene carbon was preferred. The isotactic polymer is semicrystalline and has T_g of 42 ^oC and T_m of 108 ^oC. Apart from its copolymerization, ECH was also commonly used in glycidyl ether preparation by substitution reactions of alcohol.

On the other hand, styrene oxide was found to be less reactive than propylene oxide in copolymerization with CO_2, TOF was one order of magnitude smaller.[20] At 50 ^oC, PO still had 99 % polymer selectivity but SO did not make any poly(styrene carbonate) unless pressurizing the reaction further to 7 MPa, where 91 % polymer selectivity was observe. Bearing a rigid phenyl ring, poly(styrene carbonate) has a higher T_g, 80 ^oC, than PO. The polymer selectivity of 4-chloro styrene oxide was much lower,

60 %, while reactivity maintained similar to SO, and the resulting copolymer has higher T_g at 92 ^oC. Contrarily, 4-methyl styrene oxide was non-reactive at room temperature. The activation energies for cyclic carbonate and polycarbonate formation from SO/CO_2 were measured to be 50.7 and 40.4 kJ/mol respectively. The difference between them was only 10.3 kJ/mol, much smaller than that of PO (53.5 kJ/mol). Enhanced electrophilic nature of the methine carbon facilitates backbiting for cyclic carbonate formation resulting in much lower activation barrier for cyclic styrene carbonate compared to propylene carbonate.

Vinyloxirane (VIO) is another example of this kind. In Darensbourg's 2014 report of VIO copolymerization with CO_2, it showed much lower reactivity (TOF < 10 h^{-1}) and polymer selectivity (70 % at 25 ^oC) than PO in the presence of binary Co salen catalyst system.[21] If bifunctional Co catalyst was used, TOF increased to 40.6 h^{-1} for 21 h at 40 ^oC with 92 % polymer selectivity. When terpolymerized with PO and CO_2, the conversion and polymer selectivity of VIO increased. The advantage of VIO is its postpolymerization functionalization availability due to its double bond. The resulting poly(vinyloxirane carbonate) can be functionalized by thiol-ene reaction with thiols bearing hydrophilic groups (Scheme 3). After functionalization, the hydrophobic poly(vinyloxirane carbonate) became hydrophilic and even water soluble. The T_g of poly(vinyloxirane carbonate) was 18 ^oC, of the polymer with carboxylic acid groups after functionalization was 8 ^oC. And after deprotonation of that, the T_g of polymer with carboxylate ammonium salts increased drastically to 61 ^oC.

Scheme 3

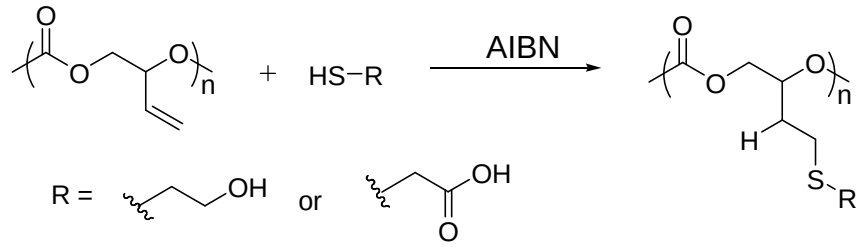

Overall, electron-withdrawing groups on the epoxide make it less reactive and less selective for polycarbonate, but can give the resulting polycarbonate different thermal or chemical properties.

Glycidyl ethers

Glycidyl ethers are of another group that are widely studied. Some of them were considered to have protected version of hydroxyl group, and after postpolymerization deprotection poly(1,2-glycerol carbonate) was formed. Unlike poly(propylene carbonate) being hydrophobic and inert to enzymes, this kind of polycarbonates are hydrophilic and biodegradable/biocompatible thus have application in biomedical field. It can be synthesized from epichlorohydrin and functionalized alcohols. The convenience of its synthesis provides possibility for epoxides to contain a variety of functional groups.

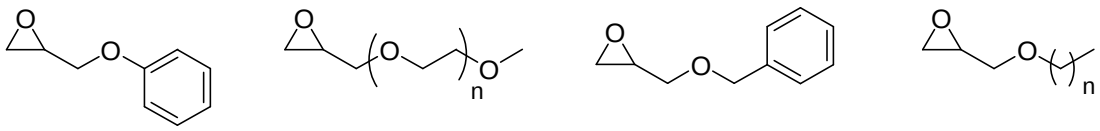

PGE ME_nMO BGE alkyl glycidyl ether

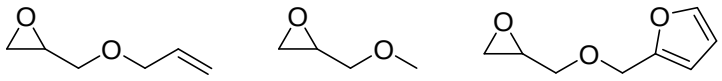

AGE GME FGE

Copolymerization of phenyl glycidyl ether (PGE) with CO_2 was studied by Lu's group, and was described to have good turnover frequency and polymer selectivity with both binary and bifunctional Co catalysts, which were similar to PO.[22] At raised temperature, 50 ^oC, TOF increased but polymer selectivity dropped to 56 %. With the rigid phenyl ring pendant groups, the resulting polymer has higher T_g (50 ^oC) than poly(propylene carbonate) but with two more atoms in between giving it flexibility, it's lower than poly(styrene carbonate) (T_g 80 ^oC). With binary Co catalyst, the activation energies for polymer and cyclic carbonate formation were determined to be 39.2 and 72.8 kJ/mol, both were similar to PO but the difference between polymer and cyclic carbonate was smaller (33.6 kJ/mol) than that of PO, accounting for the lower polymer selectivity at raised temperature.

Epoxides with oligo ethylene glycol segments like 2-((2-(2-(2-Methxyethoxy)ethoxy)ethoxy)methyl)oxirane (ME_3MO), or ME_nMO, are good candidates for hydrophilic polycarbonate preparation. Wang's group looked into terpolymerizations of ME_2MO/MEMO/CO_2 and ME_3MO/PO/CO_2 by binary catalyst system and noticed that reaction rate decreased as ethylene glycol content increased, indicating its lower reactivity than PO.[23] The T_g of ME_3MO/PO/CO_2 terpolymer's dropped as ME_3MO content enlarged in the terpolymer, while its decomposition temperature (T_d) was higher than poly(propylene carbonate). T_g and T_d for a terpolymer

with 9.7 % ME_3MO are 6.9 ^oC and 241 ^oC, respectively. Bearing oligo(ethylene glycol) pendant groups, the terpolymers were hydrophilic and had water contact angle down to 25^o with 23.6 % ME_3MO compared to 90^o with hydrophobic pure poly(propylene carbonate). Moreover, when the ME_3MO content is higher than 37%, the terpolymer became water soluble, and had reversible thermal-responsive phase transition in water, presenting lower critical solution temperature (LCST), below which the polymer is soluble in water. The LCST of the terpolymer possesses positive linear relationship with ethylene glycol content. The terpolymer with 72.6 % ME_3MO has LCST at 35.2 ^oC, which is close to body temperature, showing its potential application in biomedical area. The same LCST behavior and relationship happens in the MEMO/ME_2MO/CO_2 terpolymerization as well.

Polycarbonates derived from benzyl glycidyl ether (BGE) can be deprotected by H_2 to give poly(1,2-glycerol carbonate). Copolymerization of CO_2/BGE and subsequent deprotection were published by Grinstaff in 2013.[24] Results illustrated that BGE had somewhat lower reactivity and similar polymer selectivity compared to PO. The polymer's T_g (8 ^oC) is much lower than poly(propylene carbonate) and polycarbonate derived from phenyl glycidyl ether.[25] The deprotected polymer is more hydrophilic as expected and not soluble in CH_2Cl_2 but soluble in DMF. Faster degradation rate was observed for poly(1,2-glycerol carbonate) than the 1,3-isomer, and was attributed to the lower activation energy required for intramolecular attack of the pendant 1° OH than 2° OH.

Later, the same group also published the exploration of CO_2 copolymerization with long chain alkyl (butyl, octyl and stearyl) glycidyl ethers by bifunctional Co catalyst.[26] Glycidyl ethers' reactivities and copolymers' T_g were inversely related to the numbers of carbons in the alkyl chains, and the reactivities were lower not only than PO but than all of the above mentioned glycidyl ethers. The T_g of the polymers derived from butyl and octyl glycidyl ethers were -24 and -34 ^oC, but the polymer from stearyl (C_{18}) glycidyl ether only had a melting point at 55 ^oC due to the hydrophobic interaction between the pendant alkyl groups. T_d's were around 270 ^oC except for stearyl, 249 ^oC. The ionic conductivity of poly(butyl ether 1,2-glycerol carbonate) exhibited temperature-dependence, being 10^{-5} S/cm at 25 ^oC and. 10^{-3} S/cm at 120 ^oC. These conductivities are comparable to present PEO-based battery electrolytes make this polycarbonate a potential solid polymer electrolyte for batteries.

Expanded from their VIO/CO_2 copolymerization work, Darensbourg's group demonstrated terpolymerization of allyl glycidyl ether (AGE) with propylene oxide and CO_2.[27] With the double bond two atoms away from epoxide, AGE is more reactive than VIO. The detailed reactivity study will be addressed later. The terpolymers were cross-linked via thiol–ene reaction with dithiol or tetrathiol. Rubbery modulus and T_g of the cross-linked films increased as cross-link density increased. The surface of non-saturated cross-linked films can be functionalized via subsequent thiol-ene reaction. This surface functionalization offers application for biomolecule or metal nanoparticle immobilization.

In this year Frey reported terpolymerization of furfuryl glycidyl ether(FGE)/glycidyl methyl ether(GME)/CO_2.[28] With FGE incorporation, T_g's of terpolymers are lower than that of GME/CO_2 copolymer (1.7 ^oC), ranging from -2 to -24.7 ^oC. The terpolymer can be modified by reversible Diels-Alder reaction between the furan on the polymer and maleimides with functional groups (Scheme 4). When bismaleimide was used in the functionalization, the terpolymer was cross-linked and showed much higher T_g above 90 ^oC. The reversibility of Diels-Alder reaction gives promise for self-healing materials.

Scheme 4

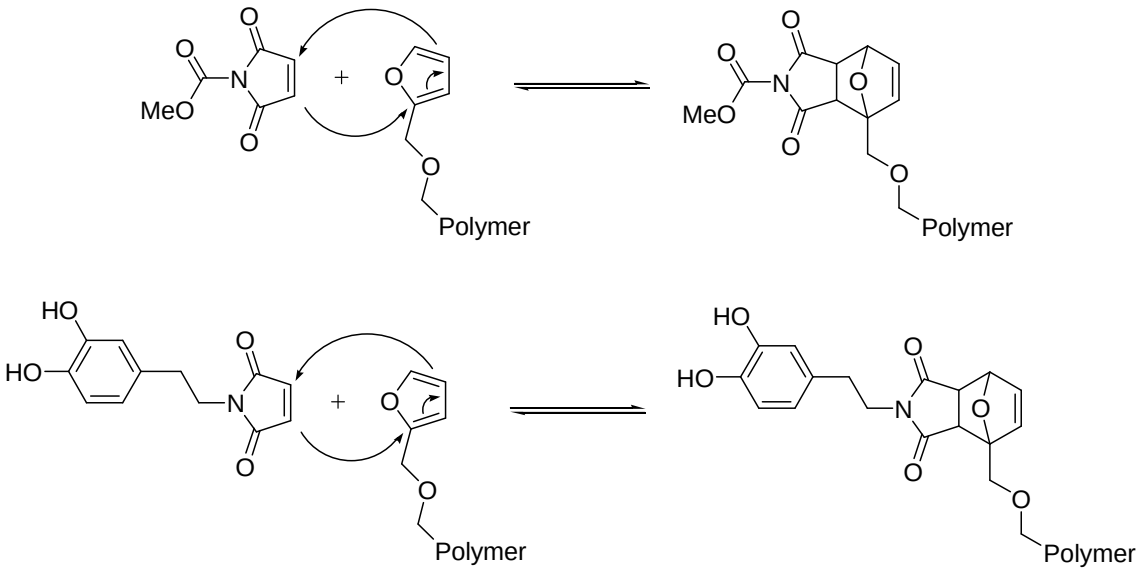

Overall, glycidyl ethers hold similar or slightly less reactivity and polymer selectivity compared to propylene oxide. Resultant polycarbonates's properties, predominantly hydrophilicity, are distinct from poly(propylene carbonate), with or

without postpolymerization functionalization. Functionalities on the glycidyl ethers spreads out the polymers' application in divergent areas.

Cyclic epoxides

In addition to terminal linear epoxides, internal cycloalkene oxides are also studied in this field. The polycarbonates from cyclic epoxides usually have higher T_g than from linear epoxides, owing to the ring fused on the backbone. Cyclohexene oxide is the most widely investigated cyclic epoxide with various catalysts. In its coupling reaction with CO_2, the cyclic carbonate is rarely generated, making high polymer selectivity. Activation energy for cyclic cyclohexene carbonate formation by Cr salen catalyst was measured by Darensbourg's group to be 133.0, higher than for cyclic propylene carbonate.[29] The activation energy difference between cyclic carbonate and polymer formation is 86 kJ/mol, higher than 32.9 kJ/mol of PO. The difficulty of making cyclic carbonate was ascribed to the five-membered ring's ring strain to accommodate the six-membered cyclohexyl ring conformation.

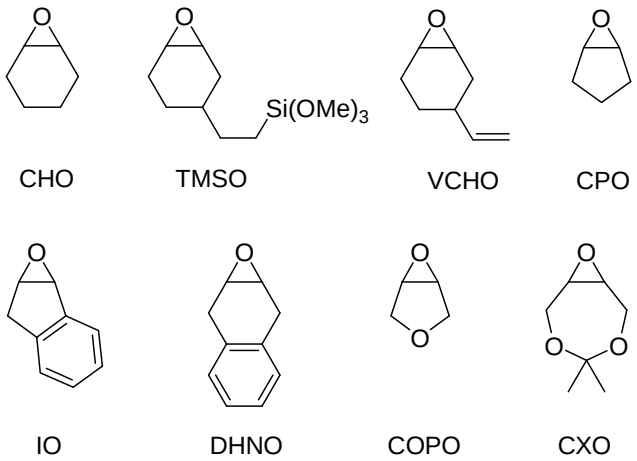

In 2006, researchers started to use binary Co salen catalysts in CHO/CO_2 copolymerization.[14,30,31] Different from Cr salen catalyst where elevated temperature was needed, Co salen catalysts work at lower temperature for coupling CO_2 and CHO. Binary Co salen catalyst alone was able to catalyzed the copolymerization with a TOF of 98 h^{-1} for 3 h at 22 ^oC, which was about the same as PO, and produce syndiotactic poly(cyclohexene carbonate) which contained 81 % r-centered tetrads.[30] With the help of PPNCl cocatalyst, the TOF remained in the same range, but was lower than that for PO in the similar condition.[30,31] Upon using chiral catalyst, the resulting polymer is isotactic-enriched 37 % enantioselectivity.[31] When the reaction temperature was raised, the Co catalyst activity rose one order of magnitude while 100 % polymer selectivity was maintained. Poly(cyclohexene carbonate) has higher T_g (117 ^oC) than most polycarbonates derived from linear epoxides because of the rigid cyclohexyl ring on the backbone.

Based on high polymer selectivity of cyclohexene oxide, 4-position functionalized CHO were studied in their copolymerization with CO_2 in the hope to make useful polycarbonates. (2-(3,4-Epoxycyclohexyl)ethyl)trimethoxysilane (TMSO) was successfully copolymerized with CO_2 by Cr salen catalyst with comparable reactivity as CHO.[32] Both epoxide monomer and copolymer from TMSO are soluble in liquid CO_2 due to the trimethoxysilane group, thus liquid CO_2 was used to separate the polymer from yellow catalyst. Random cross-linking of the trimethoxysilane was noticed and gave rise to a T_g higher than 180 ^oC. Besides, vinylcyclohexene oxide (VCHO), a good candidate for cross-linking, was terpolymerized with CO_2 and CHO by β-diiminate

zinc catalyst.[33] The thus formed terpolymer was cross-metathesized through olefin groups by Grubb's Ru catalyst. When the polycarbonate concentration was low in the cross-metathesis reaction, cross-linking occurred intramolecularly to create nanoparticles. Compare to the linear polymer, the nanoparticle has higher T_g (194 vs. 114 ^oC) caused by reduced segmental chain mobility.

While CHO was widely explored, the five-membered or seven-membered rings counter parts were not often seen in publications. In contrast to CHO, cyclopentene oxide was very unreactive in its copolymerization with CO_2 by either binary or bifunctional Co catalysts (TOF 3 h^{-1} for 48 h at 25 ^oC). However, when catalyzed by dinuclear Co salen complexes (**11**) alone or with cocatalyst, the TOF reached higher than 200 h^{-1} with 100 % polymer selectivity.[34]

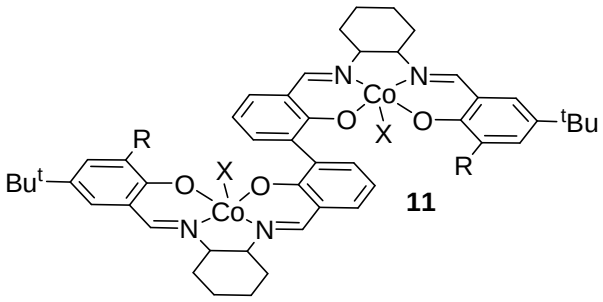

11

Bimetallic synergistic effect was observed in a way that epoxide coordinates to one metal thus being activated then the second metal's fifth axial ligand ring-opens the epoxide. They reported good TOFs' around 200 h^{-1} for 1 or 2 h at 25 ^oC and moderate with dinuclear Co catalysts alone. Isotactic poly(cyclopentene carbonate)s with ee >99 % were synthesized by the chiral catatlyst with cocatalyst. Compare to the CHO/CO_2

copolymerization with the same group of dinuclear catalysts alone, CPO showed similar reactivity but higher enantioselectivity, but in the presence of cocatalyst CHO show much higher reactivity (TOF around 1300 h^{-1} for 0.25 h). Copolymerization of CPO/CO_2 was also done by zinc catalysts.

Similar to cyclopentene oxide, with epoxide fused on a five-membered ring, indene oxide (IO) is not very reactive toward binary Co catalysts.[35] *Cis*-cyclic indene carbonate was the only product generated in IO/CO_2 coupling by binary catalyst at temperatures higher than 25 ^{o}C. Poly(indene carbonate) started to grow at 0 ^{o}C, but only with moderate polymer selectivity (45-60 %) and low TOF (<5 h^{-1} for days). Its reactivity and polymer selectivity were improved by employing bifunctional Co catalyst with tethered ammonium salt.[36] Polymer selectivity achieved >99 % even at 25 ^{o}C, and TOF went up to 11.5 h^{-1}, though still very low compare to CPO. With rigid phenyl ring fused on the five-membered ring backbone, poly(indene carbonate)'s T_g reaches 138 ^{o}C with 9.7k molecular weight, which is higher than all polycarbonates mentioned above. In an effort to increase polycarbonate's T_g, copolymerization of dihydronaphthalene oxide (DHNO), a phenyl ring fused CHO, and CO_2 was attempted by applying Cr salen catalyst, but only caused *cis*-cyclic carbonate formation along with a trace quantity of polycarbonate.[37]

Oxa-cyclic epoxides are potentially different from their hydrocarbon counter parts in the CO_2/epoxide copolymerization. In Lu's 2014 publication regarding copolymerization of 3,4-epoxytetrahydrofuran (COPO) and CO_2, dinuclear Co itself alone presented low activity, but with cocatalyst its activity was improved (TOF 170 h^{-1}

for 2 h at 25 ^{o}C) with 95% enantioselectivity and 100% polymer selectivity.[38] Interestingly, the atactic COPO derived polycarbonate of molecular weight 8200 has T_g at 122 ^{o}C, which is much higher than poly(cyclopentene carbonate)'s T_g 85 ^{o}C with molecular weight of 27k.[39] While both isotactic and atactic poly(cyclopentene carbonate)s are amorphous, isotactic COPO derived polycarbonate is crystalline.

On the other hand, copolymerization of 3,5,8-trioxa-bicyclo[5.1.0]octane derivatives (CXO) and CO_2 by dinuclear Co catalyst was demonstrated to be as efficient and selective as COPO (TOF 180 h^{-1} for 2h at 25 ^{o}C).[40] To the best of my knowledge, this is the first report of CO_2 copolymerization with epoxide fused on a seven-membered ring, and the T_g of the resulting polycarbonate being 140 ^{o}C is the highest observed in this kind. Moreover, the ketal protecting group on the seven-membered ring can be deprotected with acid back to two hydroxyl groups, and the resulting polymer can serve as a macro-initiator in lactide ring-opening polymerization to make brush copolymer.

Overall, cyclic epoxides have higher polymer selectivity and T_g compare to linear epoxides. Among them, cyclohexene oxide is the most reactive epoxide and thus widely researched. Furthermore, cyclic epoxides derived from renewable resource, such as limonene oxide and cyclohexadiene oxide, make the copolymerization thoroughly renewable.

Terpolymerization of CO_2 and Two Epoxides

Terpolymerization of CO_2 and two (or more) epoxides are beneficial in incorporation of the relatively unreactive epoxide and tuning polymer properties. For

example, when catalyzed by Cr catalyst, cyclohexene oxide copolymerizes with CO_2 at temperatures higher than 40 ^oC but displays no reactivity at room temperature. In contrast, terpolymerization of propylene oxide, cyclohexene oxide and CO_2 can cause incorporation of cyclohexene oxide at low temperature.[41] As mentioned above, this phenomenon also happened for vinyloxirane. On the other hand, the T_g of terpolymer is able to be tuned between T_gs of respective epoxides and CO_2 copolymers by varying the two epoxides' incorporation ratios based on the Flory-Fox equation (eq. 3).[42] Terpolymers with T_g ranging from -15 to 115 ^oC were prepared by terpolymerization of PO/CO_2 with CHO or 1-hexene oxide.[16]

$$\frac{1}{T_g} = \frac{w_1}{T_{g1}} + \frac{w_2}{T_{g2}} \quad \text{(w = weight fraction of respective monomer)} \qquad \text{(eq. 3)}$$

Terpolymerization also delivers information of the relative reactivity of different monomers. Fineman and Ross reported a method to analyze reactivity ratios of two monomers.[43] The reactivity ratio was defined as the self-propagation rate over the cross-propagation rate. The monomer with higher reactivity ratio has a greater tendency for self-propagation. In the early stage of polymerization (conversion lower than 10 %), the monomers feed ratio $F = M_1/M_2$, molar ratio of monomer components in copolymer $f = m_1/m_2$ and reactivity ratios r_1 and r_2 can be correlated as stated in equation 4. By comparing monomers feed ratio versus their composition in terpolymer, r_1 and r_2 can be obtained. Epoxide whose reactivity ratio is larger than 1 has great propensity to self-propagate. Epoxide that has higher reactivity ratio in a terpolymerization is more

reactive compare to the other epoxide. This section summarized reactivity ratios of different epoxides in their terpolymerization with CO_2, not limited by Co salen catalyst system.

$$\frac{(f-1)}{F} = -r_2 \frac{f}{F^2} + r_1 \qquad \text{(eq. 4)}$$

Terpolymerization involving linear epoxides

As mentioned above, Lee and coworkers examined terpolymerization of PO/CO_2 with CHO, BO and HO catalyzed by their superior four ammonium arms tethered catalyst at 70-75 ^{o}C.[16] In addition to reactivity ratio, the relationship between terpolymer's T_g and composition was explored. For BO/PO/CO_2, r_{BO} = 0.58and r_{PO} = 1.4, and T_g = -27*f_{BC} + 38. For HO/PO/CO_2, r_{HO} = 0.46 and r_{PO} = 1.9, and T_g = -62*f_{HC} + 38. For CHO/PO/CO_2, r_{CHO} = 0.37 and r_{PO} = 1.7, and T_g = 81*f_{HC} + 40. In all three cases, r_{PO} is larger than 1 and the other r is smaller than 1, pointing out that PO is more reactive. Also, as the steric bulk increasing from BO to HO to CHO, the reactivity ratio decreases. It is noteworthy here that the linear relationship of terpolymer's T_g and composition is different from Flory-Fox relationship. The same terpolymerization of CHO/PO/CO_2 was done at lower temperature using salan Cr catalyst (**12**) instead by Darensbourg's group.[44] At 25 ^{o}C, r_{CHO} and r_{PO} are 0.172 and 1.11, and they are 0.869 and 1.49 at 40 ^{o}C, presenting temperature dependence of reactivity ratios in the way that CHO gets more reactive at higher temperature.

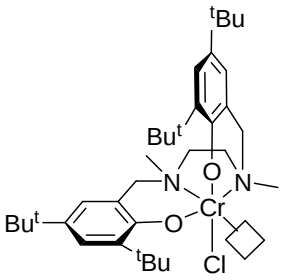

12

Darensbourg's group also investigated reactivity ratios of each epoxide in VIO/PO/CO_2 terpolymerization employing bifunctional Co catalyst.[27] In their earlier study of VIO mentioned before, VIO was way much less reactive than PO, and here the reactivity ratios reflected the trend. That is, $r_{VIO} = 0.224$ is much smaller than $r_{PO} = 3.74$. They blamed this reactivity difference on epoxide coordination ability: PO is more basic than VIO thus coordinates to metal center more easily.

The reactivity ratios of styrene oxide were measured in its terpolymerization with CO_2 and PO or CHO using binary Co catalyst.[45] In SO/PO/CO_2 terpolymerization, r_{SO} and r_{PO} are 0.18 and 2.26. The two epoxides display distinct reactivities. The terpolymer's T_d increased as styrene carbonate component increased. In SO/CHO/CO_2 terpolymerization, r_{SO} and r_{CHO} are 0.48 and 0.79. Higher reactivity of SO in terpolymerization with CHO was ascribed to the steric bulk of cyclohexene oxide.

Terpolymerization involving glycidyl ethers

Following BGE/CO_2 copolymerization, Grinstaff's group published preparation of BGE/PO/CO_2 terpolymer and a kinetic study.[25] The benzyl glycidyl ether fraction in terpolymer is always slightly larger than it feed ratio. This means it incorporates slightly

faster than PO. Reactivity ratios for BGE and PO were measured to be 1.15 and 0.93. These numbers are close to 1, with BGE's reactivity ratio be slightly larger than PO, indicating they are almost equally reactive in this terpolymerization. However, the overall TOF decreased as BGE feed ratio increased. Addition of 40 % propylene carbonate to the pure BGE/CO_2 copolymer brought about 7 times increase in storage or loss modulus. Upon deprotection to hydroxyl groups, the terpolymer's T_g droped to 10 ^oC from 15 ^oC with 60 % BGE component.

Around the same time, Luinstra's group illustrated another route to 1,2-glycerol carbonate containing polymer.[46] *O*-nitrobenzyl was chosen as the protecting group because of its easy deprotection via UV light instead of hydrogenation. Zinc glutarate catalyst was utilized for the terpolymerization of *o*-nitrobenzyl glycidyl ether (ONBGE) with PO and CO_2. This nitro-derivative of BGE is less reactive than BGE and PO in the terpolymerization. When its feed ratio was higher than 30%, no epoxide was converted to polymer. The reactivity ratios of ONBGE and PO were determined to be 0.64 and 1.46. Deprotected terpolymer has higher T_g and lower water contact angles. These changes in T_g and contact angle are proportional to *o*-nitrobenzyl glycidyl ether fraction in the terpolymer.

Likewise, reactivity ratios of allyl glycidyl ether and PO in AGE/PO/CO_2 terpolymerization by binary Co catalyst, were reported to be 0.876 and 0.755.[27] The reactivity ratio of AGE is slightly larger and AGE was found slightly more reactive than PO. The reactivity ratios of both epoxides are less than 1, meaning cross-propagation is favored and the two carbonates distribute randomly in the terpolymer.

Frey's group devoted efforts on a variety of terpolymerizations of two glycidyl ethers with CO_2 mostly using zinc pyrogallol catalyst in order to modify terpolymer physicochemical properties.[47] Those glycidyl ethers all showed similar reactivities based on the similar epoxide ratio in the terpolymer and feed. Postpolymerization modification made the terpolymers cross-linked or hydrophilic or functionalized thus have wider application in the fields of adhesives, coatings, sensors, self-healing materials, smart hydrogels, photovoltaic materials and drug delivery. Frey's group also worked on 1,2-epoxy-5-hexene terpolymerization with PO/CO_2.[48] Hydroxyl groups were attached to the terpolymer via thiol-ene reaction for "graft from" ring-opening polymerization of lactide. Unfortunately, they did not provide the reactivity data for any of their terpolymerizatoin.

Terpolymerization of CO_2 with two cyclic epoxides

In order to understand the effect of substituent group on the 4-position of CHO on reactivity, 4-vinyl cyclohexene oxide was terpolymerized with CHO and CO_2.[44] Reactivity ratios of VCHO and CHO are 0.847 and 1.03. These two close numbers show that the vinyl group at 4-position, which is away from epoxide, only has slight effect on reactivity.

As mentioned earlier, in 2014 Lu stated the results of COPO/CPO/CO_2 terpolymerization. The reactivity ratios for these two epoxides were determined to be very different, 8.49 for COPO and 0.17 for CPO, even though their reactivities towards the copolymerization with CO_2 alone were similar.[38] This large reactivity difference makes the terpolymer tapered, with one COPO enriched end and one CPO enriched end.

At the beginning of the terpolymerization, COPO incorporates dominantly. When it finishes up later CPO starts to consume. Combined with isotactic PCOPC's crystallinity, the tapered terpolymer is crystalline on one end and amorphous on the other end.

Block terpolymers

In addition to random terpolymer discussed before hand, block terpolymers have different properties and special applications. Darensbourg's group demonstrated the feasibility of di- and tri- block polycarbonates synthesis.[41] Diblock poly(propylene carbonate-b-cyclohexene carbonate) and triblock poly(propylene carbonate-b-cyclohexene carbonate-b-vinylcyclohexene carbonate) were prepared by subsequently cannulating PO/CHO/VCHO into the reactor. The success in block terpolymer synthesis expresses catalyst immortality.

Coates' group in 2011 and 2012 published their design of series block polymers of 4-substituted cyclohexen oxides.[49] Multiblock polymers were synthesized from CHO with different functionalities including vinyl, oxo, silyl and fluoro groups ranging from lipophilic to hydrophilic and fluorophilic in interchangeable sequence. Furthermore, the norbornenyl chain ends of multiblock polymer from norbornenyl acetate in the catalyst made the polymer a macromonomer in ring-opening metathesis polymerization. Core-shell and block core-shell molecular brushes were made via "grafting through" method with Grubb's catalysts.

Route to di- or triblock terpolymers of polycarbonate and polylactide was created by Darensbourg's group.[50] Poly(styrene carbonate-b-lactide) and poly(lactide-b-

propylene carbonate-b-lactide) were obtained by tandem epoxide/CO_2 copolymerization and lactide ring-opening polymerization. For diblock poly(styrene carbonate-b-lactide), SO/CO_2 copolymerization was terminated by adding water, a chain transfer/termination reagent. The thus formed hydroxyl group chain ends were deprotonated by DBU later to generate the alkoxide-terminated polymer, as a macroinitiator for the subsequent lactide ring-opening polymerization. Adding the lactide block to the polycarbonate lowered poly(styrene carbonate)'s T_g from 80 to 60 ^oC the lowest, and only one T_g was observed for every block copolymer. However, using the stereospecific D-lactide, the polylactide end started to be crystalline with melting points at about 135 ^oC. For triblock poly(lactide-b-propylene carbonate-b-lactide), water was added at the beginning of the PO/CO_2 copolymerization. Water terminated the growing chain and also hydrolyzed the trifluoroacetate initiator. This brought about poly(propylene carbonate) polyol, a poly(propylene carbonate) with hydroxyl groups on both ends. DBU and lactide were added afterwards to produce the ABA triblock terpolymer.

This dissertation focuses on expanding the scope of epoxides in order to efficiently make other polycarbonates with desirable properties. Salen metal complexes catalyzed copolymerization of CO_2 and epoxides with different electronics, sterics and structures will be discussed in terms of reactivity, polymer selectivity and resultant polycarbonate property. The final goal is to apply the knowledge of epoxides to produce useful polycarbonates from renewable resources with minimum energy input.

CHAPTER II

RELATIVE BASICITIES OF CYCLIC ETHERS AND ESTERS: CHEMISTRY OF IMPORTANCE TO RING-OPENING CO- AND TERPOLYMERIZATION REACTIONS*

Introduction

In endeavors to maintain a sustainable chemical industry, alternative feedstocks are needed to replace decreasing petroleum supplies. The utilization of carbon dioxide as a source of chemical carbon can contribute to meeting this shortage.[51] Among the processes exhibiting commercial viability are the incorporation of carbon dioxide into polymeric materials, a subject of much current interest.[1] Important among these processes is the completely alternating copolymerization of CO_2 and epoxides to provide polycarbonates (eq. 5).[2] Because there are a limited number of epoxides which provide good selectivity for copolymer formation, it may be necessary to synthesize terpolymers from two such epoxide monomers and carbon dioxide in order to obtain polycarbonates with desirable physical properties.

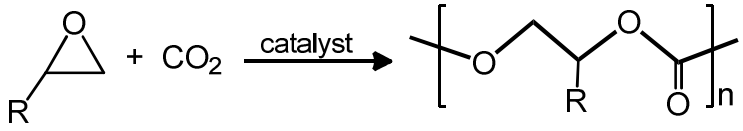

(eq. 5)

*Reproduced in part with permission from: "Relative Basicities of Cyclic Ethers and Esters. Chemistry of Importance to Ring-opening Co- and Terpolymerization Reactions." Darensbourg, D. J.; Chung, W.-C. *Polyhedron* **2013**, *58*, 139. Copyright 2013. Elsevier.

The basicity of the cyclic ether should be a factor in the copolymerization of carbon dioxide with this monomer. That is, cyclic ether activation *via* binding to the metal center should correlate with the basicity of the cyclic ether in the absence of steric hindrance, and hence facilitates ring-opening by nucleophiles (Scheme 5). At sufficiently high CO_2 concentration, insertion of CO_2 into the resulting metal alkoxide species is generally not rate-limiting. Hence, following the initiation step the rate of copolymerization should be both a function of the basicity of the cyclic ether monomer and the nucleophilicity of the growing polymer chain. The growing carbonate polymer chain in **19** serves as the recurring nucleophile in species **17**.

Scheme 5

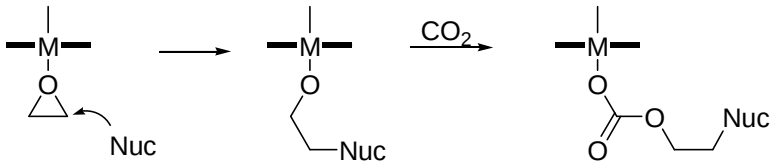

17 **18** **19**

Fineman and Ross have defined a linear method for determining the monomer reactivity ratios for two monomers in a copolymerization reaction *at low conversion* by way of equation (eq. 6).[43] M_1 and M_2 refer to the monomer composition in the feed and m_1 and m_2 to the monomer composition in the polymer. The monomer reactivity ratios are given by r_1 and r_2, which are k_{11}/k_{12} and k_{22}/k_{21} in Scheme 6, respectively.

$$\frac{dM_1}{dM_2} = \frac{M_1}{M_2}\,\frac{r_1M_1 + M_2}{M_1 + r_2M_2} = \frac{m_1}{m_2} \qquad \text{(eq. 6)}$$

Scheme 6

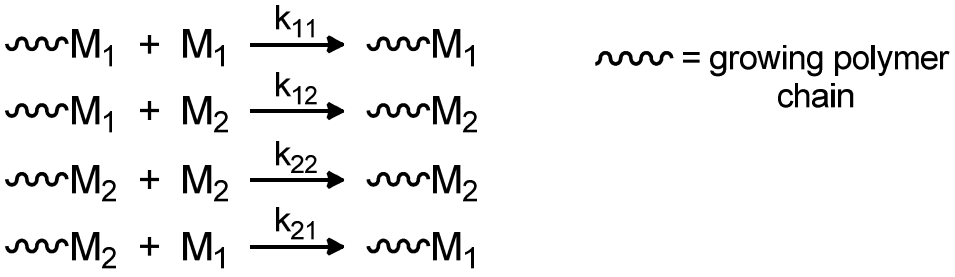

Upon examining the relative reactivity of two different cyclic ethers which differ significantly in basicities, the terpolymerization parameters should include both the rate constants for ring-opening and the binding constants for the monomers (Scheme 7).[52]

The binding constants in turn are proportional to the basicities of the cyclic ethers. Therefore, $r_1 = k_{11}K_{11}/k_{12}K_{12}$ and $r_2 = k_{22}K_{22}/k_{21}K_{21}$. In the absence of steric hindrance, if the K_b's of the two monomers are similar, K_{11} and K_{12} should be similar, and the reactivity ratio reduces to simply k_{11}/k_{12}. Hence, it is important to know the relative basicities of the two monomers involved in the polymerization process.

Scheme 7

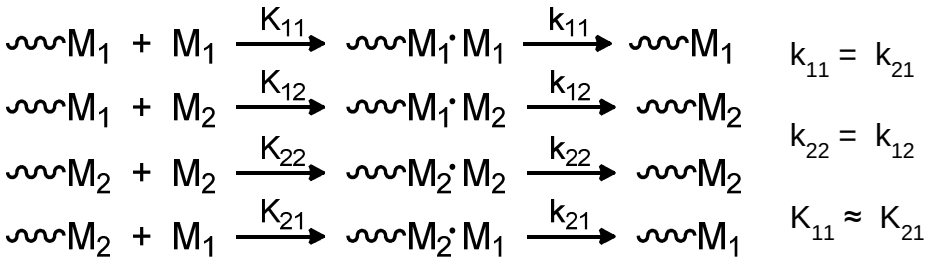

Results and Discussion

Determination of pK_bs of cyclic ethers

Over seventy years ago, Gordy and coworker established an empirical relationship between the K_b and the shift of the OD stretching vibration in methanol-d_1 dissolved in organic bases (eq. 7), where $\Delta\mu_{OD}$ = shifted value of ν_{OD} in millimicrons from that in benzene.[53] Pertinent to the subject of terpolymerization processes involving two or more cyclic ethers and carbon dioxide, it is useful at this time to revisit the Gordy equation while extending it to relevant epoxides. Originally, these researchers established a correlation between the K_b of amines and the shift of ν_{OD} of CH_3OD in amines in comparison with that in benzene. The basicity constants were determined in aqueous solution and are interpreted as the ability of the base to attract a proton from water.

$$\Delta\mu_{OD} = 0.0147 \log K_b + 0.194 \qquad \text{(eq. 7)}$$

In Figure 3, we have re-plotted Gordy's original data in more commonly used units of cm^{-1} and pK_b, leading to equation 8.[53c,d] In an analogous manner, we have measured the shifts in the ν_{OD} vibration in CH_3OD dissolved in various amines and compiled that data in Table 1, along with the literature values of the pK_b of the amines determined in aqueous solutions.[54] These ν_{OD}s are compared to the corresponding value for CH_3OD in benzene of 2667.4 cm^{-1}. Our measurements result in the linear relationship (Figure 4), which is slightly different from that of Gordy and coworker, equation 9. It should be noted that we utilized a high-resolution FTIR instrument,

whereas, Gordy and coworker employed an infrared spectrometer which utilized interchangeable 60°-prisms in a Wadworth-Littrow mounting.[55] Nevertheless, the trends are comparable.

$$\Delta\nu_{OD} = 9.011\ pK_b - 259.02 \qquad \text{(eq. 8)}$$

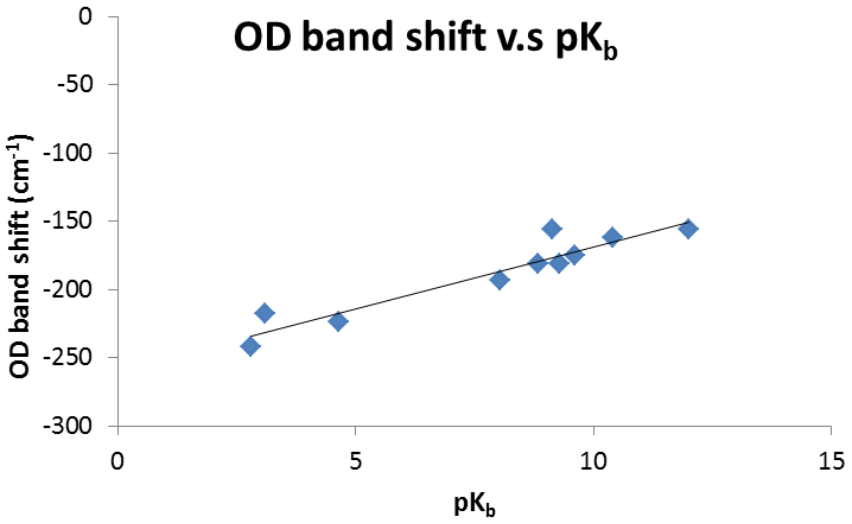

Figure 3 Re-plot of Gordy's $\Delta\nu_{OD}$ shift data of CH_3OD in amine *vs* that in benzene.

$$\Delta\nu_{OD} = 15.41\ pK_b - 299.37 \qquad \text{(eq. 9)}$$

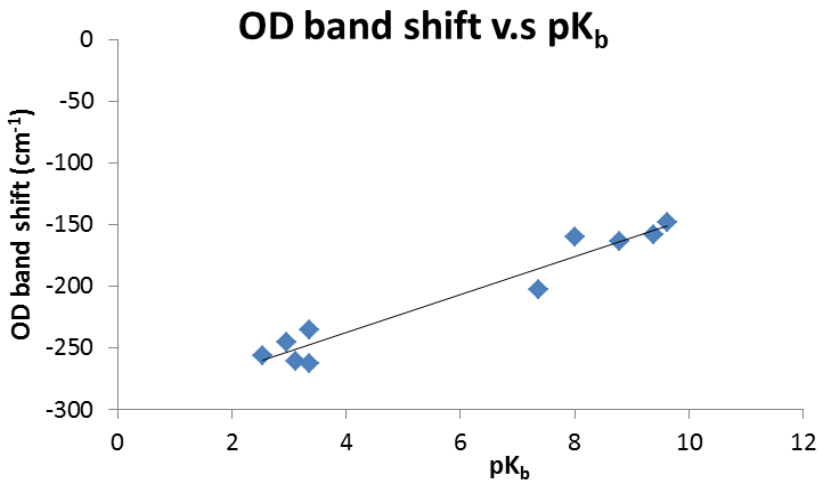

Figure 4 Plot of $\Delta\nu_{OD}$ shift data of CH_3OD in amine *vs* that in benzene. Correlation coefficient (R^2) = 0.9469.

Table 1 Basicities of amines.

Amine	MeOD peak (cm^{-1})	OD band shift from benzene (cm^{-1})	pK_b	ref
piperidine	2422.5	-244.9	2.95	10
pyridine	2503.5	-163.9	8.79	11
aniline	2509.3	-158.2	9.38	12
tributylamine	2407.0	-260.4	3.11	10
trimethylaniline	2518.9	-148.5	9.62	13
cyclohexylamine	2432.1	-235.3	3.36	12
4-picoline	2507.3	-160.1	8.00	14
triethylamine	2405.1	-262.3	3.35	10
2,6-lutidine	2464.9	-202.5	7.36	14
diisoproylethylamine	2410.9	-256.5	2.55	15

[a]ν_{OD} in benzene observed at 2667.4 cm^{-1}. [b]References are for best amine pK_b values in aqueous solution.

As mentioned earlier, our goal in these studies was to determine the *relative* pK_bs of various cyclic ethers and lactones in order to quantitatively assess their incorporation into terpolymers. Table 2 lists the spectral shifts in the ν_{OD} frequency of CH_3OD in several organic ethers and lactones relevant to our catalytic polymerization studies. In turn, these data taken together with the corresponding value of ν_{OD} in benzene of 2667.4 cm^{-1} and equations 8 and 9 were employed in computing the pK_b provided in Table 2. As is obvious in Table 2, there are significant differences in the values of the base strengths of these weak organic bases predicted by our results compared to those earlier reported by Gordy. However, the trends or relative basicities are essentially the same. Indeed, since the procedure utilizes pK_b values for amines in aqueous solution as calibration data, there should be no expectation that the absolute pK_b value will be correct in either case.

Previous studies by Arnett and Wu have reported the base strengths of several cyclic ethers in aqueous sulfuric acid.[56] The order of basicity for a series of cyclic ethers was determined to be the same as that found by others in six other acidic systems. The pK_bs of two saturated cyclic ethers (THF and 2-MeTHF) common to our reported values, along with that of diethyl ether, were measured and found to be 16.08, 16.65, and 17.59, respectively. These values show the same trend as those listed in Table 2, and lie in between those determined herein and earlier by Gordy. It should be pointed out that others have calculated pK_b values for organic bases based on Gordy's original equation incorrectly.[52,57] For example, pK_b values for the cyclic ethers, propylene oxide and THF

were reported as 7.0 and 6.0 respectively, i.e., better bases than many amines. Nevertheless, their relativity base strengths exhibited the expected trends.

Terpolymerization studies

As alluded to in the introduction, a useful means for varying the properties of copolymers derived from epoxides and CO_2 is to incorporate two chemically different epoxide monomers. In these instances, the relative reactivity patterns of the epoxide monomers are important in determining the copolymer's composition and structure. For example, if the two epoxides have significantly different reactivities diblock or tapered polymers are most likely to be produced. Hence, when carrying out such terpolymerization processes, the binding and ring-opening parameters for the two epoxides in addition to their concentrations (feed ratio) account for the extent to which each monomer is incorporated into the polymeric material. Schiff base metal complexes, in particular (salen)MX where M = Cr(III), Co(III), and Al(III), along with onium salts, are the most active and well-studied catalysts for the process defined in equation 5.[2] The inspiration for the use of these particular metal species is based on the elegant studies of Jacobsen and coworkers for the asymmetric ring-opening of epoxides.[58]

Table 2 Basicities of organic ethers and lactones.

	MeOD peak (cm^{-1})	OD band shift from benzene(cm^{-1})	pK_b	pK_b (from Gordy)
oxetane	2571.0	-96.4	13.2	18.0
3,3-dimethyl oxetane	2574.8	-92.6	13.4	18.5
indene oxide	2601.8	-65.6	15.2	21.5
cyclopentene oxide	2605.7	-61.7	15.4	21.9
cyclohexene oxide	2607.6	-59.8	15.5	22.1
vinylcyclohexene oxide	2607.6	-59.8	15.5	22.1
propylene oxide	2609.6	-57.9	15.7	22.3
methylstyrene oxide	2619.2	-48.2	16.3	23.4
styrene oxide	2621.1	-46.3	16.4	23.6
Epichlorohydrin	2625.0	-42.4	16.7	24.0
THF	2576.8	-90.7	13.5	18.7
2-methyl-THF	2578.7	-88.7	13.7	18.9
valerolactone	2588.3	-79.1	14.3	20.0
diethyl ether	2592.2	-75.2	14.5	20.4
caprolactone	2594.1	-73.3	14.7	20.6
butyrolactone	2603.8	-63.7	15.3	21.7
propiolactone	2639.5	-28.0	17.6	25.6

[a] ν_{OD} value of CH_3OD in benzene determined to be 2667.4 cm^{-1}. Our data would predict benzene to have a pK_b of 19.4, and Gordy's data would provide a value of 28.7.

Kinetic studies of terpolymerization reactions of propylene oxide (PO) and cyclohexene oxide (CHO) have been reported recently.[16,44] For example, Lee and coworkers have examined this process using a (salen)Co(III) catalyst, where the salen ligand has tethered quaternary ammonium salts. In this investigation, Fineman-Ross analysis provided r_{PO} and r_{CHO} values of 1.7 and 0.37, respectively; where $r_{PO} = k_{11}/k_{12}$ (see Scheme 8) and $r_{CHO} = k_{22}/k_{21}$. In this instance, these measured monomer reactivity ratios are good indicators of the relative rate constants since the binding constants of the two monomers are very similar based on their pK_b (15.7 *vs* 15.5). Support for the similarity of these two epoxides binding to cadmium has been provided by thermodynamic data as well as Cd-O bond distances obtained by X-ray crystallography.[59-61]

Scheme 8

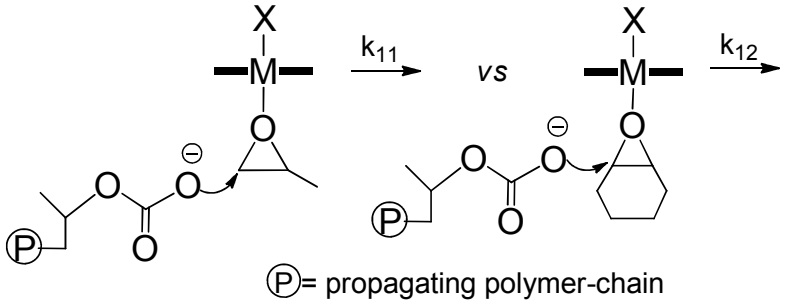

Nevertheless, it is possible with the pK_bs from Table 2 to correct the values for k_{11}/k_{12} and k_{22}/k_{21} to 2.69 and 0.234, respectively. That is, the copolymer chain ended in propylene carbonate prefers to ring open a propylene oxide monomer over a cyclohexene oxide monomer by a factor of 2.69 compared to a factor of 1.7 if binding differences are not taken into account. Likewise, $r_{CHO} = k_{22}K_b^{CHO} / k_{21}K_b^{PO}$ or

$k_{22}/k_{21} = 0.37 \times (3.16 \times 10^{-16})/(2.00 \times 10^{-16}) = 0.234$. On the other hand, in our previous study for the terpolymerization of cyclohexene oxide and vinylcyclohexene oxide (VCHO), two chemically similar monomers with identical pK_bs, with CO_2 the r_{CHO} and r_{VCHO} values determined from Fineman-Ross data of 1.03 and 0.85 are true measures of their respective rate constant parameters.[44]

VCHO

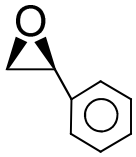

SO

Herein, we have investigated the reactivity ratios for two epoxide monomers with significantly different reactivities and basicities, i.e., the terpolymerization of propylene oxide and styrene oxide (SO) with CO_2. Individually, the rates of copolymerization of these two epoxides with CO_2 utilizing the same binary (salen)CoX catalyst system (**2**, Figure 5) and reaction conditions are quite disparate, and their respective estimated K_bs are considerably different, with K_b^{PO} being 2.00 x 10^{-16} and K_b^{SO} being 3.98 x 10^{-17}.[20b] For example, the TOFs for processes carried out under identical conditions at 25 ^oC were found to be 540 h^{-1} (PO) and 75 h^{-1} (SO), respectively. These large differences in binding affinities and self ring-opening rates make terpolymerization reaction quite challenging. Hence, it was necessary to carry out these processes to slightly greater than 10% conversion in order to achieve adequate incorporation of the less reactive monomer, styrene oxide. Table 3 contains the experimental data for the terpolymerization of

propylene oxide and styrene oxide at different feed ratios, and Table 4 summarizes the data for the monomer content in the isolated terpolymers. The Fineman-Ross plot in Figure 6 affords monomer reactivity ratios of r_{PO} = 5.37 and r_{SO} = 0.504 (eq. 10).[43] Equation 10 is derived from equation 6 assuming low conversion of reactants to product.

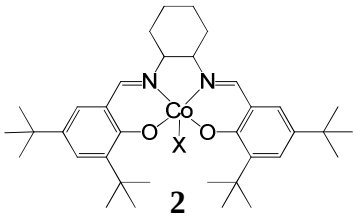

2

PPNX
PPN = *bis*(Ph_3P)N^+
X = 2,4-dinitrophenoxide

Figure 5 Binary (salen)CoX/PPNX catalyst system used in terpolymerization reactions.

$$\frac{(f-1)}{F} = -r_{PO}\frac{f}{F^2} + r_{SO} \qquad \text{(eq. 10)}$$

Based on the expected metal binding differences as indicated by their pK_bs, the reactivity ratio values, r_{PO} and r_{SO}, are a function of both the relative monomer binding ability and rate constants for self-propagation or cross-propagation. That is, $r_{PO} = k_{11}K_b^{PO}/k_{12}K_b^{SO} = 5.37$ provides a rate constant ratio of $k_{11}/k_{12} = 1.07$. Similarly,

for the styrene oxide monomer the self- and cross-ring opening rate constant ratio $k_{22} / k_{21} = 2.53$. This example points out that a critical interpretation of reactivity ratios requires some knowledge of the *relative* monomer binding ability. In cases where the binding is expected to differ significantly, assigning the reactivity ratios to differences in kinetic parameters alone can be misleading. Surprisingly, in this instance, the propylene carbonate chain end shows little preference for ring-opening propylene oxide or styrene oxide monomers, whereas, the styrene carbonate chain end displays a slight tendency to self-propagate *vs* cross-propagate.

Table 3 Terpolymerization Reactions.[a]

	feed (mmol)		monomer/catalyst		reaction	conversion (%)	
entry	SO	PO	SO	PO	time (h)	SO	PO
1	17.5	42.9	667	1632	3	2.8	13.7
2	21.9	35.7	833	1360	5	5.3	16.9
3	24.1	32.2	917	1224	3	0.3	6.3
4	26.3	28.6	1000	1088	4	2.6	16.1
5	30.6	21.4	1167	816	24	1.9	12.6

[a]Catalyst system: *N,N'*-bis(3,5-di-*tert*-butylsalicylidine)-1,2-cyclohexanediaminocobalt(III)-2,4-dinitrophenoxide/PPN(2,4-dinitrophenoxide)1:1 mol. Ratio, 2 MPa CO_2 pressure, ambient temperature.

Table 4 Monomer Content in Feed and Resulting Terpolymer.

	mole fraction in feed		mole fraction in polymer[a]		y[b]	x
entry	SO	PO	SO	PO	(f-1)/F	f/F^2
1	0.29	0.71	0.08	0.92	-2.24	0.50
2	0.38	0.62	0.13	0.88	-1.40	0.38
3	0.43	0.57	0.14	0.86	-1.12	0.29
4	0.48	0.52	0.18	0.82	-0.86	0.25
5	0.59	0.41	0.27	0.73	-0.45	0.18

[a]Determined by 1H NMR, b: F = mole ratio of SO/PO in feed, f = mole ratio of SO/PO in polymer.

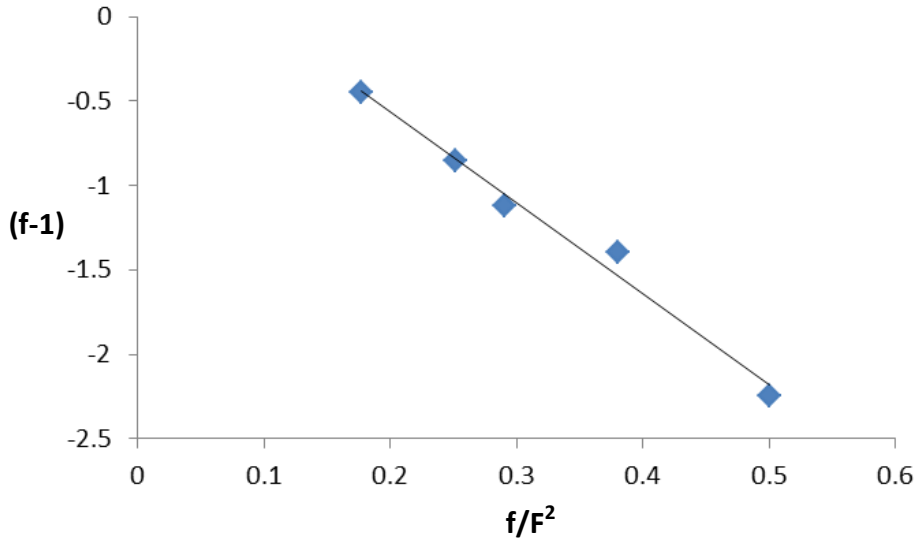

Figure 6 Fineman-Ross analysis of PO/SO/CO_2 terpolymerization reaction at ambient temperature. $y = -5.3666x + 0.5043$; $R^2 = 0.9849$.

Finally, in terpolymerization processes involving two monomers of greatly different binding abilities, where the stronger binding monomer is more difficult to ring open, no reaction takes place. For example, we have found that oxetane and propylene oxide monomers do not undergo terpolymerization with CO_2 at modest temperatures where oxetane, unlike propylene oxide, is resistant to ring-opening polymerization because of its lesser strain energy. That is, oxetane inhibits activation of propylene oxide monomer due to its lack of a metal binding site (*recall relative pK_bs of oxetane and propylene oxide are 13.2 and 15.7*).[62,63] This is, of course, the necessity for carrying out copolymerization reactions of epoxides with CO_2 in weakly binding solvents, such as methylene chloride or toluene.

Experimental Section

Spectral measurements

A calibration curve was initially made by determining the ν_{OD} of stretching vibration in CD_3OH dissolved in ten different amines with pK_a values in water spanning the range 2.55 to 9.62. The difference between the value of ν_{OD} of CH_3OD in benzene, determined to be 2667.4 cm^{-1}, and the corresponding ν_{OD} value in the amines was measured and plotted *vs* the pK_b of the amine (see Table 1 and Figure 4). As noted in Figure 4, there is a rough correlation between $\Delta\nu_{OD}$ and the amine pK_b with a correlation coefficient (R^2) of 0.9469. Similarly, the shifts of the ν_{OD} vibration in CH_3OD dissolved

in the respective cyclic ether (~ 0.2 M) and that in benzene were determined. From these shifts and the calibration curve pK_b values of the cyclic ethers were determined.

Terpolymerization reactions of styrene oxide/propylene oxide and CO_2

(S,S)-N,N'-bis(3,5-di-tert-butylsalicylidine)-1,2-cyclohexane diaminocobalt(III)-2,4-dinitrophenoxide (20.67 mg, 0.02627 mmol), *bis*(triphenylphosphine)iminium 2,4-dinitrophenoxide(18.96 mg, 0.02627 mmol), styrene oxide(2.00 mL, 17.5 mmol) and propylene oxide(3.00 mL, 42.9 mmol) were added to a 12 mL autoclave reactor which had previously been dried for six hours. For other terpolymerization with different SO/PO ratio, the SO and PO volume were varied to maintain the total volume at 5 mL. The reactor was pressurized to 2MPa with CO_2 and maintained at ambient temperature. Subsequent to the allotted time, the reactor was depressurized and a small aliquot was taken to be analyzed by ^{1}H NMR to calculate the conversion of styrene oxide and propylene oxide. The reaction solution was dissolved in CH_2Cl_2 and added to c.a. 1M HCl methanol solution to obtain pure polymer, which was dried *in vacuo* at 40 ^oC and analyzed by ^{1}H NMR and GPC.

Conclusion

We have revisited the Gordy[64] equation by assigning relative pK_b values for various common monomers employed in ring-opening polymerization processes catalyzed by coordination metal complexes based on their respective shifts in the –OD stretching vibration of CH_3OD *vs* that observed for benzene. The pK_b values for cyclic

ethers were utilized in assessing the kinetic *vs* thermodynamic components of the reactivity ratios determined by a Fineman-Ross analysis for two different monomers in terpolymerization reactions with CO_2. It was clearly illustrated that for cyclic ethers with significantly different pK_bs, the interpretation of the reactivity ratios cannot be simply based on the rate constants for self- or cross-propagation of polymer chains.

CHAPTER III

AVAILABILITY OF OTHER ALIPHATIC POLYCARBONATES DERIVED FROM GEOMETRIC ISOMERS OF BUTENE OXIDE AND CARBON DIOXIDE COUPLING REACTIONS*

Introduction

The copolymerization of epoxides and carbon dioxide to selectively afford completely alternating copolymers continues to be a challenging and important subject for study. This is the consequence of this process' ability to provide value-added chemicals from the recalcitrant CO_2 molecule, an abundant and renewable chemical feedstock.[1,65] Indeed, these polymerization processes have been commercialized and represent one of the most viable new uses of CO_2 for large-scale industrial chemical synthesis.[66] Although various epoxides have been shown to selectively undergo this CO_2 coupling process to afford copolymers, in many instances it is often accompanied by formation of the thermodynamically more stable addition product, cyclic carbonate.[2,67] These two competing pathways are illustrated in Scheme 9, specifically for propylene oxide and CO_2. Recently, the use of bifunctional salen metal catalysts have proven to be very effective at selectively providing the kinetic product, the copolymer.[12,13,36,68]

---

*Reproduced in part with permission from: "Availability of Other Aliphatic Polycarbonates Derived from Geometric Isomers of Butene Oxide and Carbon Dioxide Coupling Reactions." Darensbourg, D. J.; Chung, W.-C. *Macromolecules* **2014**, *47*, 4943. Copyright 2014. American Chemical Society.

Scheme 9

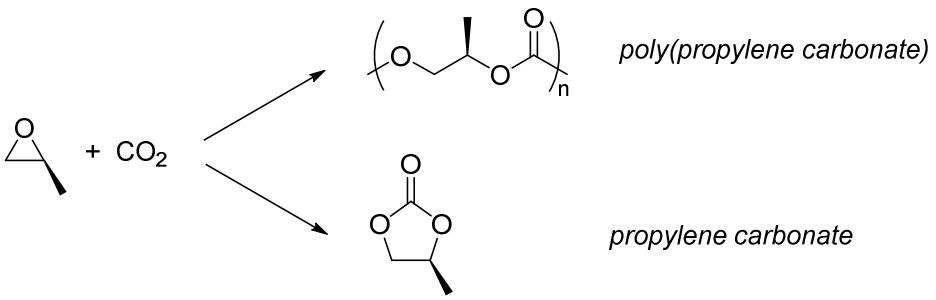

In our continuing efforts to expand the scope of epoxides that will efficiently couple with carbon dioxide to selectively afford copolymers, herein we report on the copolymerization reaction of *cis*-2-butene oxide and CO_2 (eq. 11).[69] In addition, comparative studies of the coupling reactions of CO_2 with the other isomers of butene oxide will be examined. These investigations should expand the range of thermal and mechanical properties of copolymers available based on this methodology, and hence their applications. Indeed, it is of interest to compare the large range of T_g values anticipated based on the differences in the chemical structures of the non-crystalline copolymer materials derived from the isomeric forms of butene oxide. The copolymer produced from 1-butene oxide and CO_2 has previously been reported by Lee and coworkers,[16] whereas, a brief mention of the successful copolymerization of *cis*-2-butene oxide (a meso-epoxide) and CO_2 has been cited by Nozaki and coworkers.[69]

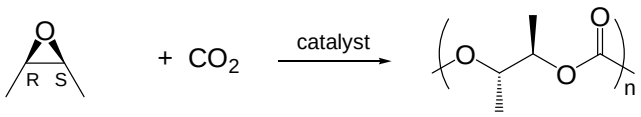

cis-2-butene oxide
(*meso*-epoxide)

(eq. 11)

Results and Discussion

In order to probe the steric effects of the substituents on the epoxide monomer on the selectivity of its coupling reaction with CO_2 to provide copolymer, we have examined the process with four different butene oxide isomers/derivatives. These include *cis*-2-butene oxide (**E1**), trans-2-butene oxide (**E2**), isobutene oxide (**E3**), and 2,3-epoxy-2-methylbutane (**E4**), initially utilizing binary (salen)Co(III) (**2**) and (salen)Cr(III) (**1**) catalyst systems (Figure 7). For both catalytic systems, *cis*-2-butene oxide was found to be the most reactive epoxide of the group (Figure 8). *Cis*-2-butene oxide was the only epoxide among these four epoxide monomers which reacted with CO_2 in the presence of the cobalt catalyst system **2** at 40 ^{o}C. In this instance, the overall conversion was 59.2% with a selectivity for copolymer formation of 75.4% along with *trans*-cyclic carbonate. On the contrary, the chromium binary catalyst system **1** at both 40 and 70 ^{o}C were efficient at coupling CO_2 and epoxides **E1**, **E2**, and **E3** to provide exclusively cyclic carbonate products. Similar to the case of catalyst **2**, catalyst **1** was completely ineffective at catalyzing the coupling of monomer **E4**, 2,3-epoxy-2-methylbutane, with CO_2. *Trans*-2-butene oxide afforded all trans-cyclic butene carbonate, whereas *cis*-2-butene oxide produced both *cis*- and *trans*-cyclic butene carbonate in a ratio of 4:1 (vide infra) at 40 ^{o}C.

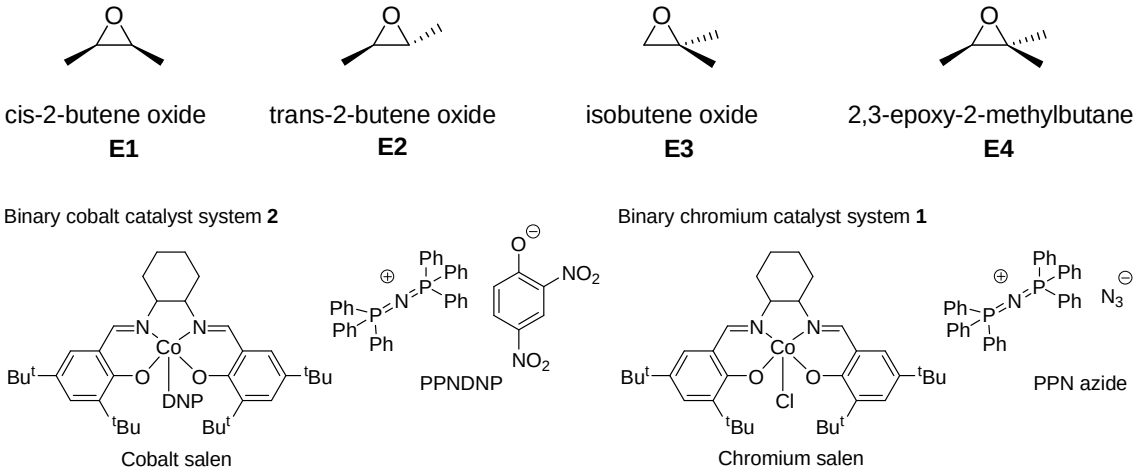

Figure 7 Coupling of CO_2 and different butene oxide isomers/derivative *via* cobalt or chromium salen complexes.

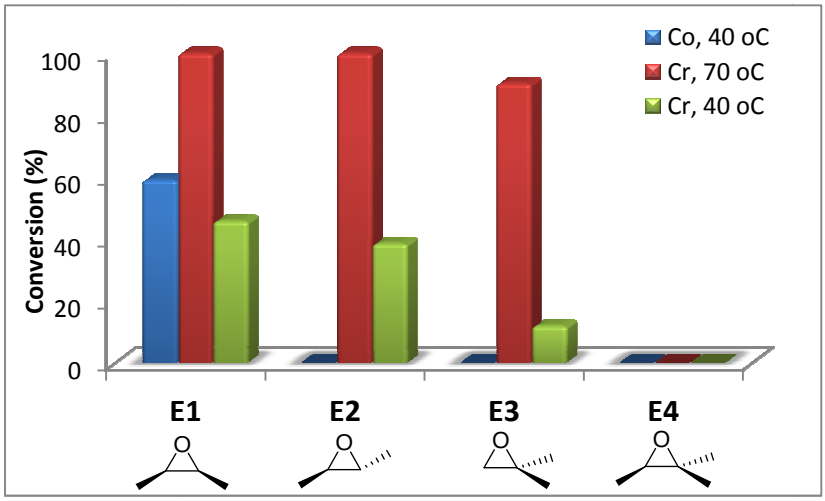

Figure 8 Reactivity of different epoxides in coupling reaction with CO_2. All monomers, except **E4**, provided cyclic carbonates with Cr catalyst **1** at 70 ^{o}C. Co catalyst **2** afforded a selectivity for copolymer of 75.4%. Reaction condition: epoxide/catalyst/cocatalyst = 500/1/1 for Co (**2**) and 500/1/2 for Cr (**1**), CO_2 20 bar, 20 h.

The bifunctional catalyst analogs, **13**, and **14** in Figure 9, have been previously shown to exhibit significant improvement over their binary analogs for the selective production of copolymers from the coupling reactions of several epoxides and CO_2.[12,36,39,68] Somewhat surprising, catalyst **14** was unreactive towards coupling CO_2 and the epoxides **E2** and **E3**. This is in sharp contrast with the binary chromium(III) catalyst system **1** which effectively catalyzed the production of the corresponding cyclic carbonates (Figure 10). This observation is presumably due to steric inhibition of the epoxide ring-opening process resulting from the restricted spatial requirements in the metal salen ligand in bifunctional Cr catalyst **14**.

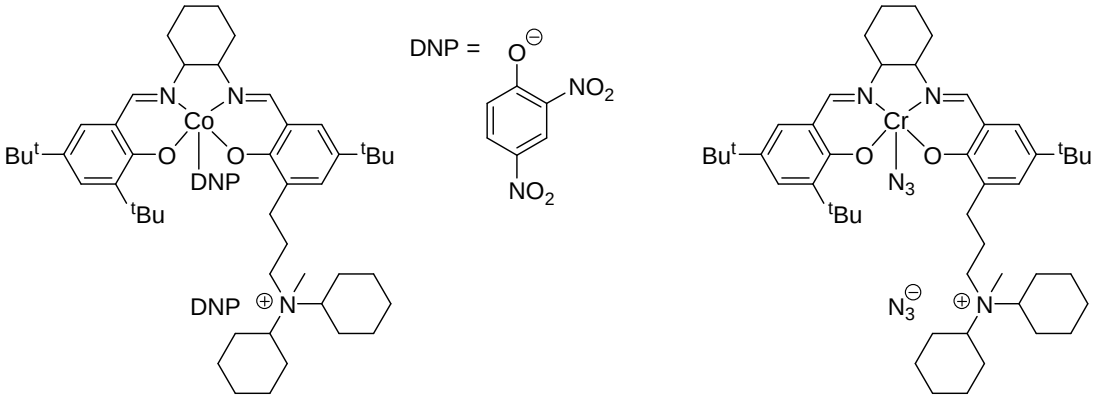

Figure 9 Bifunctional cobalt(III) and chromium(III) catalysts.

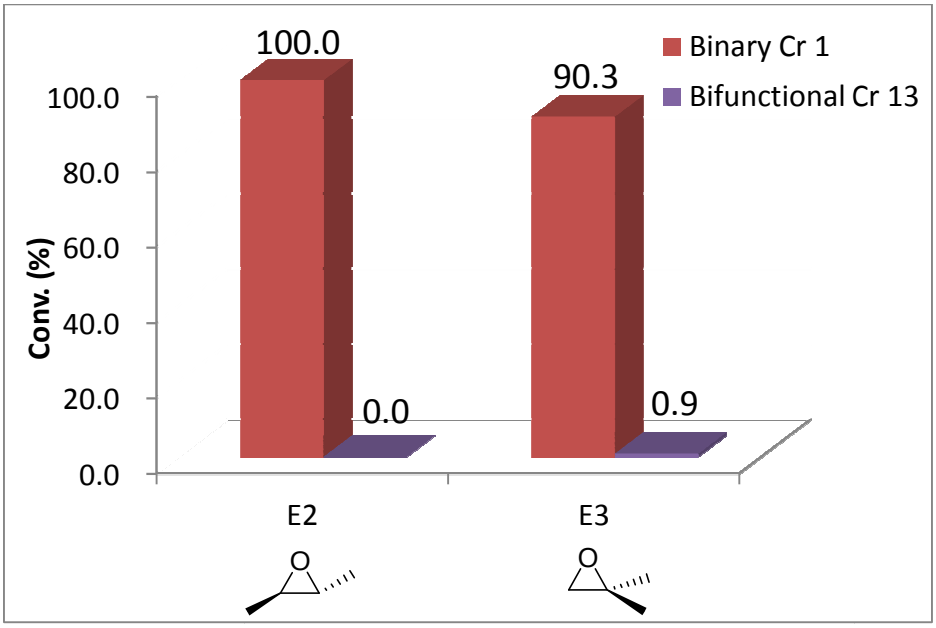

Figure 10 Conversion of epoxide **E2** and **E3** coupling with CO_2 catalyzed by binary (**1**) and bifunctional (**14**) chromium salen catalysts.

On the other hand, the cobalt(III) (**13**) and chromium(III) (**14**) bifunctional catalysts were highly selective for producing copolymer from *cis*-2-butene oxide and CO_2 (Scheme 10). Under identical reaction conditions, catalyst **14** was 79.0% selective for affording poly(2-butene carbonate), whereas catalyst **1** was 100% selective for forming cyclic butene carbonate. Catalyst **13** was found to exhibit excellent selectivity and reactivity for the coupling of *cis*-2-butene oxide and CO_2 to poly(2-butene carbonate) at 40 ^{o}C. These results are summarized in Table 5. Although the bifunctional chromium catalyst (**14**) was slightly less effective at coupling *cis*-2-butene oxide and CO_2 at 70 ^{o}C than its binary analog (**1**), unlike the catalyst **1** system which afforded cyclic carbonate exclusively, the catalyst **14** was 79% selective for copolymer formation (Table 5, entry 1 vs Table 6, entry 8). The bifunctional cobalt catalyst **13** was quite effective at

copolymerizing *cis*-2-butene oxide and CO_2 to provide 100% selectivity for copolymer at 40 oC (Table 5, entries 2 - 4). Upon increasing the reaction temperature to 70 ^{o}C, the % conversion increased with a decrease in selectivity for copolymer production (Table 5, entry 5).

Scheme 10 Coupling of *cis*-2-butene oxide and CO_2 to provide poly(2-butene carbonate) with *cis* and *trans* cyclic butene carbonate(BC) byproducts.

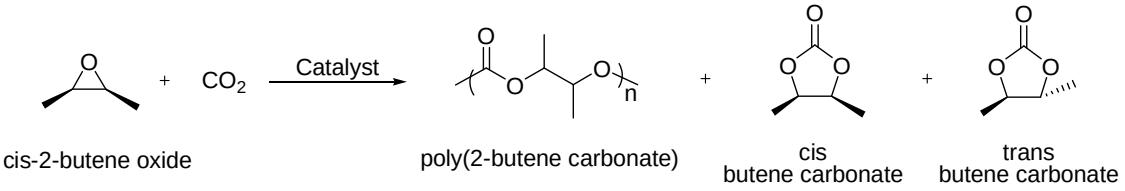

cis-2-butene oxide | poly(2-butene carbonate) | cis butene carbonate | trans butene carbonate

Table 5 Copolymerization of CO_2 and *cis*-2-butene oxide utilizing bifunctional cobalt and chromium salen catalysts.[a]

entry	catalyst	Temp (^{o}C)	time (h)	Conv. (%)[b]	TOF (h^{-1})[b]	polymer selectivity (%)[b]	M_n (kDa)	PDI	T_g (^{o}C)
1	**14**	70	20	55.1	27.6	79.0	4.5	1.08	65.3
2	**13**	40	24	67.3	28.0	> 99	13.9	1.05	69.0
3	**13**	40	12	59.0	49.2	> 99	11.6	1.04	67.9
4	**13**	40	6	46.3	77.1	> 99	11.1	1.04	65.5
5	**13**	70	6	74.5	124.2	65.0	13.9	1.12	68.0
6	mix-**13**[c]	40	48	49.5	10.3	93.1	4.8	1.05	63.6

[a.] CO_2 20 bar, monomer/catalyst = 1000/1. [b.] Determined by NMR. [c.] (*R*,*R*)-, (*S*,*S*,)-, and (*R*,*S*)- backbone mixture.

Non-crystalline polymeric materials all experience glass transitions which result in changes in polymer properties such as thermal expansion, specific heat capacity or modulus. Since the glass transition temperature is sensitive to chemical structure, there is expected to be a difference in T_g values for poly(2-butene carbonate) and poly(1-

butene carbonate). As indicated in Table 5, the glass transition temperature of poly(2-butene carbonate) is about 68 ^{o}C, or some sixty degrees higher than that reported for poly(1-butene carbonate) of 9 ^{o}C.[16] It is also of interest to compare the effect of adding methyl substituents to the copolymer backbone chain on the T_g. This is illustrated below where the T_g values increases from 18 ^{o}C for poly(ethylene carbonate) to 36 ^{o}C for poly(propylene carbonate).[70,71] Upon addition of a second methyl group in poly(2-butene carbonate) the T_g increases by about 30 ^{o}C.

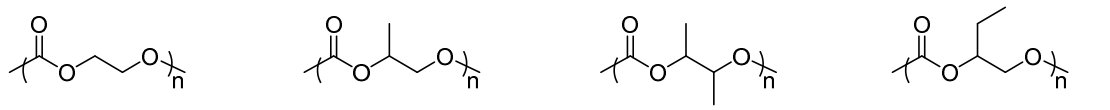

poly(ethylene carbonate) T_g = 18 ^{o}C

poly(propylene carbonate) T_g = 36 ^{o}C

poly(2-butene carbonate) T_g = 68 ^{o}C

poly(1-butene carbonate) T_g = 9 ^{o}C

As is apparent in Table 5, entries 1 and 5, catalytic runs at 70 ^{o}C utilizing catalysts **14** and **13** resulted in formation of copolymers of greatly different molecular weights. That is, the chromium derivative (**14**) afforded a polymer with a M_n value of 4.5 kDa, whereas the cobalt catalyst (**13**) yielded a polymer with M_n equals 13.9 kDa. This cannot be accounted for by the lower level of conversion for the **14** catalyst alone (55.1 vs 74.5%), and would strongly suggest that there is more adventitious water present in the chromium catalyzed process. The GPC traces are consistent with this interpretation as seen in Figure 11, where a bimodal molecular weight distribution is observed with a sizable tailing for the chain-transfer generated copolymer. On the other hand, the copolymer produced from the bifunctional cobalt catalyst displays a monomodal molecular weight distribution.

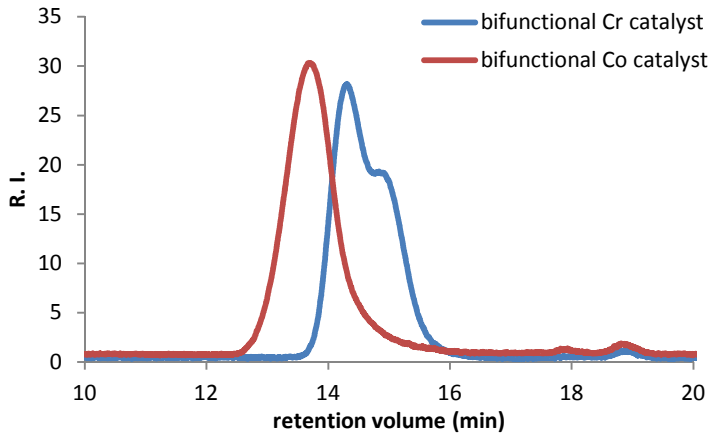

Figure 11 The GPC traces of poly(2-butene carbonate)s from Table 5 entry 1(blue) and entry 5 (red).

The ^{13}C NMR spectrum of poly(2-butene carbonate) in the carbonate region exhibits several overlapping peaks indicative of an atactic polymer (Figure 12). That is, there was no stereoselectivity in the epoxide ring-opening step, utilizing stereospecific catalysts with either *R,R*- or *S,S*-cyclohexylene diamine backbones. A catalytic run employing a mixture version of the catalyst (Table 5, entry 6) which was less effective, provided a copolymer with the same ^{13}C NMR spectrum as that shown in Figure 12a. The complex ^{13}C NMR spectrum in the methine carbon region of poly(2-butene carbonate) is also provided in Figure 12b.

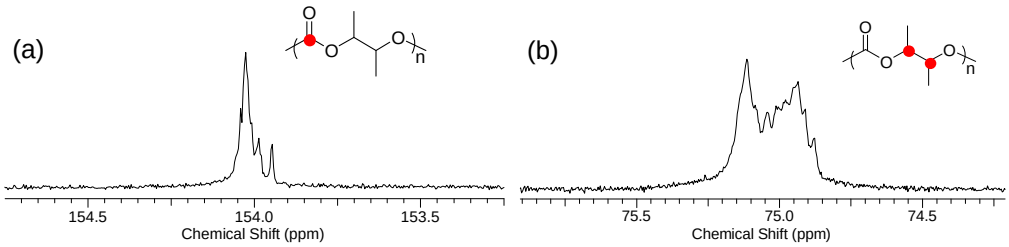

Figure 12 ^{13}C NMR spectrum of (a) the carbonate carbon and (b) the methine carbon of poly(2-butene carbonate) from Table 5 entry 2.

In studies addressing the synthesis of cyclic carbonates from *trans*-2-butene oxide and CO_2 catalyzed by iron(III) amino triphenolate complexes, Kleij and coworker have prepared both *cis* and *trans* cyclic butene carbonate in different ratio depending on reaction conditions.[72] These researchers demonstrated that with higher cocatalyst loading and higher reaction temperatures, more trans butene carbonate was formed, e.g., a [cocat]/[Fe] = 2.5, the product was mostly the trans carbonate. In the work presented herein, catalyzed by chromium salen complex bearing one chloride with two equivalent $PPNN_3$ cocatalyst, *trans* cyclic butene carbonate was also the dominant product from *trans*-2-butene oxide and CO_2. At 40 and 60 ^oC, no *cis* butene carbonate was observed, with the *cis* butene carbonate observed at 80 ^oC, in very low yield (1.4 %). On the other hand, coupling of *cis*-2-butene oxide and CO_2 gave both *cis* and *trans* cyclic carbonates in addition to poly(2-butene carbonate) (Scheme 10). Interestingly, when catalyzed by the binary Cr catalyst **1**, the major product was *cis* cyclic carbonate, but with the more polymer selective bifunctional catalysts **13** and **14** (Table 5, entries 1, 5, 6), the cyclic carbonates generated were all of the *trans* form. These observations indicated that with binary Cr salen catalyst **1**, carbonate back-biting dominated, resulting in *cis* cyclic carbonate (Scheme 11), and the leaving group could be either the polymeric alkoxide or the initiator, azide or chloride. On the contrary, alkoxide back-biting, which generates *trans* cyclic carbonate, was the only process observed with bifunctional catalysts. Depolymerization of poly(2-butene carbonate) by Cr catalyst **1** gave only trans cyclic butene carbonate (Scheme 12). This observation is consistent with back-biting of the alkoxide polymer chain end group to yield *trans* butene carbonate and explained the

selective production of the *trans* cyclic carbonate product from reaction catalyzed by **13** and **14** which were selective for copolymer formation. Unlike the result reported by Kleij and coworkers, temperature did not have a significant effect on the cis/trans ratio (Table 6), but affected the polymer selectivity as expected, i.e. higher temperature resulted in lower polymer selectivity. In addition, at 60 ^{o}C, increasing the CO_2 pressure gave higher polymer selectivity and more trans cyclic carbonate (Table 6, entries 4-6). The data in Table 6 are represented as a bar graph in Figure 13.

Table 6 Binary chromium salen complex **1** catalyzed coupling of CO_2 and *cis*-2-butene oxide at different temperature.[a]

Entry	Temp (^{o}C)	Time (h)	Conv[b] (%)	*Cis* BC (%)	*Trans* BC (%)	Polymer selectivity (%)
1	30	72	39.7	80.1	19.9	33.7
2	40	12	9.2	85.6	14.4	28.2
3	40	20	45.8	80.0	20.0	22.3
4	60	12	57.3	72.8	27.2	15.2
5	60[c]	12	80.6	76.0	24.0	0.0
6	60[d]	12	70.1	65.6	34.4	13.6
7	60	20	97.9	77.2	22.8	0.0
8	70	20	> 99	85.4	14.6	0.0
9	80	12	98.6	83.4	16.6	0.0

[a].CO_2 20 bar, monomer/catalyst = 1000/1. [b].Conversion of *cis* and *trans* butene carbonate and poly(2-butene carbonate). Determined by NMR. [c].CO_2 10 bar. [d].CO_2 30 bar.

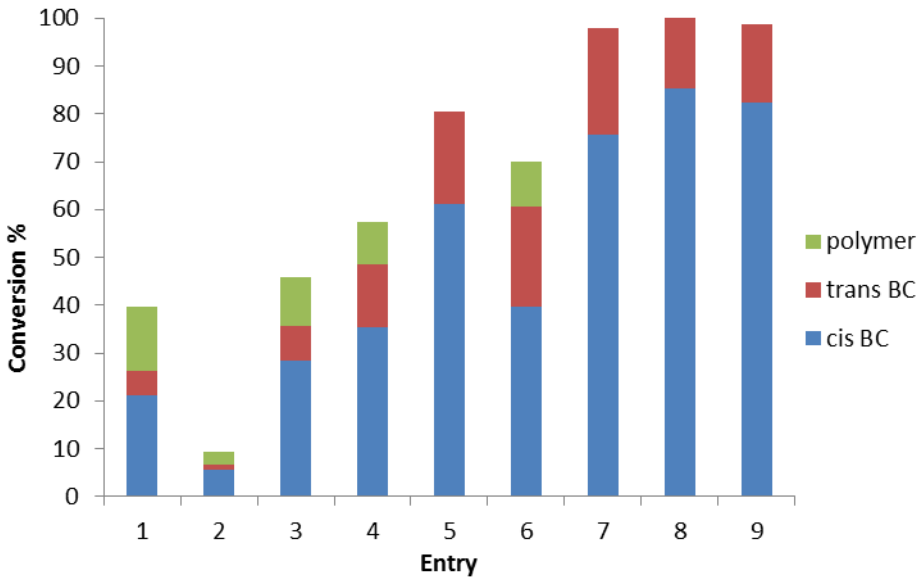

Figure 13 Conversion of *cis*-2-butene oxide to different products in the presence of catalyst **1**.

Scheme 11 Back-biting from alkoxide and carbonate to form *trans*-butene carbonate and cis butene carbonate, respectively.

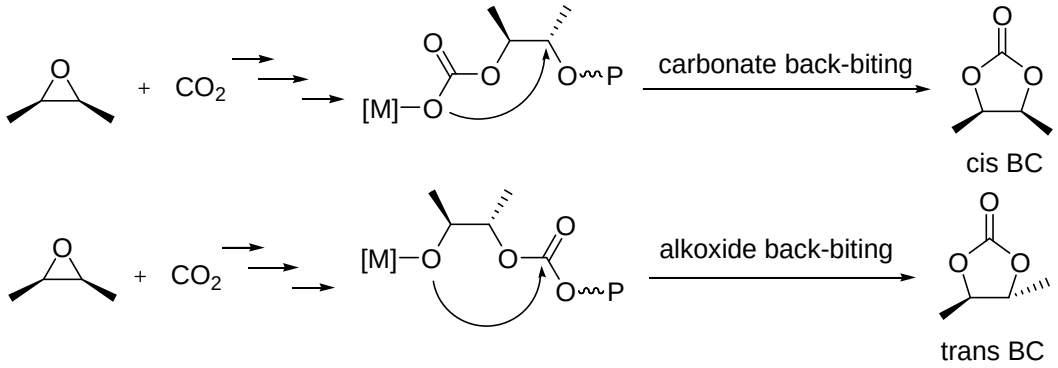

Scheme 12 Depolymerization of poly(2-butene carbonate) by **1** at 110 °C.

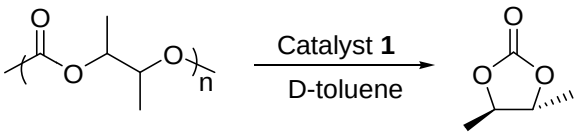

Experimental Section

General information

All manipulations involving air- and/or water-sensitive compounds were carried out in a glove box under an argon atmosphere. *Cis*-2-butene oxide (Alfa Aesar), *trans*-2-butene oxide (Alfa Aesar), isobutene oxide (Alfa Aesar) and 2,3-epoxy-2-methylbutane (Alfa Aesar) were stirred over CaH_2, distilled, and stored in an argon-filled glovebox. Research Grade 99.999% carbon dioxide supplied in a high-pressure cylinder and equipped with a liquid dip tube was purchased from Airgas. The CO_2 was further purified by passing through two steel columns packed with 4 Å molecular sieves that had been dried under vacuum at $\geq$ 200 ^{o}C. High pressure stainless steel reactors were previous dried at 170 ^{o}C for 6 h.

Representative coupling reaction of cis-2-butene oxide and CO_2

The coupling reactions of the four epoxides and CO_2 were carried out in a similar manner utilizing either binary or bifunctional catalysts **1**, **2**, **13**, **14**. For example, 9.1 mg of the cobalt catalyst **2** (11.5 μmol, 1 eq), 8.3 mg of PPNDNP (11.5 μmol, 1 eq) and 0.50 mL of *cis*-2-butene oxide (5.73 mmol or 500 eq) were charged in a 12 mL stainless steel autoclave reactor. The following loading were employed for binary chromium catalyst **1**, epoxide/Cr/cocatalyst = 500/1/2, and for bifunctional catalysts **13** and **14**, epoxide/catalyst = 1000/1. The reactor was pressurized to slightly less than 2.0 MPa and heated to the desired temperature in an oil bath with magnetic stirring. After the required reaction time, the reactor was cooled to 0 ^{o}C, depressurized, and a ^{1}H NMR spectrum of

the crude reaction mixture was obtained. The crude reaction mixture was dissolved in CH_2Cl_2 and added to about 1M HCl/methanol solution to quench the reaction and precipitate any copolymer formed. The supernatant HCl/methanol solution was removed and the polymer precipitate was re-dissolved in dichloromethane and reprecipitated from methanol. The resulting copolymer was obtained by removing the supernatant and subsequently dried in vacuo at 40 ^{o}C for further analysis by GPC and DSC.

Conclusion

This study has focused on the use of binary and bifunctional chromium and cobalt salen catalysts for the coupling of CO_2 and di-substituted epoxides to provide either copolymers and/or cyclic carbonates. Herein, we have reported that among the di-substituted epoxides, **E1** – **E3**, isobutene oxide (**E3**) bearing two methyl substituents on the same carbon center was the least reactive. Furthermore, between *cis*- and *trans*-2-butene oxides (**E1** and **E2**, respectively), the *cis* isomer was more active. This is consistent with the nucleophile being less hindered by the methyl group on the adjacent carbon during the epoxide ring-opening step. *Only cis-2-butene oxide was selective in the coupling to CO_2 to produce polycarbonates*, with the other epoxides affording the corresponding cyclic carbonates. The tri-substituted 2,3-epoxy-2-methylbutane was unreactive under the conditions of this investigation, consistent with the low reactivity of the epoxide obtainable from a renewable resource, limonene oxide (**E5**), with CO_2.[73] The production of *cis*- or *trans*-cyclic carbonate from *cis*-2-butene oxide and carbon dioxide was found to be highly dependent on the catalyst as well as the reaction

conditions, with binary catalysts favoring formation of the *cis* isomer and bifunctional catalysts showing a high preference for the *trans* isomer. The copolymer produced from *cis*-2-butene oxide and CO_2 has a T_g of 68 ^oC, which is 30 ^oC higher than that of polypropylene carbonate. Further, this glass transition temperature is 60 degrees higher than the T_g of poly(1-butene carbonate). In addition, poly(2-butene carbonate) is also less resistant to changes in shape than polypropylene carbonate, exhibiting a fracture strain value of approximately 3.0 compared to 9.0 for polypropylene carbonate.[74]

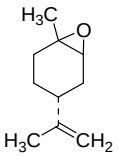

E5

CHAPTER IV

CATALYTIC COUPLING OF CYCLOPENTENE OXIDE AND CO_2 UTILIZING BIFUNCTIONAL (SALEN)C_O(III) AND (SALEN)C_r(III) CATALYSTS: COMPARATIVE PROCESSES INVOLVING BINARY (SALEN)C_r(III) ANALOGS*

Introduction

The coupling of carbon dioxide and oxiranes (epoxides) to afford either linear polycarbonates or five-membered cyclic carbonates represents encouraging technologies for CO_2 utilization (eq. 12).[2] Of importance, these processes designed for carbon dioxide capture and utilization (CCU) involve carboxylation reactions which are less energy intensive than CO_2 reduction processes.[75] Each of these processes have the potential for significantly contributing to a sustainable chemical industry. The selectivity of the reaction depicted in equation one for linear or cyclic product can presently be tuned by the appropriate selection of catalyst and/or reaction conditions. Until recently, cyclohexene oxide has been the oxiranes monomer of choice by researchers for nearly every catalyst screening for the copolymerization process. That is, researchers have typically used this cyclic ether monomer as a benchmark in order to demonstrate the viability of their catalyst for the CO_2/epoxide copolymerization reaction.

*Reproduced in part with permission from: "Catalytic Coupling of Cyclopentene Oxide and CO_2 Utilizing Bifunctional (salen)Co(III) and (salen)Cr(III) Catalysts: Comparative Processes Involving Binary (salen)Cr(III) Analogs." Darensbourg, D. J.; Chung, W.-C.; Wilson, S. J. *ACS Catal.* **2013**, *3*, 3050. Copyright 2013. American Chemical Society. Results of the coupling reaction by binary chromium salen catalyst mentioned here for comparison is from Stephanie Wilson and was included in her dissertation.

Cyclohexene oxide is an inexpensive, easy to handle material that yields high selectivity for polycarbonate over cyclic carbonate for most catalyst systems under a broad range of reaction conditions. As such, many researchers have incorrectly generalized their catalyst's high selectivity for production of poly(cyclohexene carbonate) to be translatable to all other potential monomers.

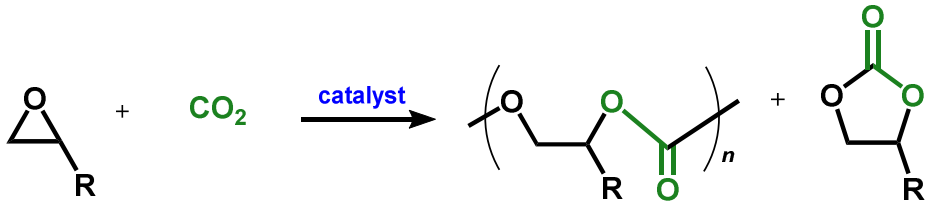

(eq. 12)

Computational studies have shown this low preference for carbonate chain-end backbiting to produce cyclohexene carbonate in this instance is due to the linear polycarbonate having to undergo an endergonic conformational change (*chair to boat*) of 4.7 kcal-mol^{-1} before traversing the activation barrier of 21.1 kcal-mol^{-1} for cyclic carbonate formation.[76] Thus, this high selectivity for copolymer formation is not necessarily typical even for all alicyclic oxiranes. Indeed, the product selectivity for the coupling of CO_2 with cyclohexene oxide and cyclopentene oxide with (salen)CrCl and an onium salt catalyst system is starkly different, though the monomers differ by only one methylene group.[76-78] Herein, we have shown that cyclohexene oxide and CO_2 will combine to form poly(cyclohexene carbonate) with 99% selectivity (< 1% *trans*-cyclohexene carbonate byproduct), cyclopentene oxide and CO_2 will instead form *cis*-cyclopentene carbonate with 100% selectivity (Scheme 13).

Scheme 13

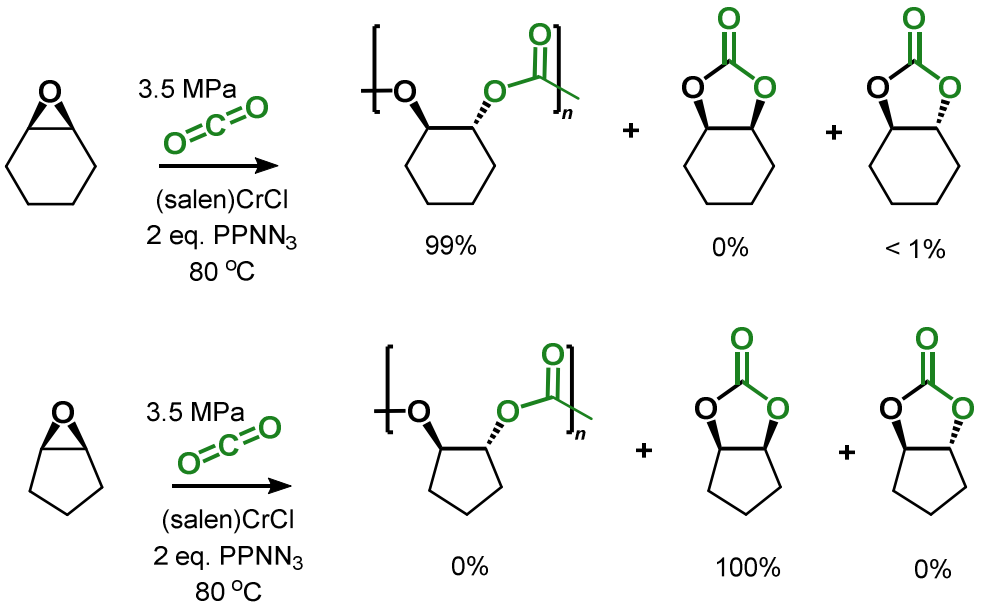

There are a few published reports for the production of poly(cyclopentene carbonate) from the completely alternating copolymerization of cyclopentene oxide and CO_2 involving zinc-based catalysts.[69,79,80] Recently, Lu and co-workers have published the successful synthesis of *isotactic* poly(cyclopentene carbonate) employing chiral dinuclear cobalt(III) complexes as catalysts.[34] Because of the significant improvements in catalytic activity, we and others have experienced using bifunctional (salen)Co(III) catalysts for selectively providing copolymers over cyclic carbonates, we choose to investigate herein the preparation of poly(cyclopentene carbonate) utilizing these catalyst systems.[12,36,68] Lu and coworkers have shown that bifunctional catalysts such as illustrated in Figure 14 exhibit a larger difference in the energies of activation for cyclic *vs* copolymer formation than their binary (salen)Co(III)/onium salt counterparts.[13]

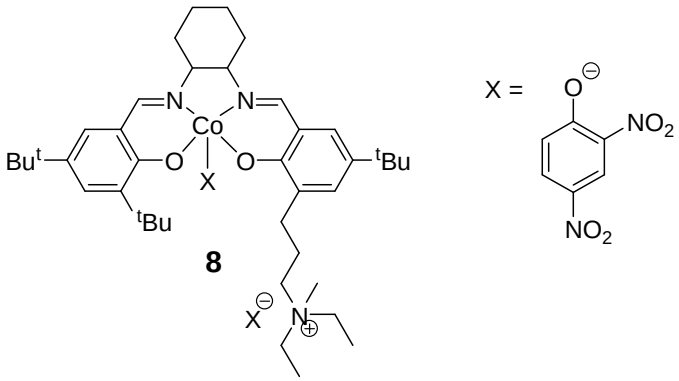

Figure 14 Asymmetric bifunctional (salen)Co(III) catalyst developed by Lu and coworkers.[13]

An added interest in developing good synthetic methods for the preparation of poly(cyclopentene carbonate) stems from the fact that this copolymer can be easily depolymerized to its monomers, cyclopentene oxide and CO_2.[77,78] Although most polycarbonates derived from carbon dioxide and epoxides can be degraded to their corresponding cyclic carbonate, copolymers capable of undergoing depolymerization which lead to a regeneration of their monomers represent the ideal method for recycling these materials. Indeed, depolymerization pathways of this type greatly enhance the sustainability of the process.

Results and Discussion

As noted earlier in Scheme 13, comparative coupling reactions of cyclohexene oxide/CO_2 and cyclopentene oxide/CO_2 were carried out in the presence of (salen)CrCl and two equivalents of $PPNN_3$ at 80 ^oC and 3.5 MPa. The preformed (salen)Cr(III) complex under these reaction conditions is anionic, containing two azide ligands.[63] The

reactions were monitored by *in situ* infrared spectroscopy in the carbonate stretching region as depicted in Figure 15 This study clearly contracts the two processes, with cyclohexene oxide/CO_2 coupling highly favoring copolymer formation, and cyclopentene oxide/CO_2 coupling leading exclusively to cyclic carbonate production.

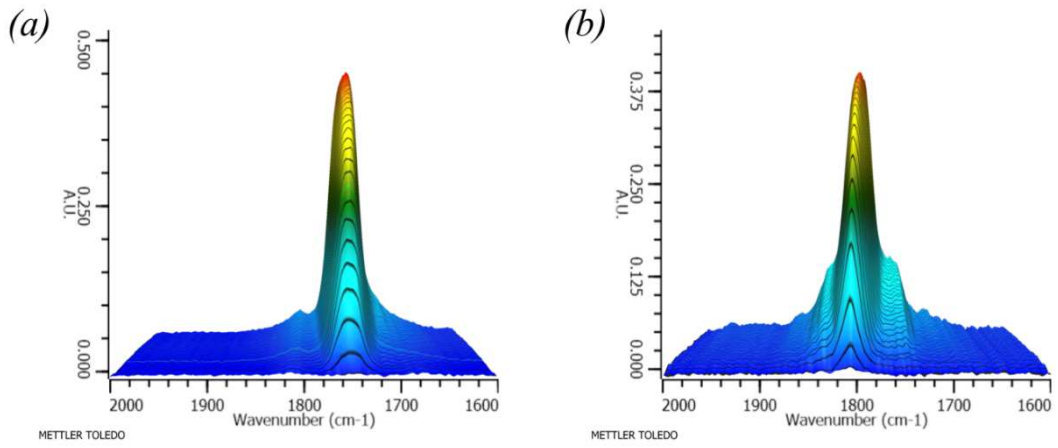

Figure 15 Product growth traces for the coupling of the alicyclic epoxides (CHO and CPO) and CO_2 utilizing *in situ* ATR-FTIR spectroscopy. *(a)* 99% selective PCHC growth at 1750 cm^{-1} and < 1% *trans*-CHC at 1810 cm^{-1} as confirmed by ^1H NMR. *(b)* 100% selectivity for CPC at 1804 cm^{-1} as confirmed by ^1H NMR. Reaction conditions: 500 eq. epoxide (15 mL), 1 eq. (salen)CrCl, 2 eq. $PPNN_3$, 3.4 MPa CO_2, 80 ^oC, 3 hours.

In a separate series of experiments, the catalytic coupling of cyclopentene oxide and CO_2 to afford *cis*-cyclopentene carbonate using (salen)CrCl and *n*-Bu_4NCl was monitored by *in situ* infrared spectroscopy at several temperatures. The observed rate constants (k_{obsd}) found in Table 7 were determined from plots of $\ln[(A_i-A_t)/A_i]$ versus time in seconds, where A_i is the absorbance of cyclic carbonate at time = infinity and A_t is the absorbance of cyclic carbonate at 1804 cm^{-1} at time = t (Figure 16). The activation

energy, E_A, of the coupling reaction was determined from the slope of the corresponding Arrhenius plot (Figure 17). The direct coupling of cyclopentene oxide and CO_2 to form *cis*-cyclopentene carbonate utilizing (salen)CrCl has an activation barrier of 72.9 ± 5.2 kJ/mol. The *cis*-nature of the product was confirmed both by ^{1}H NMR and X-ray diffraction analysis of single crystals grown from the final product mixture (Figure 18). Separate attempts were made to produce *trans*-cyclopentene carbonate from *trans*-1,2-cyclopentanediol and ethyl chloroformate, but these were unsuccessful. This is due to the extreme angle strain at the bridgehead carbons linking the fused 5-membered rings.[76,78] *Trans*-isomers are possible for the corresponding trithiocarbonate, however.[77,81,82]

Table 7 Observed rate constants for the coupling of cyclopentene oxide and CO_2 to afford *cis*-cyclopentene carbonate.[a]

Temperature (^{o}C)	**k_{obsd} x 10^5 (s^{-1})**
43.0	5.80
53.0	12.8
63.0	23.5
73.0	63.8

[a]CPO: (salen)CrCl: *n*-Bu_4NCl equals 500:1:2 in the absence of added solvent at 3.5 MPa CO_2 pressure.

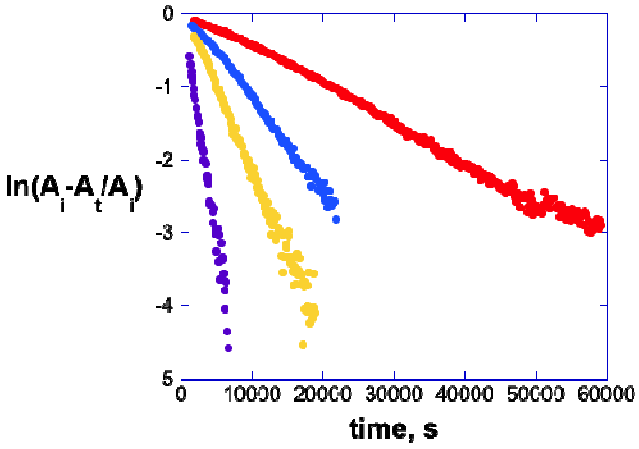

Figure 16 Kinetic plots of $\ln[(A_i-A_t)/A_t]$ vs. time for *cis*-cyclopentene carbonate production. Red (43.0 ^{o}C), Blue (53.0 ^{o}C), Yellow (63.0 ^{o}C), and Purple (73.0 ^{o}C).

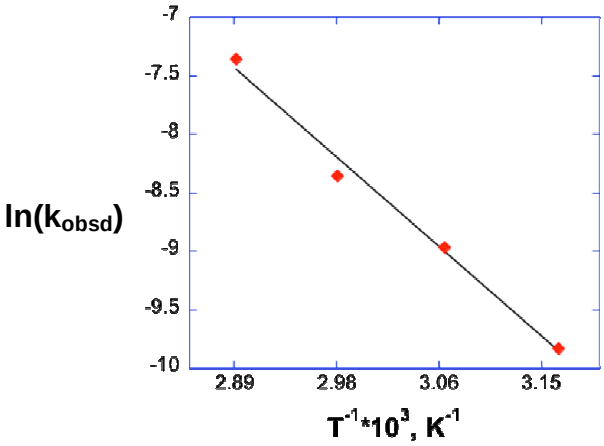

Figure 17 Arrhenius plot of *cis*-cyclopentene carbonate production in the presence of (salen)CrCl/*n*-Bu_4NCl. $R^2 = 0.989$.

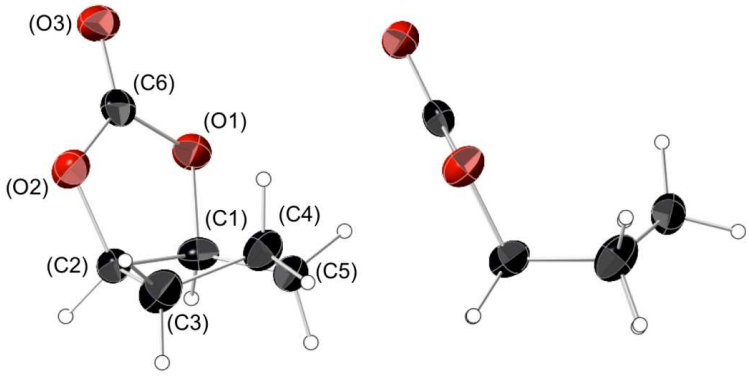

Figure 18 Thermal ellipsoid representation of *cis*-cyclopentene carbonate with ellipsoids at 50% probability surfaces. At right, looking down the plane created by C2-C1-C3-C5 to show the near-planarity of the cyclic carbonate ring (O1-C1-C2-O2 = 0.347^{o}).

The reaction pathway for the formation of cyclopentene carbonate in the presence of CO_2 (3.5 MPa) is proposed to proceed *via* backbiting by a free carbonate end group following epoxide ring-opening by chloride and carboxylation (eq. 13). This pathway is most likely since *no* copolymer chain growth was observed during cyclic carbonate formation. Furthermore, it has been shown by experimental and computational studies that the activation barrier for the backbiting process involving the carbonate polymer chain end is significantly higher than that for the process illustrated in equation 13.[76,78] High level *ab initio* calculations reveal this pathway to have a $\Delta G^{\ddagger}$ of 57.3 kJ/mol which is consistent with the activation energy measured herein when considering the positive entropy of activation expected for the process in equation 13.

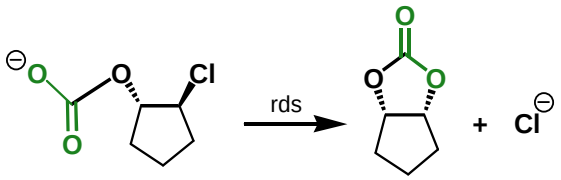

(eq. 13)

By way of contrast, we have initiated studies utilizing the bifunctional (salen)Cr(III) analog of the binary system used in the preceding coupling reaction of cyclopentene oxide and CO_2. The (salen)Cr(III) complex (**15**) depicted in Figure 19 was shown to be selective for copolymer formation even at elevated temperatures. Although we have not optimized the reaction conditions, for a five hour reaction of cyclopentene oxide and 2.0 MPa CO_2 at 100 ^oC, the TOF for copolymer production was 50.3 h^{-1} with 94.3% selectivity. For an epoxide:catalyst loading of 1000/1, the afforded poly(cyclopentene carbonate) following 25.1% conversion displayed a M_n of 11900 with a PDI of 1.10.

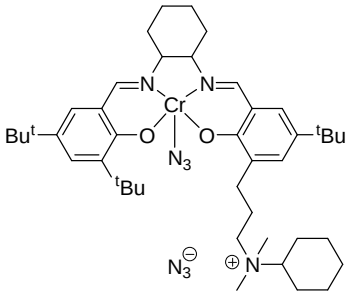

Figure 19 Asymmetric bifunctional (*R*,*R*)-(salen)CrN_3 catalyst, **15**.

The bifunctional (salen)Cr(III) catalyst system shown in Figure 19 shows the azide anion ion-paired with the ammonium cation. Unfortunately, we have thus far been

unable to obtain single crystals for X-ray structural analysis, however, the solution structure clearly indicates the azide ion is bound to the chromium center, similar to what is observed in the binary catalyst system in both the solid-state and in weakly interacting solvents.[63] That is, the infrared spectrum in dichloromethane of complex **15**, like its binary analog complex **1**, was shown to have *no* free azide band at 2000 cm^{-1} and metal bound azide bands at 2044 cm^{-1} with a shoulder at 2060 cm^{-1} as illustrated in Figure 20. This is an important observation, for it indicates the metal is the preferred site for anion binding, where, during the polymerization reaction, the anion is the growing polymer chain. Furthermore, the infrared spectra of complex **15** and **1** (shown in Figure 21) in pure cyclopentene oxide clearly show that under identical reaction conditions, the initial azide epoxide ring-opening step is faster in the binary catalytic process. It is important to note, however, that this step is not rate limiting in the coopolymerization process, which is, in the presence of high CO_2 pressures, ring-opening of the metal bound epoxide by the growing polymeric carbonate chain.

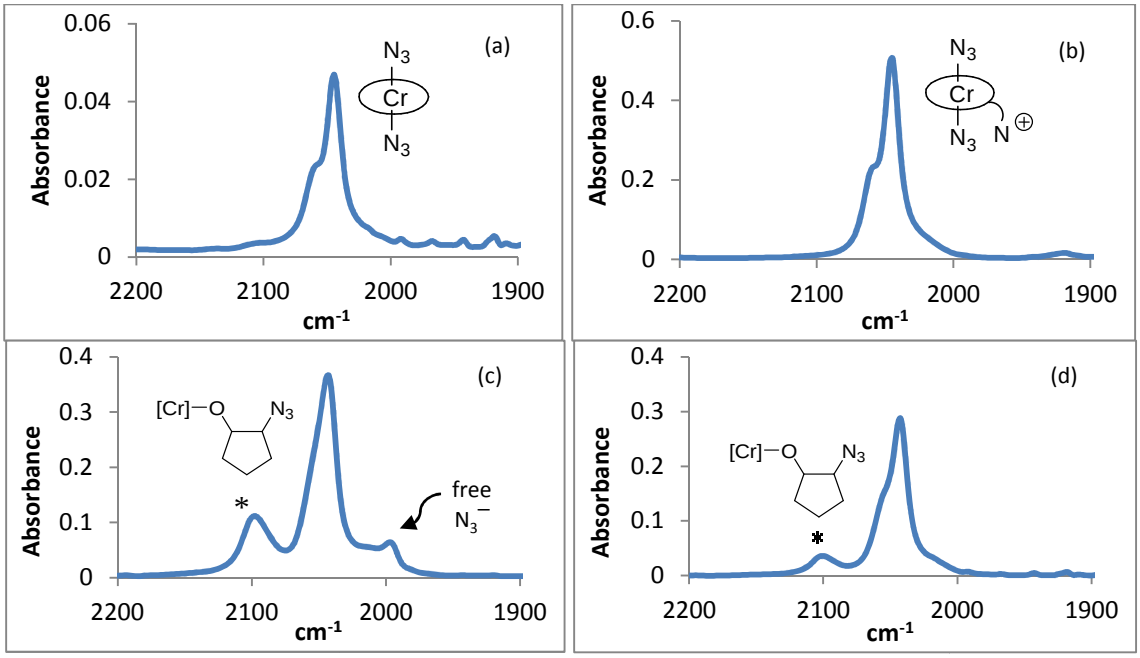

Figure 20 IR spectra of (a) binary *bis*-azide chromium catalyst **1** in dichloromethane, (b) bifunctional chromium catalyst **15** in dichloromethane, (c) binary *bis*-azide chromium catalyst **1** in cyclopentene oxide after 40 minutes at ambient temperature and (d) bifunctional chromium complex **15** in cyclopentene oxide after 40 minutes at ambient temperature. The asterisk (*) in (c) and (d) represents the ν_{N_3} vibration in the ring-opened epoxide.

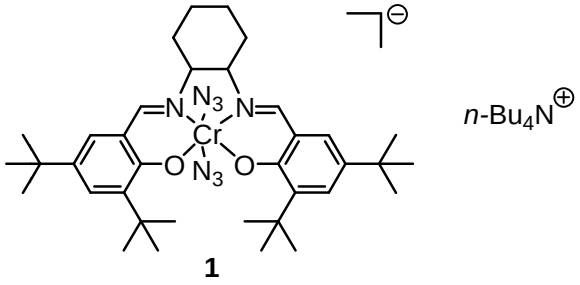

1

Figure 21 Binary (*R*,*R*)-(salen)CrN_3/*n*-Bu_4NN_3 catalyst system.

As anticipated, based on copolymerization studies involving other epoxides, the (*R*,*R*)-cobalt(III) analog of the bifunctional chromium(III) catalyst, complex **16**, was

found to be significantly more active for selective production of copolymer from cyclopentene oxide and CO_2 than complex **15**.[2i] For example, for a five hour reaction carried out at 70 ^oC and 2.0 MPa, the corresponding TOFs were 56.5 *vs* 2.20 h^{-1} (Table 8 and 9). Table 8 lists the effects of temperature, CO_2 pressure, reaction time, and catalyst loading for the copolymerization of cyclopentene oxide and CO_2 in the presence of complex **16** (eq. 14). As noted in Table 2, upon increasing the reaction temperature from 40 to 70 ^oC (*entries 1-3*), the catalytic activity increased along with the molecular weight of the copolymer. However, a further increase in temperature to 100 ^oC (*entry 4*) led to a significant decrease in catalytic activity, concomitantly with a decrease in selectivity for copolymer production (62% selectivity), as compared with > 99% selectivity at the lower temperatures. The drop in reactivity is the result of catalyst instability at this elevated temperature. Although there is a slight increase in copolymer production with increasing CO_2 pressure (*entries 5-7*), clearly the process can be performed successfully at a modest pressure of 1.0 MPa with little loss in activity. There was good molecular weight control as indicated in *entries 3, 8,* and *9* where an increase in reaction time led to an increase in % conversion and corresponding M_n values. Furthermore, albeit the copolymers exhibited a bimodal molecular weight distribution (Figure 22), the measured molecular weights were not grossly different from those calculated based on each cobalt center averaging two polymer chains. Additionally, a decrease in catalyst loading (*entries 7-10*) had no negative effect on TOFs or M_n and PDI. The T_g of the high molecular weight copolymer (*entry 9*) was found to be 84.5 ^oC, considerably lower than the 116 ^oC value reported for its cyclohexene oxide derived

analog.[83] The ^{13}C NMR spectrum of the synthesized poly(cyclopentene carbonate) is shown in Figure 23, indicative of an atactic copolymer as previously reported by Lu and coworkers utilizing similar catalysts.[34]

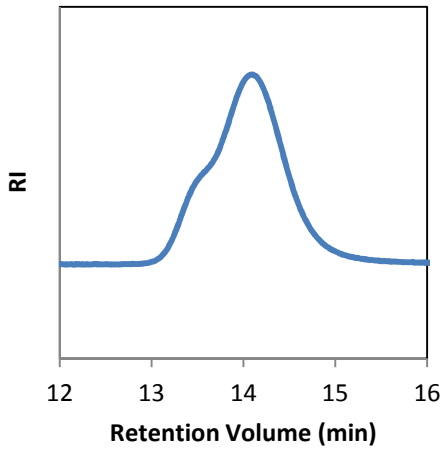

Figure 22 GPC trace of poly(cyclopentene carbonate) from Table 8, *entry 9*. Deconvolution of the two overlapping peaks revealed the smaller peak to account for 10% of the total area.

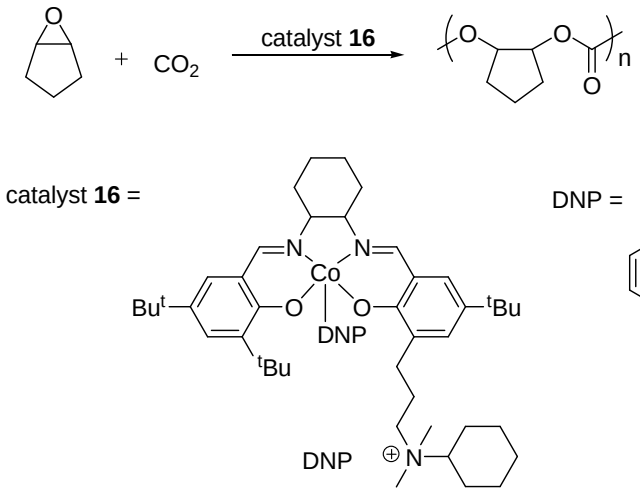

(eq. 14)

Table 8 Effects of variables on the copolymerization of cyclopentene oxide and CO_2.[a]

Entry	Temp (^oC)	Pressure (MPa)	Time (h)	Conv. (%)	TOF (h^{-1})	M_n[b] (Da)	PDI
1	40	2.0	5	9.43	18.9	5680 (6035)	1.04
2	50	2.0	5	20.9	41.8	9380 (13376)	1.10
3	70	2.0	5	28.2	56.5	19300 (18048)	1.10
4	100	2.0	5	10.8	21.6	7410 (10432)	1.20
5	70	1.0	5	30.5	61.0	17620 (19520)	1.08
6	70	1.5	5	28.0	56.0	15250 (17920)	1.13
7	70	2.5	5	36.8	73.5	20450 (23552)	1.06
8	70	2.0	2	21.6	108	12220 (13824)	1.06
9	70	2.0	10	44.1	44.1	27000 (28224)	1.05
10	70	2.0	5	18.3	73.3[c]	18100 (23424)	1.06

[a] Catalyzed by catalyst **15**.Catalyst loading = 1000/1. Polycarbonate selectivity over cyclic carbonate for all entries is >99% except for entry 4 which is 62%. [b]Theoretical values provided in parentheses. [c]Catalyst loading = 2000/1.

For comparative purposes, we have examined the coupling of cyclopentene oxide and CO_2 with various catalyst systems under similar reaction conditions. These are tabulated in Table 9, where complexes **13** and **8** are illustrated in Figure 24. As seen in *entries 3-5*, the bifunctional chromium catalyst (**15**) is thermally more stable than complex **16**, maintaining good catalytic activity at 120 ^oC. Nevertheless, as would be expected, there is a loss in copolymer selectivity at this elevated temperature. Finally, it is noted, as previously reported, that there is a correlation between the bulkiness of the

ligand tethered ammonium ion and catalytic activity (*entries 1*, *6*, and *7*), with greater steric bulk leading to greater reactivity.[36]

Table 9 Coupling of cyclopentene oxide and CO_2 catalyzed by different bifunctional catalysts.[a]

Entry	catalyst	temp (^oC)	conv (%)[b]	TOF (h^{-1})[b,c]	M_n[d]	PDI[d]	polymer selectivity (%)[b,e]
1	**16**	70	28.2	56.5	19300	1.10	> 99
2	**15**	70	1.1	2.2	N/A	N/A	> 99
3	**15**	100	25.1	50.3	11900(16064)[f]	1.10	94.3
4[g]	**15**	100	19.4	38.8	8550	1.13	92.6
5	**15**	120	26.7	53.5	15400	1.16	75.8
6	**13**	70	38.3	76.6	18500	1.12	88.5
7	**8**	70	0.3	0.6	N/A	N/A	> 99

[a]CPO/catalyst = 1000/1, CO_2 2.0 MPa. [b]Determined by ^1H NMR. [c]Moles of CPO converted/moles of catalyst/time. [d]Determined by GPC. [e]Polycarbonate/(polycarbonate + cyclic carbonate). [f]Calculated value. [g]CO_2 1.5 MPa.

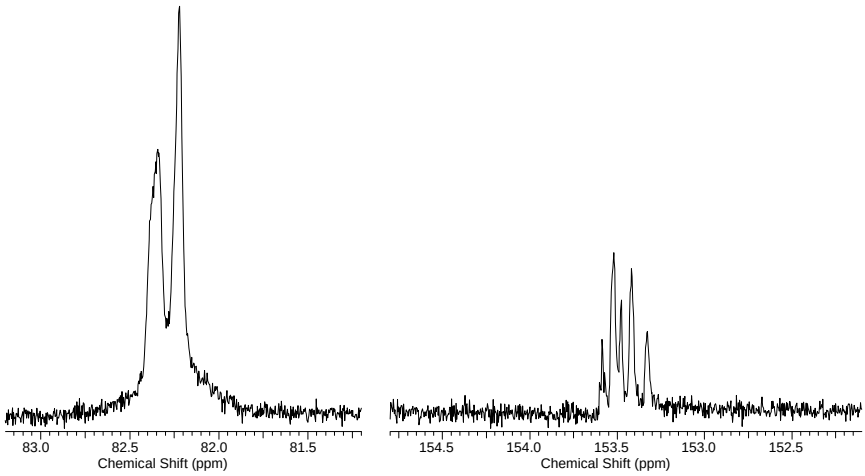

Figure 23 ^{13}C NMR spectrum of poly(cyclopentene carbonate) from Table 8, *entry 9*. Methine region (left) and carbonate region (right).

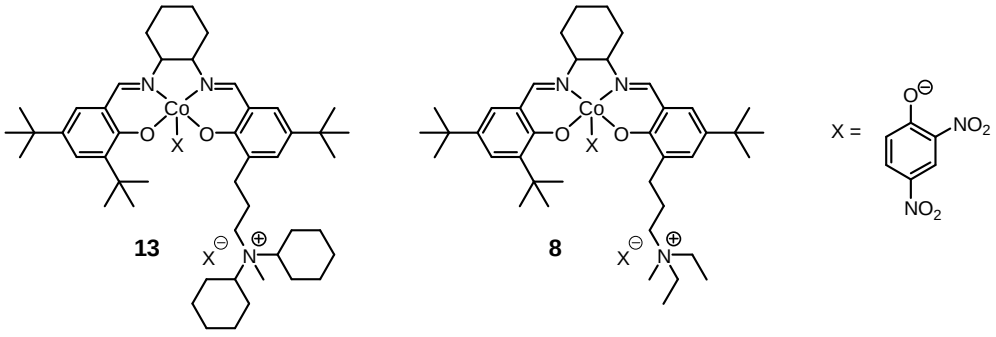

Figure 24 Asymmetric bifunctional (salen)Co(III) catalysts developed by Lu and coworkers.[13]

Experimental Section

General information

All manipulations involving air- and/or water-sensitive compounds were carried out in a glove box under an argon atmosphere or with standard Schlenk techniques under

dry nitrogen. Toluene was distilled from sodium/benzophenone and stored in an argon-filled glovebox. Cyclopentene oxide (GL Biochem (Shanghai), Ltd.) was stirred over CaH_2, distilled, and stored in an argon-filled glovebox. Tetra-*n*-butylammonium chloride (Aldrich) was recrystallized from acetone/diethyl either before use and stored in an argon-filled glovebox. *(R,R)-N,N'*-bis(3,5-di-*tert*-butylsalicylidene)-1,2-cyclohexanediaminochromium(III) chloride, (salen)CrCl, was purchased from Strem, stored in an argon-filled glovebox, and used as received. Research Grade 99.999% carbon dioxide supplied in a high-pressure cylinder and equipped with a liquid dip tube was purchased from Airgas. The CO_2 was further purified by passing through two steel columns packed with 4 Å molecular sieves that had been dried under vacuum at ≥ 200 ^{o}C. High pressure reaction monitoring measurements were performed using an ASI ReactIR 1000 reaction analysis system with a 300 mL stainless steel Parr autoclave modified with a permanently mounted ATR crystal (SiComp) at the bottom of the reactor (purchased from Mettler Toledo). Infrared spectra were recorded on a Bruker Tensor 37 spectrometer in CaF_2 solution cells with a 0.1 mm path length.

X-ray crystal study

For the crystal structure of *cis*-cyclopentene carbonate, a Bausch and Lomb 10× microscope was used to identify suitable crystals. A single crystal sample was coated in mineral oil, affixed to a Nylon loop, and placed under streaming N_2 (110 K) in a single-crystal APEXii CCD or Bruker GADDS/Histar diffractometer. X-ray diffraction data were collected by covering a hemisphere of space upon combination of three sets of

exposures. The structure was solved by direct methods. H atoms were placed at idealized positions and refined with fixed isotropic displacement parameters and anisotropic displacement parameters were employed for all non-hydrogen atoms. The following programs were used: for data collection and cell refinement, APEX2;[84a] data reductions, SAINTPLUS, version 6.63; [84b] absorption correction, SADABS; [84c] structure solutions, SHELXS-97; [84d] structure refinement, SHELXL-97. [84e]

Synthesis of bifunctional catalysts

Asymmetric salen ligands (**L1**). Asymmetric bifunctional ligand **L1** was synthesized following the literature.[17] However, instead of bearing two cyclohexyl groups and one methyl group on ammonium, the ligand obtained had one cyclohexyl group and two methyl groups. In the deprotection step to convert methoxyl group to hydroxyl group on the phenyl ring using BBr_3, one cyclohexyl group on amine was shown to be replaced by hydrogen, making a secondary amine as outlined below. In the following formylation step, this secondary amine reacted with formaldehyde and underwent reductive amination to give a tertiary amine with one methyl group and one cyclohexyl group. ^{1}H NMR (300 MHz, $CDCl_3$): δ 8.34 (s, 1H), 8.29 (s, 1H), 7.32 (d, 1H, J = 3 Hz), 7.18 (d, 1H, J = 3 Hz), 7.07 (d, 1H, J = 3 Hz), 7.00 (d, 1H, J = 3 Hz), 3.52 (m. 3H), 3.29-2.41 (m, 2H), 3.24 (s, 3H), 3.19 (s, 3H), 2.72 (m, 2H), 2.09 (m, 4H), 1.89 (m, 6H), 1.75-1.63 (m, 4H), 1.40 (br s, 15H), 1.24 (s, 9H), 1.22 (s, 9H) ppm. ^{13}C NMR (75 MHz, $CDCl_3$): δ 165.54, 165.17, 157.96, 141.40, 140.06, 136.54, 130.40, 126.86, 126.81, 126.12, 126.10, 125.82, 72.91, 72.28, 71.77, 62.22, 48.94, 34.96, 34.07, 33.91, 33.50,

32.98, 31.44, 31.37, 29.37, 27.32, 26.29, 25.18, 24.61, 24.31, 24.17, 22.27 ppm. MS for(**L1**-I^-): m/z = 658.5011.

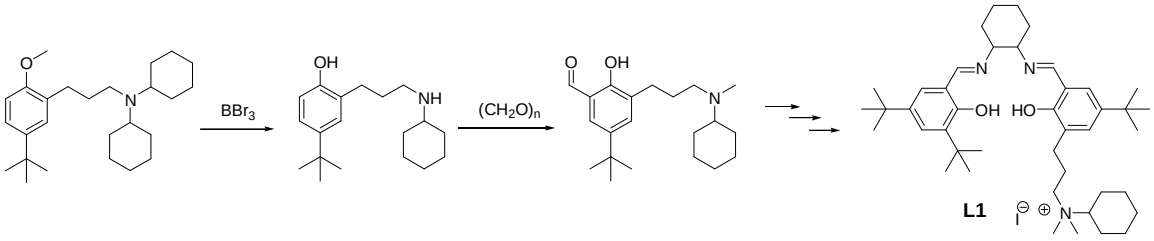

Bifunctional chromium catalyst **15.** Bifunctional chromium catalyst **15** was synthesized via a modified literature procedure.[85] 103 mg of ligand **L1** (0.131 mmol, 1 eq.) and 19.5 mg chromium(II) chloride (0.158 mmol, 1.2 eq.) were dissolved in THF and stirred for one day under Ar and another day under air. After being washed by NH_4Cl and NaCl aqueous solution, the reaction mixture was dried, redissolved in acetonitrile and transferred to a Schlenk flask charged with 51.4 mg $AgBF_4$ (0.263 mmol, 2 eq.). After one day stirring in the dark, the reaction mixture was filtered into another Schlenk flask with 51.4 mg sodium azide (0.788 mmol, 6 eq.) and stirred for one day. Subsequently, the solvent was removed *in vacuo* and the mixture was redissolved in dichloromethane. After being washed by NaCl aqueous solution, the solvent was removed *in vacuo* overnight affording 61.3 mg chromium catalyst **15** (0.0773 mmol, 58.8 % yield). MS for (**15**-N_3^-): m/z = 750.4571, for (**15**-2(N_3^-)): m/z = 354.2231. Anal. Calc. for $C_6H_8O_3$: C, 65.1; H, 8.39. Found: C, 64.33; H, 8.38.

Bifunctional cobalt catalyst **16.** This complex was synthesized following the literature procedure starting from 29.6 mg of cobalt(II) acetate (0.165 mmol, 1.3 eq) and

99.9 mg of **L1** (0.127 mmol, 1 eq). The yield of complex **16** was 81.9 mg (0.0757 mmol) or 59.5%.

Coupling of cyclopentene oxide and CO_2 using binary chromium catalyst

72.5 mg (salen)CrCl (114.7 μmol) and 133.4 mg $PPNN_3$ (229.2 μmol, 2 eq.) were charged in a vial, dissolved in dry CH_2Cl_2, and allowed to stir at room temperature under argon for ~30 minutes in order to activate the catalyst. The solvent was thoroughly removed *in vacuo*, and the vial was charged with 15.0 mL dry cyclopentene oxide (171.9 mmol, 1500 eq.). The homogeneous solution was cannulated into a 300 mL stainless steel autoclave with a permanently mounted SiComp crystal. The reactor was pressurized with 3.4 MPa CO_2 and heated to 80 ^{o}C. The course of the reaction was monitored for 3 hours. The system was cooled to room temperature, depressurized, and both ^{1}H NMR and FT-IR spectra were obtained of the crude reaction mixture. 56% conversion to *cis*-cyclopentene carbonate was observed from ^{1}H NMR.

Cis-cyclopentene carbonate

Following the completion of the coupling of CPO and CO_2, the mixture was concentrated *in vacuo*, redissolved in dichloromethane, and passed through a short column of silica gel in order to remove residual catalyst and cocatalyst. Clear, slightly colored crystals were grown from slow evaporation of the resulting solution. ^{1}H NMR (300 MHz, $CDCl_3$): δ 3.39 (s, 2H), 1.94 (dd, 2H, J = 5.1, 7.8 Hz), 1.45-1.54 (m, 3H), 1.23-1.34 (m, 1H) ppm. ^{13}C NMR (125 MHz, $CDCl_3$): δ 155.6, 82.0, 33.2, 21.6 ppm.

FT-IR ν_{CO3}1796 cm^{-1} (CH_2Cl_2); 1838sh, 1807 cm^{-1} (C_7H_8). Anal. Calc. for $C_6H_8O_3$: C, 56.24; H, 6.29. Found: C, 56.22; H, 6.15.

Coupling of cyclohexene oxide and CO_2

62.5 mg (salen)CrCl (98.8 μmol) and 115.0 mg $PPNN_3$ (197.7 μmol, 2 eq.) were charged in a vial, dissolved in dry CH_2Cl_2, and allowed to stir at room temperature under argon for ~30 minutes in order to activate the catalyst. The solvent was thoroughly removed *in vacuo*, and the vial was charged with 15.0 mL dry cyclohexene oxide (148.3 mmol, 1500 eq.). The homogeneous solution was cannulated into a 300 mL stainless steel autoclave with a permanently mounted SiComp crystal. The reactor was pressurized with 3.4 MPa CO_2 and heated to 80 ^oC. The course of the reaction was monitored for 3 hours. The system was cooled to room temperature, depressurized, and both ^1H NMR and FT-IR spectra were obtained of the crude reaction mixture. 64% conversion to poly(cyclohexene carbonate), 0.7% conversion to *trans*-cyclohexene carbonate, 0.2% ether linkages was observable from ^1H NMR.

Poly(cyclohexene carbonate)

The crude reaction mixture from the coupling of CHO and CO_2 was added dropwise to acidified methanol (~5% HCl). The off-white polymer precipitate was collected by filtration, redissolved in dichloromethane, and reprecipiated using the same method. The resulting white solid was dried under vacuum with heating. ^1H NMR (300 MHz, $CDCl_3$): δ 4.64 (br s, 2H), 2.10 (br s, 2H), 1.70 (br s, 2H), 1.23-1.55 (br m, 4H)

ppm. ^{13}C NMR (75 MHz, $CDCl_3$): broad peaks centered at δ 153.4, 29.5, 22.8 ppm. FT-IR ν_{CO3} 1850 (CH_2Cl_2); 1851 (C_7H_8). Anal. Calc. for $(C_7H_{10}O_3)_n$: C, 59.14; H, 7.09. Found: C, 59.21; H, 7.09.

Kinetic measurements for the direct coupling of cyclopentene oxide and CO_2 utilizing (salen)CrCl/n-Bu4NCl

In an argon-filled glovebox, 90.2 mg (salen)CrCl (0.142 mmol), 79.3 mg *n*-Bu_4NCl (0.285 mol, 2 eq), 6.00 g cyclopentene oxide (71.3 mmol, 500 eq), and 5.22 g toluene (6 mL) were charged into a vial. The reactants were cannulated into a 300 mL stainless steel Parr autoclave modified with a permanently mounted ATR crystal (SiComp) at the bottom of the reactor. This initial mixture served as the background signal for the measurements. CO_2 (3.4 MPa) was charged into the system, and the reactor was heated to the desired temperature (43, 53, 63, 73 ^oC). Infrared spectra were taken periodically throughout the course of the reaction, and the reaction's progress was monitored through the growth of cyclic carbonate peak at 1804 cm^{-1}. No activity was ever observed at 1750 cm^{-1}, indicating that polymer formation did not take place or was not appreciable. The reaction was followed to 100% completion.

Coupling of cyclopentene oxide and CO_2 utilizing bifunctional catalysts

The copolymerization reactions of cyclopentene oxide and CO_2 were carried out in a similar manner utilizing either of the metal complexes **1, 2, 15 or 16** as catalyst. For example, 6.2 mg of the bifunction cobalt catalyst **2** (5.7 μmol) and 0.50 mL of

cyclopentene oxide (5.77 mmol or 1000 eq) were charged in a 12 mL stainless steel autoclave reactor which had previously been dried at 170 ^{o}C for six hours. The reactor was pressurized to the appropriate pressure (1.0 – 2.5 MPa) and heated to the desired temperature in an oil bath with magnetic stirring. After the required reaction time, the reactor was cooled to 0 ^{o}C, depressurized, and a ^{1}H NMR spectrum of the crude reaction mixture was obtained.

Poly(cyclopentene carbonate)

The crude reaction mixture from coupling of cyclopentene oxide and CO_2 was dissolved in CH_2Cl_2 and added to about 1 M HCl/methanol solution to quench the reaction and precipitate the copolymer. The supernatant HCl/methanol solution was removed and the polymer precipitate was re-dissolved in dichloromethane and reprecipitated from methanol. The resulting copolymer was obtained by removing the supernatant and subsequently dried *in vacuo* at 50 ^{o}C for further analysis by GPC and DSC. ^{1}H NMR (300 MHz, $CDCl_3$): δ5.00 (br s, 2H), 2.13 (br s, 2H), 1.84-1.77 (br m, 4H). ^{13}C NMR (75 MHz, $CDCl_3$): δ153.5, 82.3, 30.0, 21.2 ppm.

Conclusion

Herein we have successfully prepared high molecular weight poly(cyclopentene carbonate) from the completely alternating copolymerization of cyclopentene oxide and carbon dioxide utilizing bifunctional (salen)M(III) catalysts (M = Cr, Co). The copolymers were synthesized in a very selective manner with little to no production of

cyclic carbonate byproduct. By way of contrast, it was demonstrated that, whereas under identical reaction conditions (80 ^{o}C/3.5 MPa) in the presence of the binary (salen)CrN_3/$PPNN_3$ catalyst system, the coupling of cyclohexene oxide and CO_2 produces poly(cyclohexene carbonate) with > 99% selectivity, the corresponding reaction of the alicyclic cyclopentene oxide and CO_2 affords > 99% selectivity for *cis*-cyclopentene carbonate. This cyclic carbonate was structurally characterized by X-ray crystallography. Kinetic studies for *cis*-cyclopentene carbonate formation revealed an activation energy of 72.9 ± 5.2 kJ/mol proceeding *via* backbiting of the anionic carbonate species generated in the initial epoxide ring-opening process subsequent to carboxylation, consistent with theoretical predictions.

For reactions carried out at 70 ^{o}C employing the bifunctional Co(III) catalyst in 0.1% catalyst loading at 2.0 MPa CO_2 pressure, 44% conversion to poly(cyclopentene carbonate) occurred within 10 hours leading to a copolymer with a M_n value of 27,000 (PDI = 1.05). Although the analogous chromium catalyst is less active, it is thermally more stable and hence coupling reactions can be carried out at higher temperatures while maintaining a high selectivity for copolymer production. The T_g of the resulting atactic poly(cyclopentene carbonate) was determined to be 84.5 ^{o}C. Importantly, these polycarbonates have been shown to be depolymerized to their comonomers, cyclopentene oxide and CO_2, thereby making their production from epoxide and CO_2 sustainable.

CHAPTER V

COPOLYMERIZATION AND CYCLOADDITION PRODUCTS DERIVED FROM COUPLING REACTIONS OF 1,2-EPOXY-4-CYCLOHEXENE AND CO_2. POSTPOLYMERIZATION FUNCTIONALIZATION VIA THIOL−ENE CLICK REACTIONS*

Introduction

There are numerous reports involving a wide variety of metal catalysts of the coupling of cyclohexene oxide and carbon dioxide to selectively provide copolymer as opposed to the alternative, thermodynamically more stable cyclic carbonate product.[2] The propensity of the cyclohexene oxide/CO_2 coupling reaction to afford copolymer *vs* cyclic carbonate results from the high activation barrier for cyclic carbonate production in this instance.[5,86] As a result of this reactivity pattern, this epoxide monomer is most often the subject of catalytic studies of this process. At the same time, poly(cyclohexene carbonate) is a brittle, hydrophobic polymer which has thus far found limited applications. An epoxide monomer which has some features in common with cyclohexene oxide, 1,2-epoxy-4-cyclohexene (**E6**), provides reactivity which allows for postfunctionalization of the derived copolymer with CO_2.[87] This can be achieved by the thiol-ene click reaction (Scheme 14).[21,48,88-90] Of further importance, the self-metathesis

*Reproduced in part with permission from: "Copolymerization and Cycloaddition Products Derived from Coupling Reactions of 1,2-Epoxy-4-cyclohexene and Carbon Dioxide. Postpolymerization Functionalization via Thiol-ene Click Reactions." Darensbourg, D. J.; Chung, W.-C.; Arp, C. J.; Tsai, F.-T.; Kyran, S. J. *Macromolecule.* **2014**, *47*, 7347. Copyright 2014. American Chemical Society.

of some polyunsaturated fatty acids derived from plant oils provides 1,4-cyclohexadiene as a waste byproduct, thereby affording a renewable source of epoxide **E6**.[91]

Scheme 14

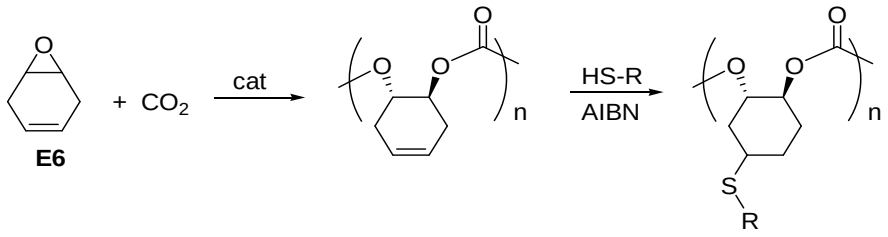

E6

Of further interest, the cyclic carbonate product (**C6**) which results from the cycloaddition of **E6** and carbon dioxide represents the *simplest* of the numerous non-macrocyclic and macrocyclic organic carbonates that originate from both plant and bacterial/fungi natural sources.[92] That is, *cis*-cyclohexadiene carbonate (**cis-C6**) is obtained from a microbial source, *Escherichia coli*, and was observed covalently bonded to a serine residue at the active stie of a (-) γ-lactamase enzyme of an *Aurebacterium* species (Figure 25).[93,94] Ethylene carbonate and propylene carbonate were also shown to be good substrates for the (-) γ-lactamase enzyme.

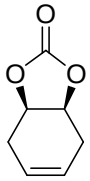

***Cis*-C6**

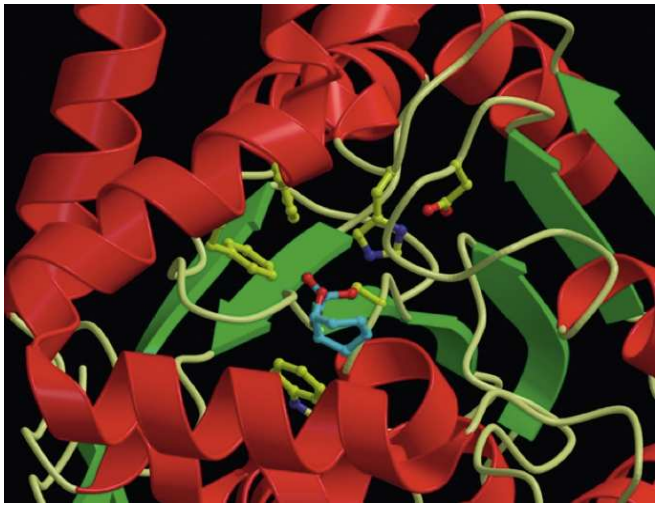

Figure 25 Ribbon diagram of the subunit of (-) γ-lactamase showing the active site cavity with the binding ligand (***cis*-C6**) in blue.[94]

In this chapter we wish to report on the chemistry outlined in Scheme 15, where the synthesis of the copolymer derived from epoxide **E6** and carbon dioxide is described. This was achieved using both binary and bifunctional (salen)Cr(III) catalysts (**1** and **14**) as well as a binary (salen)Co(III) catalyst (**2**) under solventless conditions (Figure 26). Furthermore, by way of thiol-ene coupling reactions with RSH (R = -CH_2CH_2OH and –CH_2COOH) in postfunctionalization processes, amphiphilic copolymers with a cyclohexylene backbone have been prepared. In addition, the preparation and full characterization, including an X-ray structure, of *cis*- and *trans*-cyclohexadiene carbonates are provided. These cyclic carbonates were synthesized from the corresponding diols, as well as from **E6** and CO_2. Although the details of the biosynthesis of **C6** are not presently understood, it is conceivable that it could arise *via* the cycloaddition of one of the naturally occurring cyclohexene oxides and CO_2.[95]

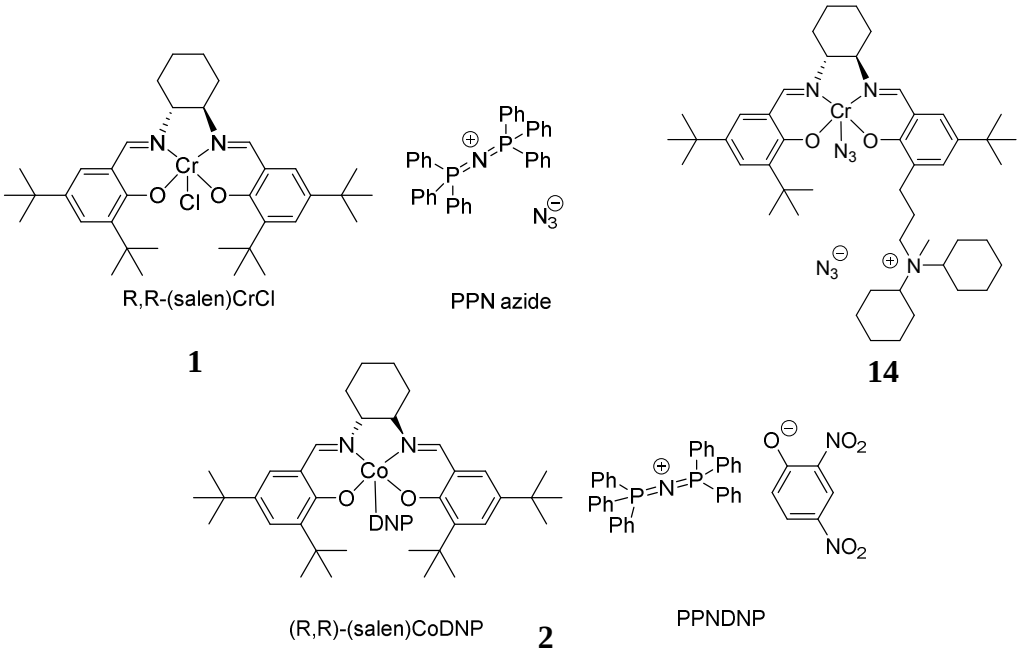

Figure 26 Binary (**1**) and bifunctional (**14**) chromium and binary cobalt (**2**) catalysts.

Scheme 15

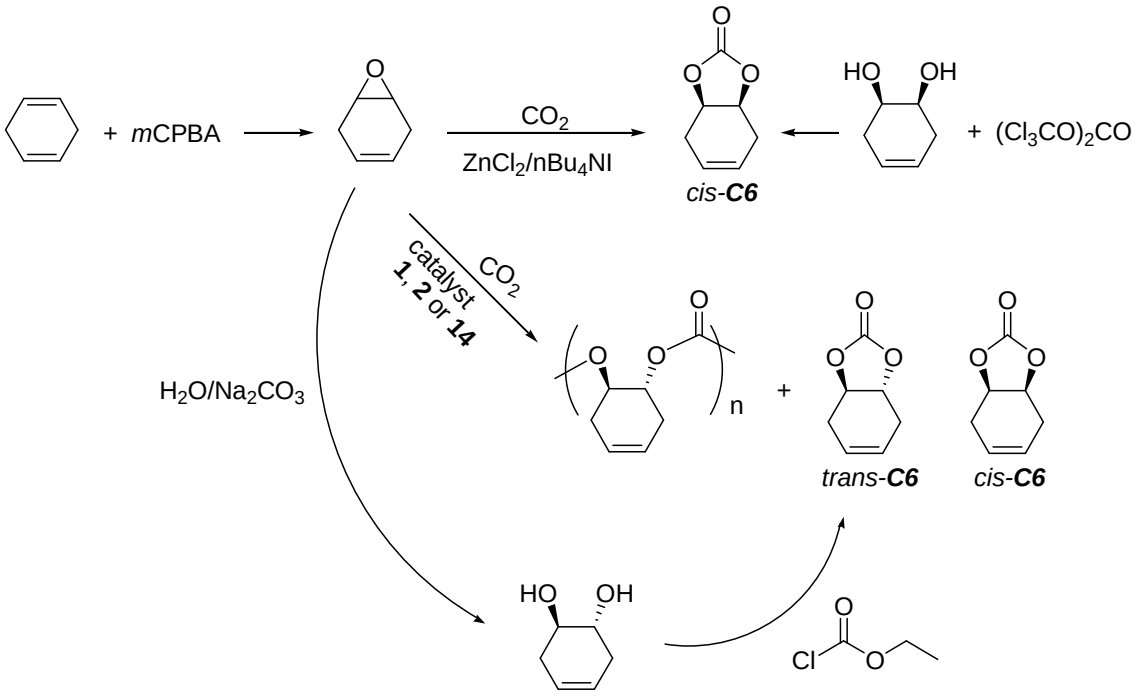

Results and Discussion

Coupling reactions of 1,4-cyclohexadiene oxide (1,4-CHDO) and carbon dioxide

Cyclohexadiene oxide was synthesized from 1,4-cyclohexadiene using *meta*-chloroperbenzoic acid (*m*CPBA) as an oxidant following the literature procedure.[96] Our initial studies were designed to synthesize the naturally occurring *cis* isomer of cyclohexadiene carbonate. To this end, we prepared 4-cyclohexene-*cis*-1,2-diol by acetylation of the diene followed by methanolysis.[97] The *cis*-diol was converted to the corresponding *cis* cyclic carbonate using triphosgene.[98] The infrared spectrum of *cis*-cyclohexadiene carbonate (*cis*-CHDC) in THF solution in the ν(C=O) region displayed a band at 1805 cm^{-1}, with a ^{13}C NMR signal at 155.0 ppm.[94] The crystal structure of *cis*-CHDC is depicted in Figure 27.[99] Alternatively, *cis*-CHDC is readily prepared *via* a greener route from CHDO and CO_2 using the $ZnCl_2$/*n*Bu_4NI catalyst system at 70 ^oC and 3.0 MPa CO_2 pressure in the absence of added solvent. This catalyzed pathway has been shown to proceed by double-inversion at the ring-opened carbon center of 1,4-CHDO.[100]

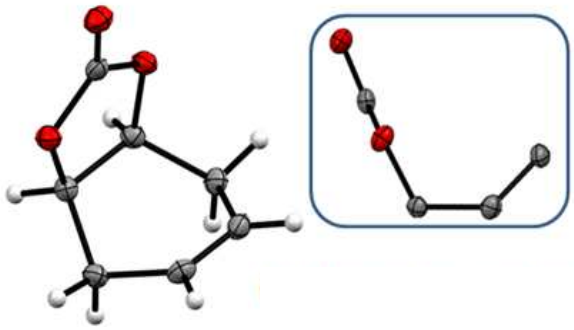

Figure 27 X-ray crystal structure of *cis*-cyclohexadiene carbonate.[99]

Because (salen)CrX complexes in the presence of onium salts have been successful for catalyzing the copolymerization of cyclohexene oxide and CO_2, catalyst (**1**) was initially chosen to investigate the copolymerization of epoxide **E6** and CO_2. As summarized in Table 10 using this catalyst afforded copolymer, along with smaller quantities of both *cis*- and *trans*-cyclohexadiene carbonate. At 90 ^{o}C and 2.0 MPa of CO_2 under solventless conditions, the conversion increased with increasing reaction time (2 – 10 hours) from 23.2 to 69.6% (entries 2-4) as would be expected for a controllable polymerization process. There was also an increase in copolymer selectivity with conversion, as well as the *trans*/*cis* cyclic carbonate ratio, eventually reaching 77.8% and 1.18, respectively. Decreasing the reaction temperature to 80 ^{o}C resulted in an increase in copolymer selectivity to 86.8% as is generally observed for these processes (entry 1). Upon employing the bifunctional chromium catalyst **14** (entry 5), the reaction proceeded more slowly, but with 100% selectivity for copolymer production. This decrease in reactivity is most likely the consequence of the steric bulk of the pendant ammonium group. In all instances, using the chromium(III) catalysts (**1** and **14**) the polymer molecular weights were less than 9000 Daltons and bimodal. The bimodality of these processes results from chain transfer reactions with water, and accounts for the enlarged PDI values noted.

Table 10 Coupling of 1,4-cyclohexadiene oxide and CO_2.[a]

Entry	Cat	Temp (°C)	Time (h)	Conv. (%)[b]	TOF (h^{-1})[b]	Polym. Selec. (%)[b,c]	M_n (kDa)	PDI	T_g (^oC)
1	**1**	80	6	35.0	58.3	86.8 (1.53)	7.6	1.2	105
2	**1**	90	2	23.2	116	48.9 (2.98)	2.1	1.1	100
3	**1**	90	5	57.0	114	36.6 (1.74)	3.8	1.1	104
4	**1**	90	10	69.6	69.6	77.8 (0.845)	8.8	1.2	104
5	**14**	90	10	9.5	9.5	> 99	3.8	1.5	n.d.
6	**2**	40	5	26.0	52.1	> 99	12.2	1.4	n.d.
7	**2**	40	20	33.9	16.9	> 99	35.9	1.5	123
8[d]	**2**	40	10	31.1	15.6	> 99	20.6	1.3	118
9[d]	**2**	r.t.	10	59.8	29.9	> 99	17.6	1.3	n.d.

[a] Reaction condition: 1,4-CHDO/Cr/$PPNN_3$ = 1000/1/2, 1,4-CHDO/Co/PPNDNP=1000/1/1, CO_2 pressure 2.0 MPa.
[b] Determined by ^1H NMR. [c] The number in the parenthesis represents the *cis*-/*trans*- CHDC ratio.
[d] 1,4-CHDO/Co = 500/1.

More importantly, upon utilizing the binary cobalt catalyst system (**2**), the copolymerization reaction could be carried out under milder reaction conditions with >99% selectivity for affording high-molecular weight copolymers. For example, at ambient temperature the copolymerization of **E6** and CO_2 selectively provided poly(cyclohexadiene carbonate) with a molecular weight (M_n) of 17.6 kDa at a TOF of 59.8 h^{-1} for a 10 hr reaction (Table 10, entry 9). It should be noted here that Williams and coworkers have shown the cobalt complex (*R*,*R*)SalcyCo(III)Cl in the presence of PPNCl to be an effective catalyst for selectively coupling **E6** and CO_2 to copolymer.[87] Consequent to increasing the catalyst loading by twofold, the conversion to copolymer remained approximately constant for a reaction performed in one-half the reaction time

(Table 10, entries 7 and 8). Furthermore, as expected for the lower catalyst loading reaction (entry 7) the molecular weight (M_n) of the copolymer was almost twice as large at 35.9 kDa *vs* 20.6 kDa. Both of these observations suggest good control of the copolymerization process. Nevertheless, based on the ambient temperature result (entry 9) *versus* those at 40 ^oC, there is clearly some catalyst degradation occurring at the higher temperature as has previously been observed.

The ^{13}C NMR spectrum of poly(cyclohexadiene carbonate) displayed two broad peaks for the carbonyl carbon indicating no stereoselectivity (Figure 28). This was further confirmed when using the *S,S*-counterpart of the binary cobalt catalyst. That is, the coupling catalyzed by the *S,S*-catalyst exhibited similar reactivity to the *R,R*-version under the same reaction conditions (TOF = 14.7 h^{-1}, M_n = 19.6 kDa, PDI = 1.3) compared to Table 10, entry 8. Relative to the structurally similar epoxide, cyclohexene oxide, under the same reaction conditions as entry 1 in Table 10, epoxide **E6** is less reactive and selective for copolymer formation (TOFs 58.3 h^{-1} *vs* 118 h^{-1} and polymer selectivity 86.8% *vs* 97.5%). The double bond of epoxide's **E6** backbone acts as a weak electron withdrawing group, thereby making **E6** slightly less basic than cyclohexene oxide which reduces its coordinating ability to the metal center and also increases the probability for backbiting to provide cyclic carbonate byproduct. However, there are structural differences between these two related epoxides which might contribute to their behavior differences. The T_g of the high molecular weight (M_n = 35.9 kDa) purified poly(cyclohexadiene carbonate) was found to be 123 ^oC with lower T_gs observed for polymers of lower molecular weights, e.g., 118 ^oC for M_n = 20.6 kDa and 104 for M_n =

8.8 kDa. The corresponding value for the completely alternating copolymer derived from cyclohexene oxide and CO_2 has been reported to be 116 ^{o}C.[85]

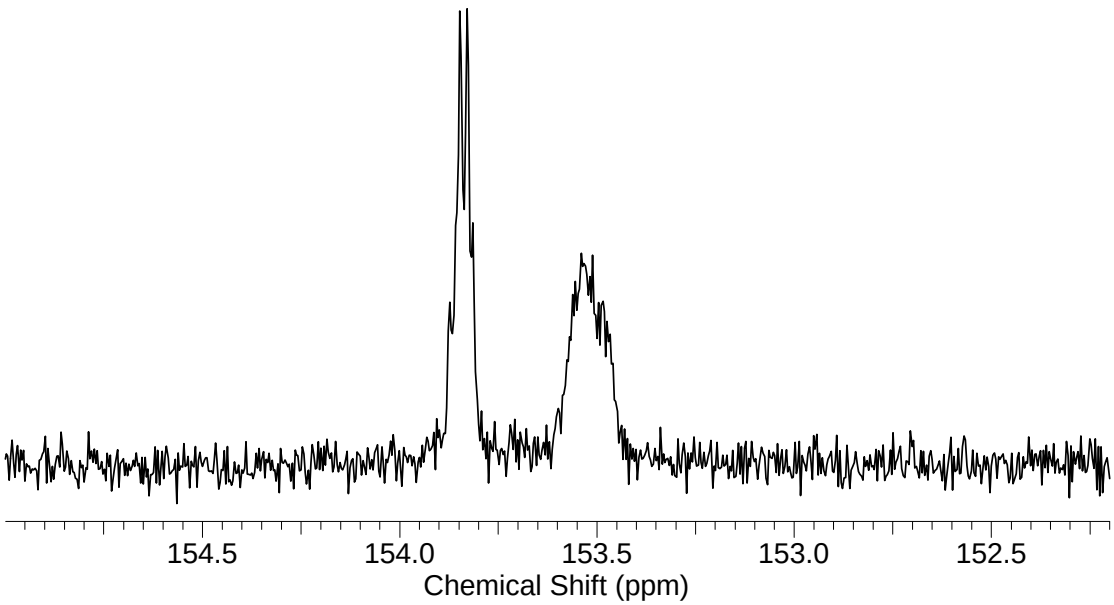

Figure 28 ^{13}C NMR spectrum in the carbonate region of poly(cyclohexadiene carbonate) in $CDCl_3$.

Depolymerization of poly(cyclohexadiene carbonate) to trans-cyclohexadiene carbonate

Of additional interest are studies of the thermal depolymerization of polycarbonates derived from epoxides and CO_2 under anaerobic conditions. In the past, we have examined numerous such processes and found them to generally occur *via* backbiting of the deprotonated copolymer chain end resulting in an unzipping of the polymer chain to provide the cyclic carbonate.[101] Herein, the depolymerization of poly(cyclohexadiene carbonate) is reported to proceed *via* a similar end-scission pathway subsequent to the hydroxyl chain end being deprotonated by the strong base

sodium bis(trimethylsilyl)amide (eq. 15). In order to stabilize these hydroxyl chain end polycarbonates towards base degradation, it is necessary to add an acetate end-group employing acetyl chloride.

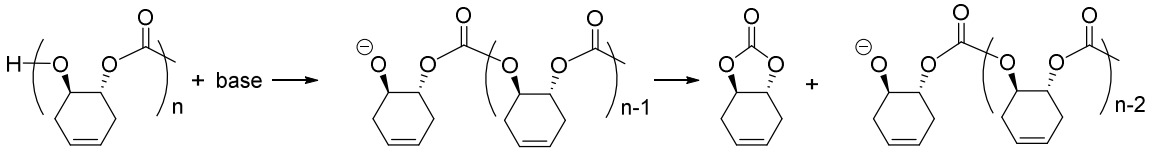

(eq. 15)

This depolymerization reaction, like that of poly(cyclohexene carbonate), proceeded slowly in toluene at 110 ^{o}C to produce exclusively *trans*-cyclohexadiene carbonate.[101] The identity of the *trans* isomer of the cyclic carbonate was confirmed by an independent synthesis of this compound as described in Scheme 15. That is, *trans*-CHDC was prepared from epoxide **E6** in two steps. First, hydrolysis of **E6** in the presence of Na_2CO_3 provided the *trans*-diol, followed by carbonylation with ethyl chloroformate to afford the *trans*-cyclic product. *Trans*-cyclohexadiene carbonate has two infrared bands in the carbonate region, while the *cis* isomer has only one (Figure 29). As illustrated in Figure 30, in the ^{1}H NMR spectra of the two isomeric forms of the cyclic carbonate, the *trans* isomer signals in the olefinic and methine regions are more upfield.

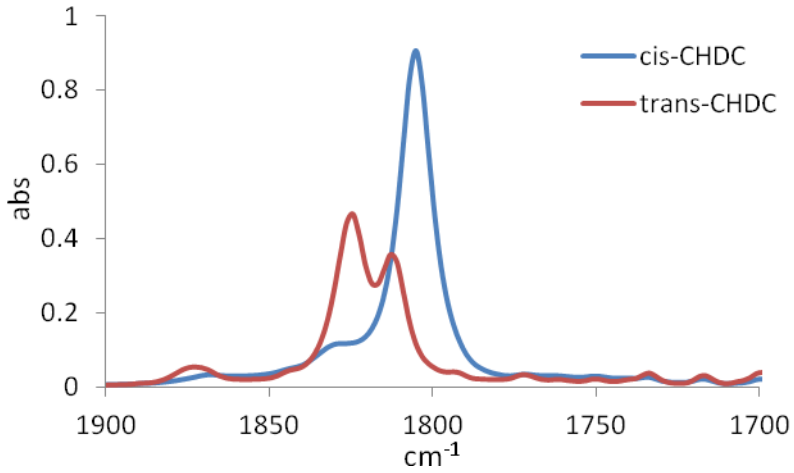

Figure 29 Infrared spectra of *cis*- (blue) and *trans*- (red) cyclohexadiene carbonate.

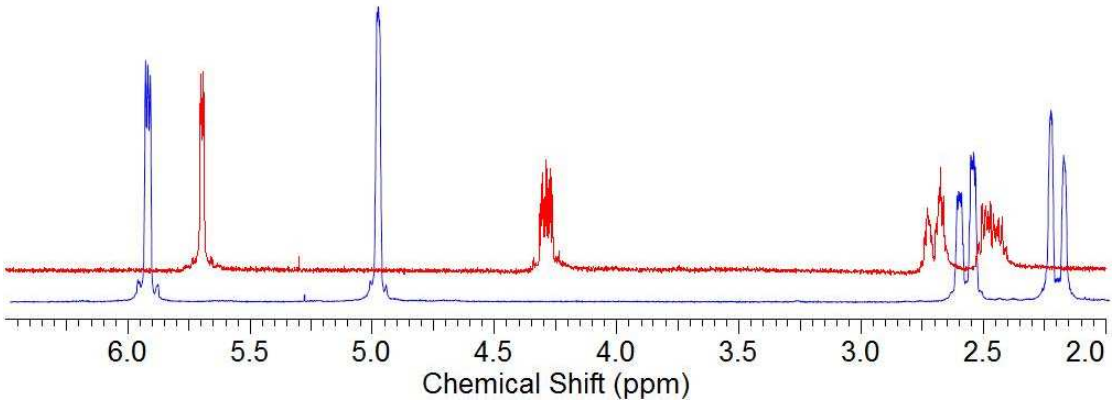

Figure 30 ^{1}H NMR spectra of *cis*- (blue) and *trans*- (red) cyclohexadiene carbonate.

Postpolymerization functionalization of poly(cyclohexadiene carbonate)

As mentioned in the introduction, the carbon-carbon unsaturated bond provides a site for modifying this hydrophobic copolymer by introducing functional groups for attaching other useful molecules, as well as providing amphiphilic or water soluble materials. Recently, Sugimoto and coworkers have chlorinated and brominated

poly(cyclohexadiene carbonate) in unsuccessful efforts to enhance its glass transition temperature.[102] Alternatively, we and others have used thiol-ene click chemistry to alter copolymer properties.[21,48,89,90] In this instance, this was achieved in a postpolymerization functionalization process of poly(cyclohexadiene carbonate) (M_n = 11.5 kDa) using the thiol, thioglycolic acid, in the presence of AIBN (azobis(isobutyronitrile)) to quantitatively afford an amphiphilic polymer (M_n = 20.9 kDa, M_n(theory) = 19.0 kDa) with a reduced T_g of 90 ^oC. Upon deprotonation of this amphiphilic copolymer with an aqueous solution of NH_4OH, a water-soluble polymer material was obtained (eq. 16). This modified copolymer was shown to be water soluble by dynamic light scattering analysis. Because of the intrinsic ionic property of the ammonium salt of this copolymer, it exhibited an enhanced T_g of 120 ^oC.

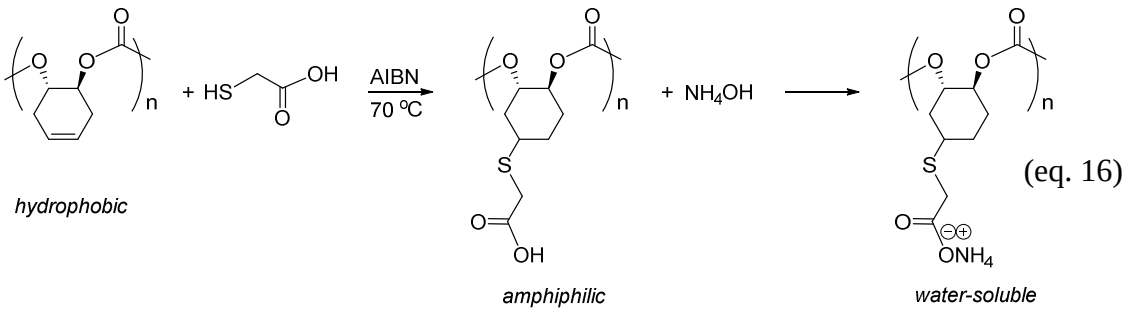

(eq. 16)

The thermogravimetric analysis traces of poly(cyclohexadiene carbonate) and its functionalized polymers are shown in Figure 31, along with the summarized data in Table 11. As seen, the functionalized polymers exhibit broader profiles. The weight loss

observed for the deprotonated polymer at about 100 °C is due to its decarboxylation. Except for this latter observation the three polymers share similar thermal stability.

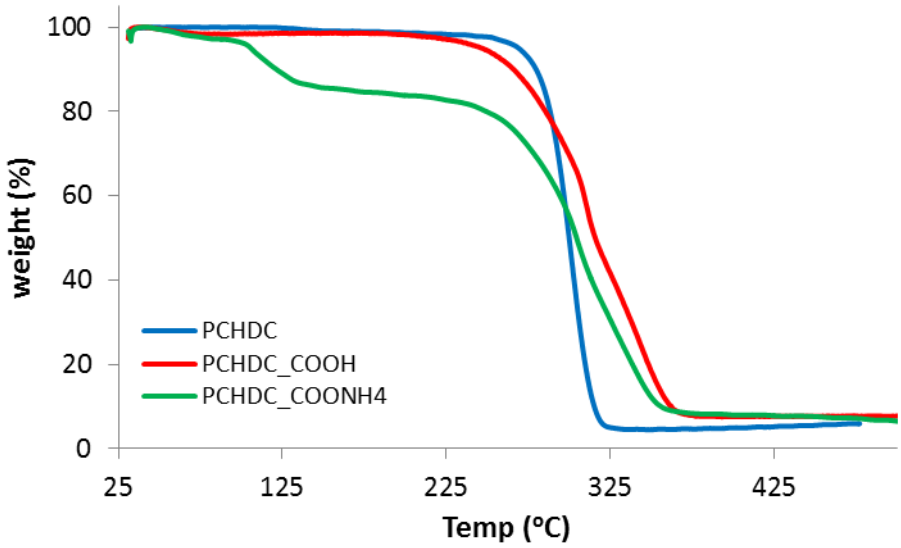

Figure 31 TGA traces for the three polymer samples.

Table 11 Summary of T_g and TGA data.[a]

polymer	T_g (°C)	T_{d5} (°C)	T_{d50} (°C)
PCHDC	116	269	300
PCHDC_COOH	90	247	316
PCHDC_$COONH_4$	120	106	305

[a]Data obtained of a PCHDC polymer of molecular weight 11.5 kDa and its functionalized derivatives.

Unfortunately, under similar reaction conditions the corresponding 2-mercaptoethanol reagent was not effective for this thiol-ene coupling process. Currently, we are examining other epoxide monomers that do not have too different reactivity ratios

for providing terpolymers with epoxide **E6**, thereby potentially affording amphiphilic/water-soluble polymeric materials with a range of thermal and physical properties.

Experimental Section

General information

All manipulations involving air- and/or water-sensitive compounds were carried out in a glove box under an argon atmosphere. 1,4-cyclohexadiene (Alfa Aesar) and *meta*-chloroperbenzoic acid (70-75%, Acros Organics) were used as received. Research grade 99.999% carbon dioxide supplied in a high-pressure cylinder and equipped with a liquid dip tube was purchased from Airgas. The CO_2 was further purified by passing through two steel columns packed with 4 A molecular sieves that had been dried under vacuum at $\geq$ 200 ^{o}C.

Measurements

Molecular weight determinations (M_n and M_w) were carried out with a Malvern Modular GPC apparatus equipped with ViscoGEL I-series columns (H+L) and Model 270 dual detector comprised of RI and light scattering detectors. Samples were weighed into a 2 mL volumetric cylinder, dissolved in THF and filtered with 0.2 μm syringe filter before injection. Glass transition temperatures (T_g) were measured using a Mettler Toledo polymer DSC. Samples (~6 mg) were weighed into 40 μL aluminum pans and subjected to two heating cycles. The first cycle covered the range from 25 to 150 °C at

10 °C/min heating rate and was cooled down to 0 °C at −10 °C/min cooling rate. The second cycle ranged from 0 ^{o}C to 150 ^{o}C at 5 ^{o}C/min heating rate and was where T_g was obtained (Figure 32). Dynamic light scattering (DLS) measurements were conducted using Delsa Nano C (Beckman Coulter, Inc., Fullerton, CA) equipped with a laser diode operating at 658 nm. All measurements were made in water (n = 1.3328, η = 0.8878 cP) at 25 ± 1 °C. The concentration of water-soluble polymer was 1 mg/mL. Scattered light was detected at 15° angle and analyzed using a log correlator over 70 accumulations for a 0.5 mL of sample in a glass size cell (0.9 mL capacity). Prior to measurement, solutions were filtered through a 0.2 μm PTFE membrane filter to remove dust particles. The photomultiplier aperture and the attenuator were automatically adjusted to obtain a photon counting rate of ca. 10 kcps. Thermogravimetric analyses were performed under an Ar atmosphere using a Mettler-Toledo model TGA/DSC1 STARe system. Sample (~6 mg) was weighed in tared aluminum pan, stabilized at 25 °C and heated to 500 °C at 10 °C/min heating rate.

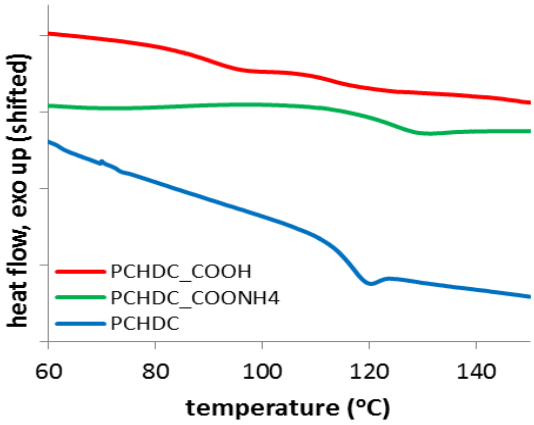

Figure 32 DSC traces of the parent poly(cyclohexadiene carbonate) (blue), and its functionalized polymer (red), along with the deprotonated analog (green).

Synthesis of 1,4-cyclohexadiene oxide[96]

To a flask charged with 20 mL 1,4-cyclohexadiene (0.21 mol, 1.06 eq.), 27.3 g $NaHCO_3$ (0.33 mol, 1.6 eq.), 160 mL H_2O, and 240 mL CH_2Cl_2 co-solvent, 46.8 g *m*CPBA (0.20 mol, 1 eq.) was added in small portions in ice bath, and the reaction mixture was allowed to warm up to ambient temperature. After stirring for 19 h, 100 mL of a saturated $Na_2S_2O_3$ aqueous solution was added and the solution was stirred for another hour. The organic layer was collected and combined with the CH_2Cl_2 extracts from the separated aqueous layer, and was further washed with saturated $NaHCO_3$ aqueous solution, dried over anhydrous Na_2SO_4 and concentrated under reduced pressure. The afforded clear liquid was further dried over CaH_2, followed by distillation under reduced pressure at 90 ^oC. The distillate was collected as colorless liquid (12.6 g, 0.13 mol, 65% yield). ^1H NMR (300 MHz, $CDCl_3$): δ 5.43 (s, 2H), 3.23 (s, 2H) and 2.49 (q, 4H) ppm. ^{13}C NMR (75 MHz, $CDCl_3$): δ 121.5, 51.0 and 24.9 ppm.

Synthesis of trans-cyclohexadiene carbonate.[103,104]

The synthesis of *trans*-CHDC involves two steps from CHDO. In the first step, cyclohexadiene oxide (0.761 g, 7.92 mmol) was added to 8 mL of 0.2 M Na_2CO_3 aqueous solution and the reaction mixture was heated to 90-100 ^oC. After 12 h the reaction was cooled down and neutralized to about pH 6 by adding HCl aqueous solution. It was then extracted with CH_2Cl_2, and the water layer was distilled to reduce water to about 3 mL, followed by CH_2Cl_2 extraction. The combined organic layers were dried over Na_2SO_4 and concentrated under reduced pressure followed by being fully dried in vacuo. 0.481 g (4.21 mmol, 53.2% yield) of white powder was obtained as the desired *trans*-diol product. In the second step, triethylamine (0.15 mL, 1.09 mmol, 2.07 eq.) was added to THF solution of *trans*-diol (60.3 mg, 0.528 mmol, 1 eq.) and ethyl chloroformate (0.1 mL, 1.06 mmol, 2 eq.) under an argon atmosphere in ice bath. The reaction was allowed to warm up to ambient temperature and stirred for 40 h. The solvent was removed under vacuum and the resultant mixture was redissolved in CH_2Cl_2 and filtered through a silica pad to purify. The eluent was concentrated and dried to afford a yellow powder (38.6 mg, 0.276 mmol, 52.2% yield) with a melting point of 128 ^oC. ^1H NMR (300 MHz, $CDCl_3$): δ 5.70 (s, 2H), 4.29 (m, 2H) and 2.59 (m, 4H) ppm. ^{13}C NMR (75 MHz, $CDCl_3$): δ 154.9, 124.2, 79.8 and 29.8 ppm. Infrared (THF): 1825, 1813 cm^{-1}.

Synthesis of cis-cyclohexadiene carbonate

$ZnCl_2$ (7.5 mg, 56 μmol, 1 eq.), *n*Bu_4NI (82.8 mg, 224 μmol, 4 eq.) and cyclohexadiene oxide (0.5 mL, 5.6 mmol, 100 eq.) were charged in a 12 mL stainless steel autoclave reactor which had been previously dried at 170 ^oC for 6 h. The reactor was pressurized to slightly less than 3.0 MPa and heated to 70 ^oC in an oil bath with magnetic stirring. After 24 h, the reactor was cooled to 0 ^oC, depressurized, and a ^1H NMR spectrum of the crude reaction mixture was taken immediately, which showed the exclusive production of the *cis*-cyclic carbonate product.

Representative coupling reaction of 1,4-cyclohexadiene oxide and CO_2

(*R*,*R*)-(salen)CrCl (3.5 mg, 5.6 μmol, 1 eq.), $PPNN_3$ (6.5 mg, 11 μmol, 2 eq.) and cyclohexadiene oxide (0.5 mL, 5.6 mmol, 1000 eq.) were charged in a 12 mL stainless steel autoclave reactor which had been previously dried at 170 ^oC for 6 h. The reactor was pressurized to slightly less than 2.0 MPa and heated to 90 ^oC in an oil bath with magnetic stirring. After 10 h, the reactor was cooled to 0 ^oC, depressurized, and a ^1H NMR spectrum of the crude reaction mixture was taken immediately. The crude reaction mixture was dissolved in CH_2Cl_2 and added to about 1M HCl/methanol solution to quench the reaction and precipitate any copolymer formed. The supernatant HCl/methanol solution was removed and the polymer precipitate was re-dissolved in dichloromethane and reprecipitated from methanol. The resulting copolymer was obtained by removing the supernatant and subsequently drying *in vacuo* at 40 ^oC for further analysis by GPC and DSC. ^1H NMR (300 MHz, $CDCl_3$): δ 5.57 (s, 2H), 4.97 (s,

2H) and 2.45 (d, 4H) ppm. ^{13}C NMR (125 MHz, $CDCl_3$): δ 153.7, 123.2, 73.3 and 29.4 ppm. Infrared (THF): 1753 cm^{-1}.

Thiol-ene click reaction between copolymer and thioglycolic acid

The procedure for synthesis of amphiphilic polymer was started with the ratio of reagents $[C=C]_o$ / $[thiol]_o$ / $[AIBN]_o$=1/40/0.8. The thiol-ene click reaction between polycarbonate (0.06 g, 0.43 mmol of C=C groups, M_n(GPC (THF)): 11.5 kDa) and thioglycolic acid (1.3 mL, 18 mmol) was conducted in a 25 mL Schlenk flask under argon atmosphere with 10 mL THF as solvent and AIBN (0.056 g, 0.34 mmol) as initiator. The reaction mixture was stirred for 24 h at 70 ^oC. After filtration, the solvent and excess thiol were removed under vacuum. The crude product was dissolved in THF and precipitated in diethyl ether. Since the conversion of the first thiol-ene coupling was around 55%, the secondary thiol-ene coupling was conducted. After removal of excess thiol and solvents, amphiphilic polymer with 100% conversion was obtained by vacuum dry. M_n(GPC(THF)): 20.9 kDa; M_n (theory): 19.0 kDa; T_g (DSC): 90 ^oC.

Deprotonation of amphiphilic polymer using aqueous ammonium hydroxide

0.9 equiv (based on mole of olefinic groups of former polycarbonate) of aqueous ammonium hydroxide (30% wt $NH_4OH_{(aq)}$) was added to a THF solution of the amphiphilic polymer dropwise *via* syringe under positive argon atmosphere. This was done to avoid the presence of unreacted reagents from contaminating the produced polymers. The reaction mixture was stirred for 5 min at ambient temperature. The

resulting suspension was filtered, and the white solid was collected and vacuum dried. Dynamic light scattering (DLS) analysis showed no hydrodynamic diameter distribution was observed in aqueous solution, demonstrating the resulting polymer could completely dissolve in water. T_g (DSC): 120 ^oC.

Conclusion

1,2-epoxy-4-cyclohexene (1,4-CHDO), which can readily be synthesized from 1,4-cyclohexadiene and *m*CPBA in good yield, was shown to be effectively coupled with carbon dioxide to either produce the *cis*-cyclic carbonate or the corresponding copolymer selectively. Product selectivity was observed to be dependent on the catalyst system utilized. That is, in the presence of $ZnCl_2$/*n*Bu_4NI, CHDO reacts with CO_2 to produce the naturally occurring *cis*-cyclohexadiene carbonate, whereas, employing (salen)Cr(III) or (salen)Co(III) derivatives along with onium salts as catalysts, selective formation of poly(cyclohexadiene carbonate) was achieved. In the case utilizing the Cr(III) derivative as catalyst, small quantities of both *cis*- and *trans*-cyclic carbonate were produced. On the other hand, the binary (salen)CoDNP/PPNDNP catalyst was most effective at selectively producing high molecular weight copolymers. For example, at ambient temperature and 2.0 MPa CO_2 pressure poly(cyclohexadiene carbonate) was produced with a TOF of 59.8 h^{-1} for a 10 hr reaction with a M_n of 17.6 kDa. The T_g of a high molecular weight copolymer (35.9 kDa) was found to be 123 ^oC, some 7 degrees higher than that of its saturated analog, poly(cyclohexene carbonate). Depolymerization of an hydroxyl terminated copolymer was initiated by the strong base sodium

bis(trimethylsilylamide) occurred under anaerobic conditions at 110 ^{o}C in toluene to quantitatively afford *trans*-cyclohexadiene carbonate. *Trans*-cyclohexadiene carbonate was independently synthesized from the *trans*-diol and ethylchloroformate, and was fully characterized spectroscopically. Postpolymerization functionalization of this well-defined alicyclic carbonate was achieved by the radical addition of thioglycolic acid to the unsaturated carbon-carbon bond. The resulting amphiphilic copolymer was subsequently deprotonated with ammonium hydroxide to produce the ionic ammonium salt which displayed a T_g of 120 ^{o}C and was completely water-soluble.

CHAPTER VI

DRAMATIC BEHAVIORAL DIFFERENCES OF THE COPOLYMERIZATION REACTIONS OF 1,4-CYCLOHEXADIENE AND 1,3-CYCLOHEXADIENE OXIDES WITH CARBON DIOXIDE*

Introduction

Several recent contributions have been published on the copolymerization reactions of 1,2-epoxy-4-cyclohexene (**E6**) with carbon dioxide (eq. 17).[87,102,105] This epoxide monomer with carbons 3 and 4 unsaturated reacts with CO_2 to provide copolymer more sluggishly under the same catalytic conditions than its saturated counterpart, cyclohexene oxide (CHO).[87,105] As expected, the physical and thermal properties of the two copolymer are similar, with the added feature that the copolymer derived from epoxide **E6** has the ability to be postmodified and the epoxide can be obtained from renewable resources.[4]

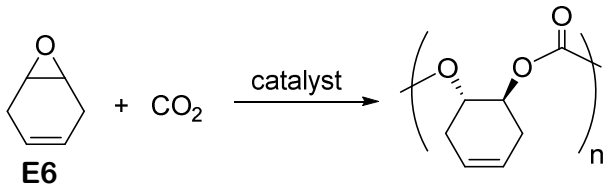

E6 (eq. 17)

We were interested in whether the location of the double bond in the six-membered carbon ring system would alter the reactivity of the epoxide monomer.

*Reproduced in part with permission from: "Dramatic Behavioral Differences of the Copolymerization Reactions of 1,4-Cyclohexadiene and 1,3-Cyclohexadiene Oxides with Carbon Dioxide." Darensbourg, D. J.; Chung, W.-C.; Yeung, A. D.; Luna, M. *Macromolecule* **2015**, *48*, 1679. Copyright 2015. American Chemical Society.

Hence, we report herein an examination of the analogous process in equation 17, instead using 1,2-epoxy-3-cyclohexene (**E7**). As might be anticipated, the structural parameters, and therefore the steric requirements of these three epoxides, CHO, **E6**, and **E7** are all very similar. Similarly, the pK_b's of the three epoxides are not very different, with CHO being slightly more basic towards a proton than epoxides **E6** and **E7**.[106] That is, the ν_{OD} shifts from MeOD in benzene (2667.4 cm^{-1}) are 2600.0, 2605.8, and 2603.8 cm^{-1} for CHO, **E6**, and **E7**, respectively. Therefore, it is expected that all three epoxides have similar binding abilities to the metal centers of the cobalt or chromium catalysts, and hence any differences in reactivity can mainly be ascribed to the kinetics of the ring-opening step.[107]

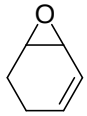

E7

In this chapter, we present the synthesis and characterization of the copolymer derived from epoxide **E7** and carbon dioxide, along with the corresponding cyclic carbonates. Further, the terpolymerization reactions of epoxide **E7** with propylene oxide and CO_2 were investigated, as well as the depolymerization of the copolymer derived from epoxide **E7** and CO_2, for comparison with analogous studies involving epoxide **E6**.[87,105] This study has provided some striking differences in reactivity patterns for

copolymers produced from the two isomeric forms of cyclohexadiene oxide, epoxides **E6** and **E7**.

Result and Discussion

Initially, we synthesized the epoxide monomer, 1,2-epoxy-3-cyclohexene (**E7**), *via* the commonly employed route of epoxidation of 1,3-cyclohexadiene with *m*-CPBA, however in very low yield. Alternatively, the required epoxide was synthesized by reacting the diene with NBS to afford bromohydrin followed by ring closure (eq. 18). This procedure also provided a yield of only 20%.[108] Hence, we resorted to obtaining the epoxide from commercial sources.

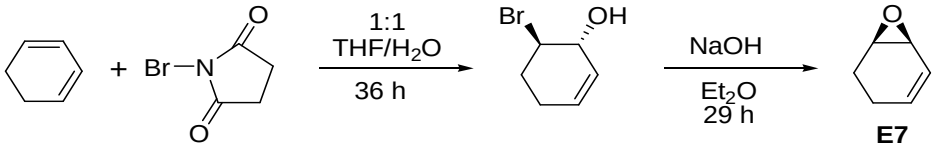

(eq. 18)

Coupling of epoxide **E7** (1,3-CHDO) and CO_2 using cobalt salen **catalyst 2** (shown in Figure 33) at 40 ^{o}C under solventless conditions afforded poly(1,3-cyclohexadiene carbonate) exclusively with a decent TOF of 30 – 70 h^{-1}. The epoxide/CO_2 coupling reactions are summarized in Table 12.

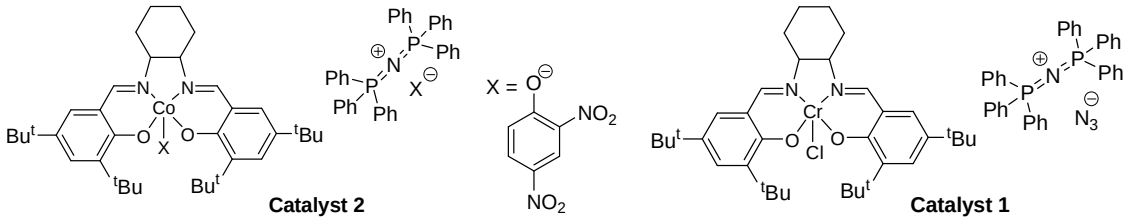

Figure 33 Binary cobalt salen **catalyst 2** and chromium salen **catalyst 1**.

Table 12 Coupling of 1,3-CHDO and CO_2.[a]

entry	cat	Temp (^oC)	time (h)	Conv. (%)[b]	TOF (h^{-1})[b]	polymer selectivity (%)[b]	M_n (kDa)	PDI	T_g (^oC)
1	**2**	40	5	33.3	66.5	100	8.7	1.09	105
2	**2**	40	10	53.3	53.3	100	16.5	1.06	104
3	**2**	40	20	66.9	33.5	100	22.0	1.07	108
4	**2**	RT	10	58.2	58.2	100	24.6	1.05	104
5	**1**	90	1	55.2	552	69.2	11.4	1.10	n.d.
6	**1**	90	2.5	90.0	360	55.6	10.8	1.14	107
7	**1**	90	5	100.0	200	40.8	8.9	1.25	104

[a] Reaction condition: 1,3-CHDO/Co/PPNDNP=1000/1/1, 1,3-CHDO/Cr/$PPNN_3$=1000/1/2, CO_2 pressure 2.0 MPa. [b] Determined by ^1H NMR.

As to be anticipated, upon increasing reaction times the TOFs decreased while higher conversions and molecular weights were observed (entries 1-3). At lower temperature, **catalyst 2** exhibited similar reactivity while affording higher molecular weight copolymer due to reduced chain transfer processes (entries 2 and 4). When the CO_2/1,3-CHDO coupling reaction was catalyzed using the chromium salen complex, **catalyst 1**, at 90 ^{o}C both copolymer and *cis*-1,3-cyclohexadiene carbonate were

produced (eq. 19). *Of importance, no trans-cyclic carbonate was observed* (*vide infra*). Although, the conversion to products increased with reaction time, there was no increase in the molecular weights of the copolymer produced (entries 5-7). Presumably, as the monomer is consumed, the rate of enchainment decrease relative to the backbiting process depicted in equation 20.

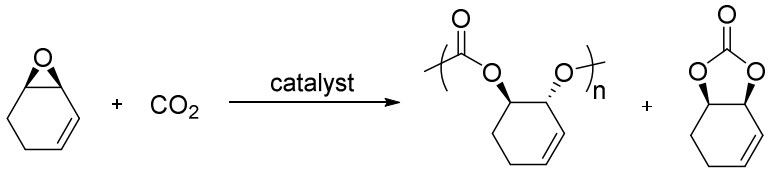

(eq. 19)

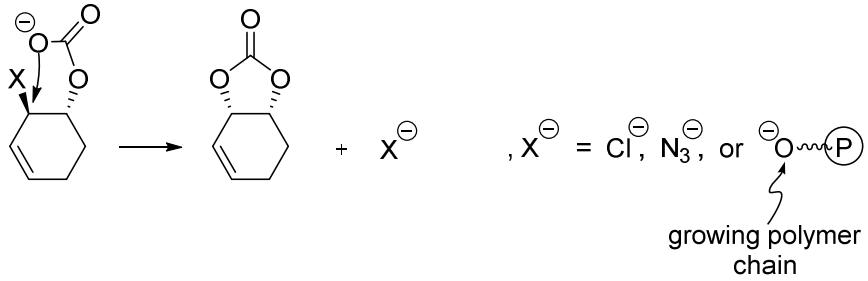

(eq. 20)

Compared to 1,4-cyclohexadiene oxide and carbon dioxide copolymerization reactions catalyzed by **catalyst 2**, 1,3-cyclohexadiene oxide is observed to be more reactive. For example, under the same reaction conditions as in entry 3, the 1,4-cyclohexadiene oxide/CO_2 coupling reaction exhibited 33.9% conversion, or about one-half the reactivity of the 1,3-isomeric form. Similarly, in the presence of **catalyst 1** in entry 7, 1,3-CHDO provided 40.8% polymer selectivity with 100% conversion, whereas, 1,4-CHDO under identical conditions afforded 36.6% polymer selectivity with 57%

conversion. Noteworthy, in the latter process *trans*-cyclic carbonate was produced. On the other hand, using cyclohexene oxide (CHO) as epoxide monomer where all carbon bonds are saturated, in the presence of the cobalt **catalyst 2** 1,3-CHDO was slightly less reactive (33.3% conversion, TOF = 66.5 h^{-1}) in entry 1 compared to CHO (42.2% conversion, TOF = 84.4 h^{-1}). However, under the reaction conditions in entry 7 where the chromium **catalyst 1** is used, CHO was less reactive with a 63% conversion to copolymer.

As indicated in the introduction, based on a relative basicity study of epoxides using the ν_{OD} shift of MeOD in epoxides from the corresponding shift in benzene, CHO is slightly more basic ($\Delta\nu$ = −67.4 cm^{-1}) than 1,3-CHDO ($\Delta\nu$ = −63.6 cm^{-1}) and 1,4-CHDO ($\Delta\nu$ = −61.6 cm^{-1}). That is, the sp^2 carbons of the double bond in both cyclohexadiene oxides act as weak electron withdrawing groups. Hence, 1,3-CHDO which bears a double bond next to the epoxy carbon, should be the easiest to ring-open because the π-electrons can stabilize the ring-opening transition state (*vide infra*).

The glass transition temperature of poly(1,3-cyclohexadiene carbonate) is lower (104 – 108 ^{o}C) than its 1,4-counterpart (123 ^{o}C),[105] and as well as poly(cyclohexene carbonate) (116 ^{o}C).[85] This is likely due to the unsymmetric nature of the double bond in 1,3-cyclohexadiene carbonate. The ^{13}C NMR spectrum of poly(1,3-cyclohexadiene carbonate) is similar to the 1,4-isomer except for exhibiting an additional set of peaks in the methylene and olefinic regions. The two ^{13}C NMR spectra are shown in Figure 34 for comparisons.

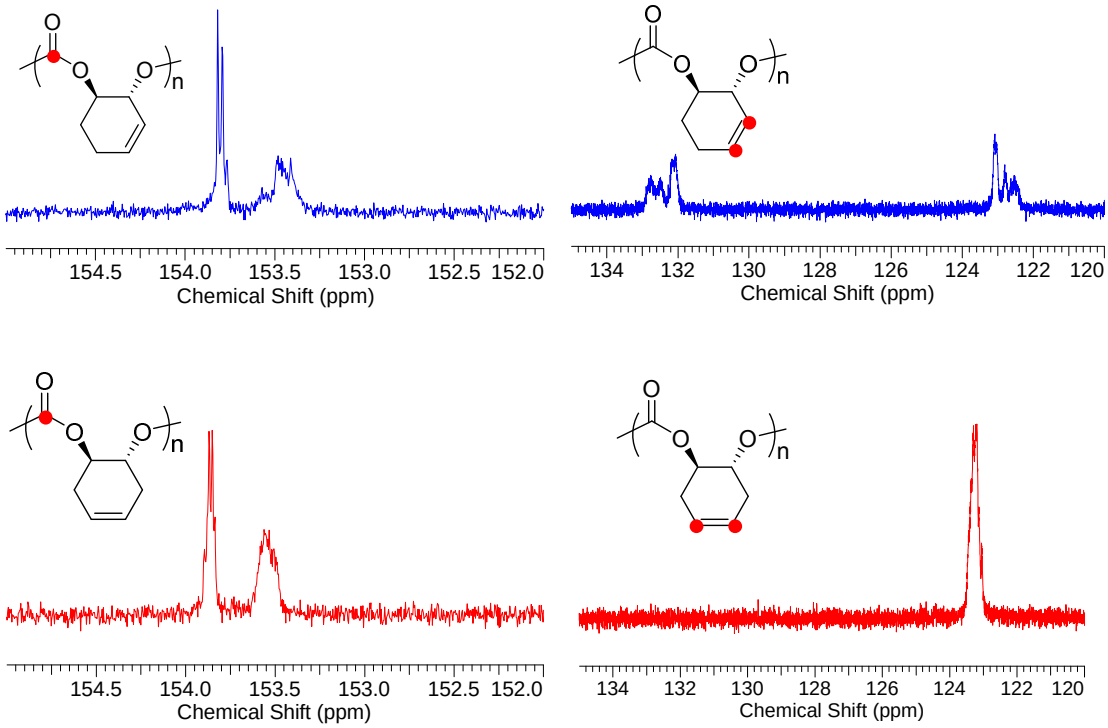

Figure 34 ^{13}C NMR spectra of poly(1,3-cyclohexadiene carbonate) (blue) and poly(1,4-cyclohexadiene carbonate) (red) in the carbonate region (left) and olefin region (right).

Attempts to depolymerize poly(1,3-cyclohexadiene carbonate) by deprotonation of the hydroxyl polymer end-group, which normally leads to an unzipping of the polymer chain to provide the cyclic carbonate, were unsuccessful.[77,101] That is, poly(1,3-cyclohexadiene carbonate) was stable in toluene in the presence of the strong base NaHMDS at 110 ^{o}C, with no degradation to *trans*-1,3-cyclohexadiene carbonate (eq. 21). *This is in stark contrast to poly(1,4-cyclohexadiene carbonate) which, under similar conditions, readily unzip quantitatively to trans-1,4-cyclohexadiene carbonate.*[105] As anticipated based on the process depicted in equation 20 where the thermodynamically more stable *cis*-1,3-cyclohexadiene carbonate is produced, if the depolymerization

reaction is carried out in the presence of CO_2, slow formation of the *cis*-cyclic carbonate is afforded. That is, upon deprotonation of the copolymer with a strong base, CO_2 addition occurs at the polymeric anionic alkoxy end group and backbiting proceeds *via* unzipping of the carbonate intermediate.

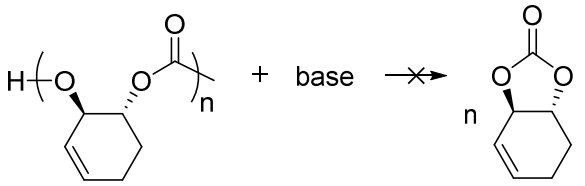

(eq. 21)

However, the ring-opening polymerization (ROP) of *trans*-1,3-cyclohexadiene carbonate was found to occur in the presence of the organo-based catalyst system TBD (1,5,7-triazabicyclo[4.4.0]dec-5-ene) and benzyl alcohol (see Experimental Section). The conversion of *trans*-1,3-cyclohexadiene carbonate was observed to proceed at a significantly faster rate under similar reaction conditions than reported for *trans*-1,4-cyclohexadiene carbonate.[109] The higher reactivity for the ROP of the 1,3-isomer is consistent with computational results which predicts the driving force for this process to be greater than that for the 1,4-isomer (*vide infra*). Similar to the polymer derived from the ROP of the *trans*-1,4-isomeric form, the ^{13}C NMR spectrum in the carbonate region of the polymer resulting from the ROP of *trans*-1,3-cyclohexadiene carbonate differs in tacticity from that obtained from the corresponding copolymerization of CO_2 and epoxide.

Nevertheless, hydrolysis of poly(1,3-cyclohexadiene carbonate) with NaOH was successful to provide *trans*-diol.[110] Subsequent carbonylation of *trans*-diol with

ethylchloroformate in the presence of triethylamine provided *trans*-1,3-cyclohexadiene carbonate (*trans*-1,3-CHDC) in 42.5% isolated yield (eq. 22).

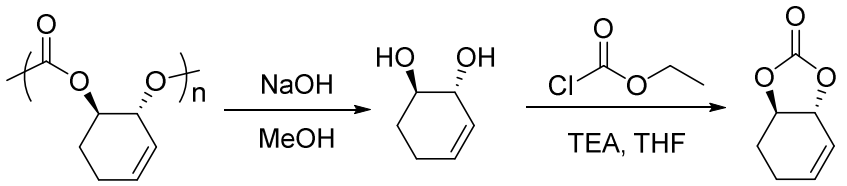

(eq. 22)

The *trans* conformation was confirmed by X-ray crystallography. The solid state structure is similar to *trans*-cyclohexene carbonate (*trans*-CHC), but exhibits a more twisted cyclohexyl ring (Figure 35).[25,111] *Trans*-1,3-CHDC has a larger O1-C1-C6-O2 dihedral angle of 39.2^{o} compared to that of *trans*-CHC of 23.9^{o} (Table 13). Also, *trans*-1,3-CHDC exhibits a small H4B-C4-C5-H5A dihedral angle of 34.7^{o}, whereas, *trans*-CHC has a nearly perfectly staggered conformation with a H3A-C3-C4-H4B dihedral angle of 58^{o}. *Cis*-1,3-cyclohexadiene carbonate (*cis*-1,3-CHDC) was prepared by an established route which involved the coupling of epoxide **E7** and CO_2 in the presence of $ZnCl_2$ and PPNI at 70 ^{o}C and 3.0 MPa pressure.[100,105] *Cis*-1,3-CHDC synthesized in this manner with 100% conversion displayed identical spectroscopic properties (ν_{CO_3} and ^{1}H, ^{13}C-NMR) as the byproduct produced in equation 19. *Trans*-1,3-CHDC in dichloromethane showed three carbonate infrared bands at 1867.0, 1834.3, and 1809.2 cm^{-1}; whereas, *cis*-1,3-CHDC exhibited only one band at a lower frequency (1799.5 cm^{-1}), Figure 36. A similar situation was noted in the isomeric forms of 1,4-CHDC

where the *trans*-isomer had two carbonate bands at higher frequencies (1824.6 and 1809.2 cm^{-1}) compared to one band at 1797.6 cm^{-1} for the *cis*-isomer.[105]

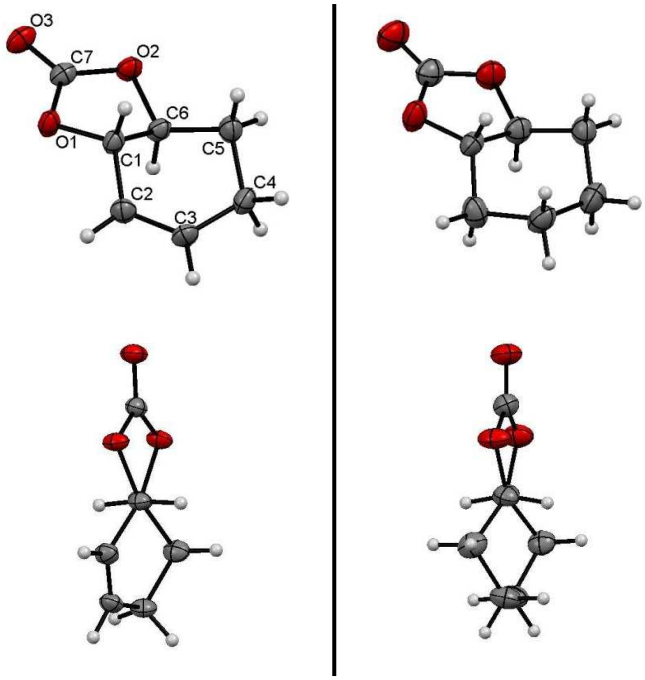

Figure 35 Crystal structures of *trans*-1,3-CHDC (left) and *trans*-CHC (right). The bottom ones are the views along C1-C6 axis.

Table 13 Dihedral angles of trans-1,3-CHDC and trans-CHC.

	trans-1,3-CHDC	*trans*-CHC
O1-C1-C6-O2	39.2(1)	23.9(9)
H4B-C4-C5-H5A	34.6(2)	58(2)
C2-C1-C6-C5	67.3(2)	72(1)

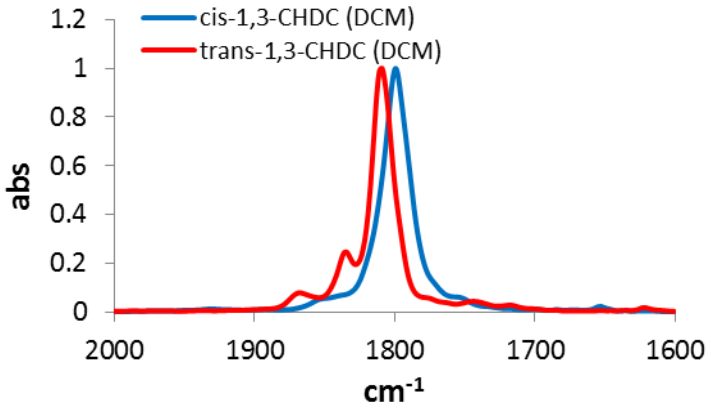

Figure 36 Normalized infrared spectra of cis-1,3-CHDC and trans-1,3-CHDC in the carbonyl region.

In order to enhance the applicability of polymers derived from carbon dioxide and cyclohexene oxide or its derivatives, it is desirable to incorporate other less rigid epoxide monomers, e.g., propylene oxide (PO). Unfortunately, when 1,4-cyclohexadiene oxide is terpolymerized with propylene oxide and CO_2, very little 1,4-CHDO is incorporated into the propylene carbonate backbone. Indeed, it has been shown that cyclohexene oxide itself is much more reactive than 1,4-CHDO in terpolymerization reactions with CO_2.[87,105] By way of contrast, the 1,3-CHDO isomer's reactivity compares favorably with propylene oxide in terpolymerization processes with CO_2 (eq. 23). Herein, we have investigated the reactivity ratios (ratio of self- to cross-propagation) of propylene oxide and 1,3-CHDO by a Fineman-Ross analysis (Scheme 16).[43]

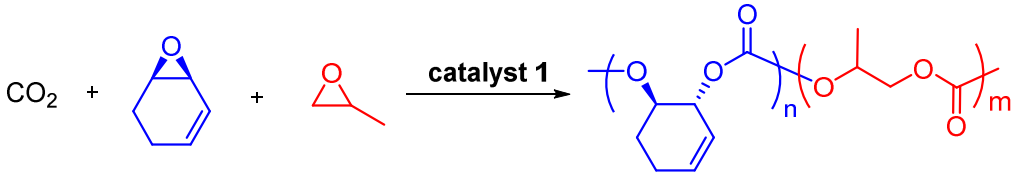

(eq. 23)

Scheme 16 Self- and cross-propagation pathways and reactivity ratios of both epoxides in the CO_2/1,3-CHDO/PO terpolymerization reaction.

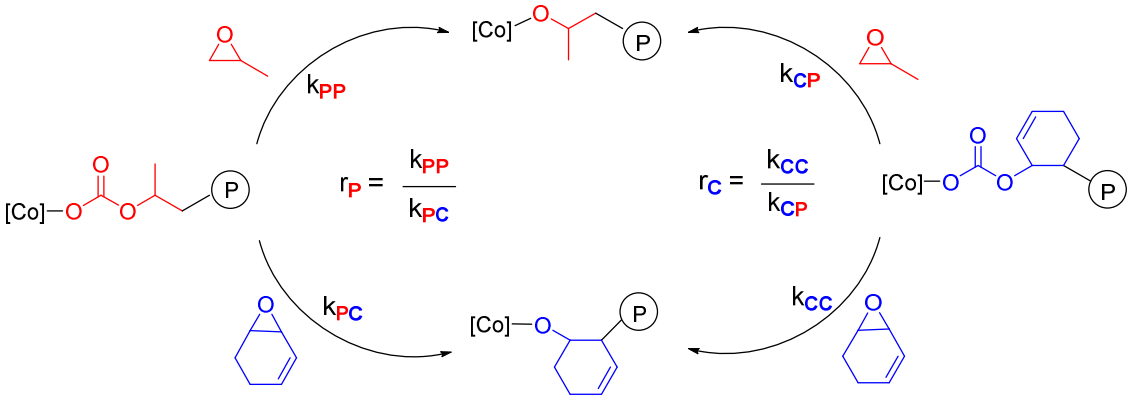

A set of terpolymerization reactions with different epoxide feed ratios were conducted and the components of the resulting terpolymers were analyzed by ^{1}H NMR spectroscopy. The results of this study are summarized in Table 14 and Figure 37. The reactivity ratio of propylene oxide for self- *vs* cross-propagation was found to be 0.553, whereas for 1,3-cyclohexadiene oxide was determined to be 0.846. The observation that propylene carbonate incorporates 1,3-CHDO faster than propylene oxide is ascribed to the π-orbital of the adjacent olefin stabilizing the transition state in the ring-opening step of 1,3-CHDO. This effect was also observed in the terpolymerization reaction of propylene oxide/styrene oxide/CO_2, where styrene oxide was more easily ring-opened.[106] On the other hand, cyclohexadiene carbonates incorporate propylene oxide slightly faster

than 1,3-CHDO as the result of propylene oxide better metal binding and less steric hindrance than 1,3-CHDO.

Table 14 Terpolymerization of CO_2/1,3-CHDO/PO.[a]

1,3-CHDO/Co	PO/Co	time (min)	1,3-CHDO conv. (%)[b]	PO conv. (%)[b]	PPC/PCHDC (m/n)[b]
600	1800	60	24.4	15.8	2.04
800	1600	30	17.9	9.6	1.43
1200	1200	30	13.6	9.0	0.855
1600	800	40	8.4	2.5	0.489
1800	600	43	6.9	5.6	0.330

[a]Reaction condition: CO_2 pressure 2.0 MPa, ambient temperature. [b] Determined by ^{1}H NMR.

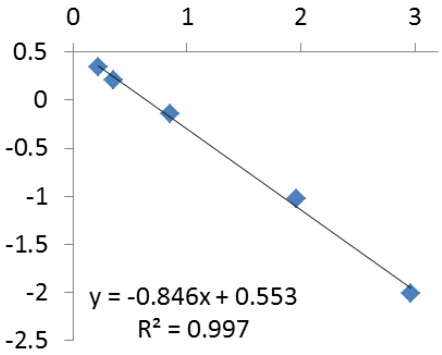

Figure 37 Fineman-Ross analysis of CO_2/1,3-CHDO/PO terpolymerization. The slope indicates reactivity ratio of 1,3-CHDO and the intercept indicates that of PO.

As has been previously reported for the copolymer derived from carbon dioxide and 1,4-cyclohexadiene oxide or 2-vinyloxirane, poly(1,3-cyclohexadiene carbonate) can be functionalized with thioglycolic acid using thiol-ene chemistry in the presence of AIBN (eq. 24).[21.105] All olefinic groups were coupled with the thiol bearing acetic acid pendant group, with the resulting polymer having a M_n value of 15.70 kDa and PDI of

1.2 (theoretical M_n 16.6 kDa for a parent copolymer with M_n of 10.0 kDa). The functionalized polycarbonate exhibited a lower T_g of 89 ^oC compared to its parent (108 ^oC).

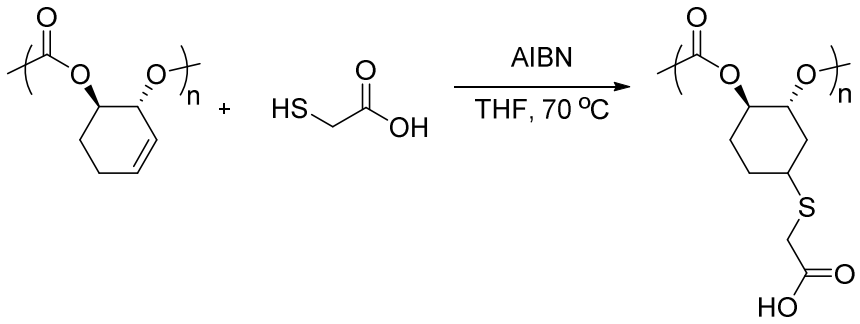

(eq. 24)

Computational studies

Computational modeling has the potential to provide deeper insight into experimental observations at a qualitative and quantitative level, and its application toward the CO_2-epoxide copolymerization has been surveyed.[86] We have employed such studies to quantify the thermodynamics of polymerization *vs* cyclic carbonate formation, the kinetics of metal-catalyzed chain growth, and associated degradation reactions.[76,107] Such calculations indicate that displacement of the growing polymer strand (terminated with carbonate) with an epoxide, followed by epoxide ring-opening (Scheme 17), is the rate-limiting step in the overall enchainment reaction.[107] That is to say, the last step, carboxylation of the polymeric alkoxide, is rapid for these systems, and does not constrain the catalytic reaction.

Scheme 17 Ring-opening of a metal-bound epoxide by a polymeric carbonate nucleophile.

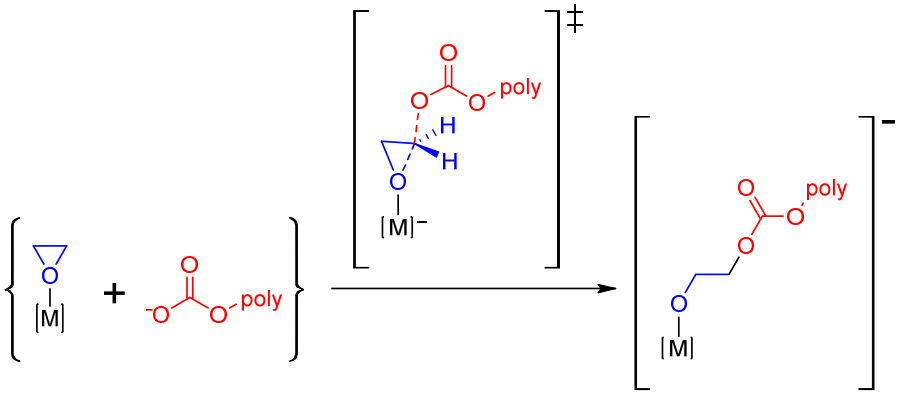

Pertinent to the observations noted on the epoxide/CO_2 coupling reactions reported herein, the enthalpies and free energies of the respective processes involving cyclohexene oxide, 1,4-cyclohexadiene oxide, and 1,3-cyclohexadiene oxide were calculated and are presented in Figure 38 and Figure 39, respectively. As is typical for these processes, copolymer formation was found to be exothermic by 18-22 kcal/mol, making it the enthalpic product. On the other hand, formation of cyclic carbonates are much less exothermic, and are the thermodynamic products of these coupling reaction due to entropy (Table 15).

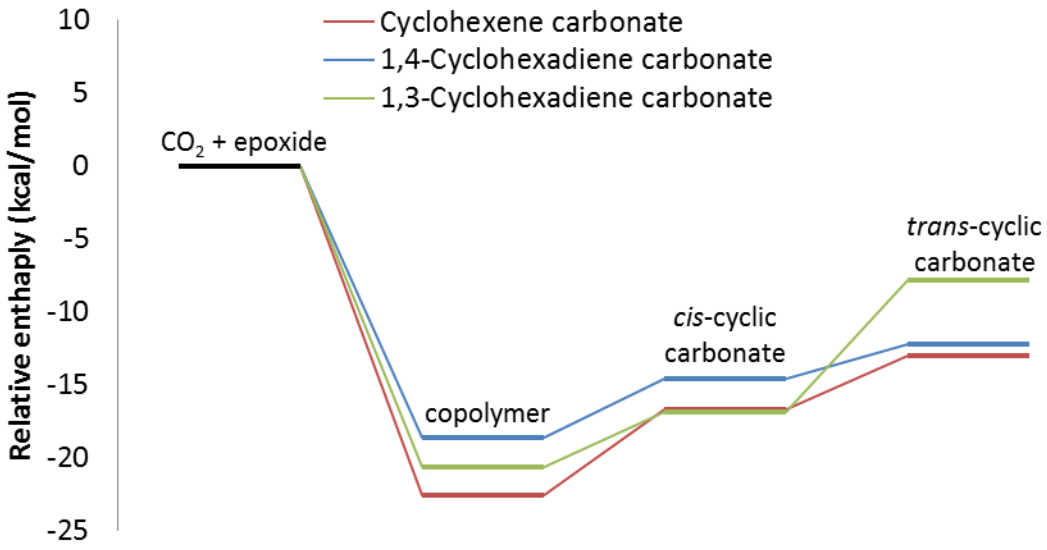

Figure 38 Enthalpies of the reactions between CO_2 and cyclohexene, 1,4-cyclohexadiene, and 1,3-cyclohexadiene oxides.

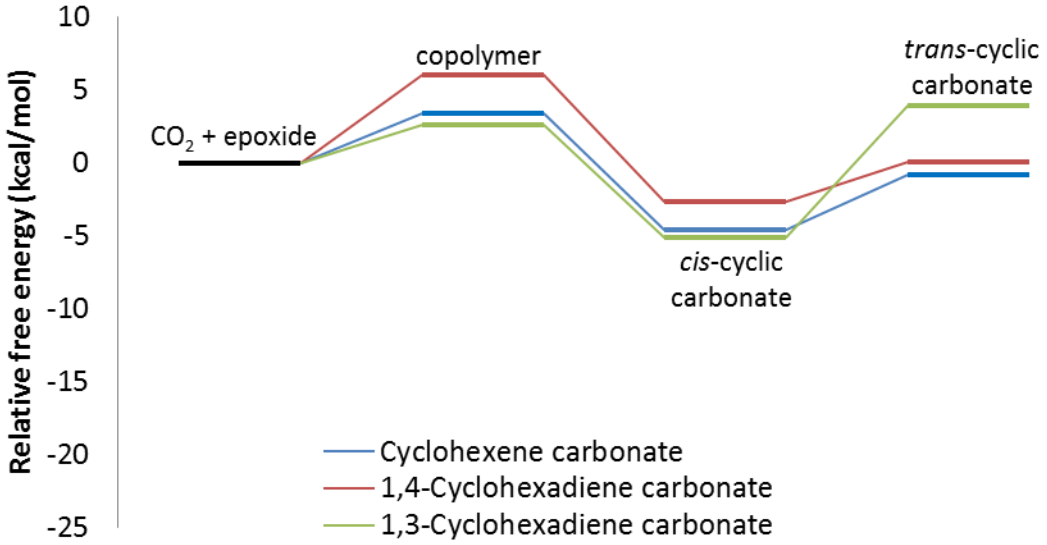

Figure 39 Free energies of the reactions between CO_2 and cyclohexene, 1,4-cyclohexadiene, and 1,3-cyclohexadiene oxides.

While formation of *trans*-cyclic carbonate from the backbiting process involving all three polycarbonates are endothermic, they are exergonic for poly(cyclohexene carbonate) and poly(1,4-cyclohexadiene carbonate) with ΔG values of −4.3 and −5.9 kcal/mol, respectively. By way of contrast, poly(1,3-cyclohexadiene carbonate) degradation to *trans*-1,3-cyclohexadiene carbonate was endergonic by 1.3 kcal/mol due to the enthalpic component of the free energy. The computed kinetic barriers for the alkoxide backbiting reactions for the three alicyclic epoxide derived copolymers were quite similar (*vide infra*), therefore, thermodynamic explains why treatment of poly(1,3-cyclohexadiene carbonate) with a strong base yields *no trans*-1,3-cyclohexadiene carbonate (eq. 21).

Table 15 Thermodynamic Data (Enthalpies and Free Energies) for the CO_2 Coupling Reactions with CHO, 1,4-CHDO and 1,3-CHDO.[a]

Epoxide	ΔH (ΔG) Copolymerization	ΔH (ΔG) *cis*-cyclic carbonate	ΔH (ΔG) *trans*-cyclic carbonate
Cyclohexene oxide	−22.6 (+3.4)	−16.7 (−4.6)	−13.0 (−0.9)
1,4-cyclohexadiene oxide	−18.6 (+6.0)	−14.6 (−2.6)	−12.3 (+0.1)
1,3-cyclohexadiene oxide	−20.6 (+2.6)	−16.9 (−5.2)	−7.8 (+3.9)

[a] Energies provided in kcal/mol. with free energies included in parentheses.

The ~4.0 kcal/mol difference in free energy for formation of *trans*-cyclic carbonate from the other two epoxides is ascribed to the small H-C-C-H dihedral angle of 35.1^{o} (synconformation) of *trans*-1,3-cyclohexadiene carbonate (Figure 40). Such intramolecular steric repulsion is greater than that for the corresponding dihedral angles

for the 1,4-isomer, whereas, this angle is close to the ideal 60^{o} for cyclohexene carbonate (gauche conformation).

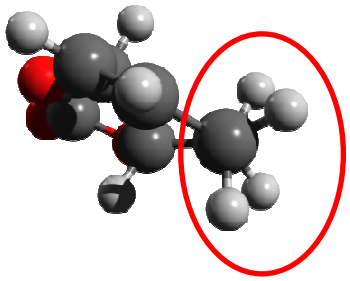

H-C-C-H dihedral angles
trans-1,3-CHDC: 35.1°
trans-1,4-CHDC: 76.8°, 42.9°
trans-CHC: 56.5°

Figure 40 *trans*-1,3-Cyclohexadiene carbonate, highlighting the syn conformation between two adjacent carbon atoms in the ring.

As alluded to earlier, the kinetic barriers for the copolymers to undergo alkoxide backbiting to afford *trans*-cyclic carbonates were determined to be non-rate limiting (Table 16 and Figure 41). On the other hand, formation of the *cis*-cyclic carbonates from the carbonate backbiting process have activation barriers about 10 kcal/mol higher. While the energy barrier leading to *trans*-1,3-cyclohexadiene carbonate via alkoxide backbiting is the highest, these barriers are quite typical, and should not, in themselves, preclude cyclic carbonate formation. Experimentally, attempts to prepare *trans*-1,3-cyclohexadiene carbonate via treating the polymer with a strong base were not successful. These calculations emphasize that the failure is attributed to the thermodynamics of the overall reaction (ΔH = +12.8 kcal/mol, ΔG = +1.3 kcal/mol). Indeed, the reverse process of ROP of *trans*-1,3-cyclohexadiene should be favored as observed experimentally.

Table 16 Energy barriers (kcal/mol) for metal-free alkoxide backbiting.

	$\Delta H^{‡}$	$\Delta G^{‡}$
CHC	15.3	14.6
trans-13CHDC-up[a]	16.2	15.7
trans-13CHDC-down[a]	15.9	15.1
trans-14CHDC	15.0	14.9

[a] See Figure 41.

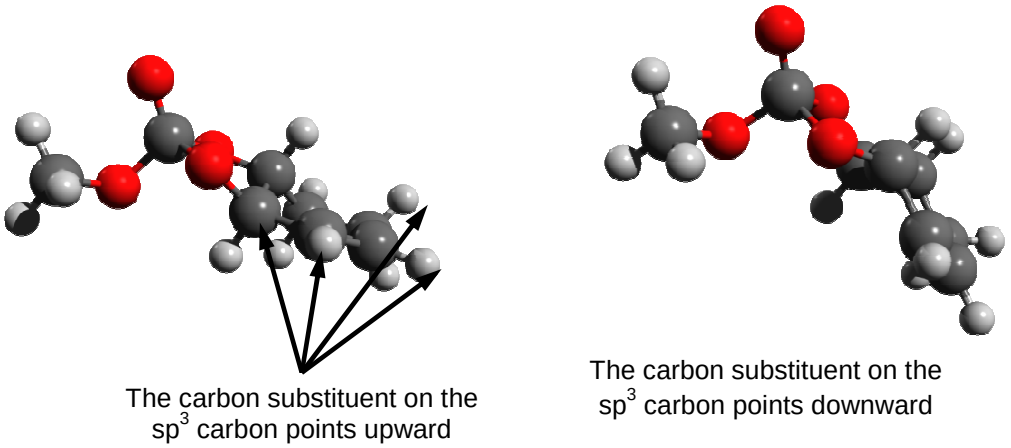

Figure 41 Tetrahedral intermediates involved in the alkoxide backbiting reaction for trans-13-CHDC-up (left) and trans-13-CHDC-down (right).

The rate-limiting step for the (salen)M(III)Cl-catalyzed CO_2-epoxide copolymerization has previously been established to be displacement of the metal-bound polymeric carbonate with an epoxide molecule, followed by ring-opening the metal-bound epoxide (Scheme 17). The overall energy barriers presented here are calculated as:

$\Delta E^{‡}$ = E(transition state) – E([M]-polymeric carbonate) – E(epoxide)

As a further refinement, the growing polymer chain is represented by cyclohexyl carbonate ($C_6H_{11}OCO_2^-$) that better represents the steric bulk of the incoming

nucleophile than methyl carbonate ($CH_3OCO_2^-$). Between the bulkier nucleophile and a more typical cyclohexylene salen backbone, we would preclude a transition states over-stabilized by dipolar interactions between the carbonate oxygen atoms and the hydrogen atoms on the salen ligand's ethylene backbone that are adjacent to the electron-withdrawing nitrogen atoms.

The overall free energy barriers for these two steps are 22-27 kcal/mol; carboxylation has trivial barriers in comparison ($\Delta G^{\ddagger}$ = 6-8 kcal/mol).[107] The overall energy barriers for cyclohexene, 1,3-, and 1,4-cyclohexadiene oxides to yield polycarbonates are presented in Table 17. In this table, "-1" refers to the polymeric carbonate (represented by cyclohexyl carbonate) ring-opening the activated epoxide at the vinylic carbon for aliyclic epoxides, whereas "-2" refers to attack at the adjacent methylene position. As before, the chromium-catalyzed reactions have higher energy barriers than the cobalt-catalyzed reactions.

Consistent with the case for styrene oxide, attack at the methine positions of vinylic epoxide (1,3-cyclohexadiene oxide) has a free energy barrier lower by ca. 2-6 kcal/mol than for methylene attack.[107] This occurs despite the steric hindrance at the more substituted carbon atom, whereas methine attack has a higher barrier for propylene oxide. The large difference in methine/vinylic vs. methylene attack suggest that [Cr] may catalyze analogous reaction with cyclohexadiene oxide in a regioselective head-tail manner. The calculated results predict that the ease of copolymerization is in the order: 1,3-CHDO > 1,4-CHDO > CHO for both [Cr] and [Co] catalyzed reactions. These results are in general agreement with experimental observations. To be specific, such

experiments indicate that 1,3-cyclohexadiene oxide is expected to react more readily than cyclohexene oxide.

Table 17 Overall energy barriers (kcal/mol) for various epoxides to copolymerize with CO_2.

	[Cr]-bound		[Co]-bound	
Epoxide	$\Delta H^{‡}$	$\Delta G^{‡}$	$\Delta H^{‡}$	$\Delta G^{‡}$
CHO[a]	16.8	29.1	16.7	29.1
1,3-CHDO-1[a]	13.1	24.2	12.2	24.1
1,3-CHDO-2[a]	16.8	30.0	14.5	26.6
1,4-CHDO[a]	15.1	27.5	13.8	26.4

CHDO = cyclohexadiene oxides. [a]Cyclohexyl carbonate nucleophile.

How well these epoxide ligands bind to the Lewis acid catalysts were calculated (Table 18). As was observed previously, R-epoxides bind more weakly to the Lewis acid catalyst than S-epoxides, due to conformational reasons.[107] The corresponding Lewis basicities toward [Cr] and [Co] are determined here to be in the order: CHO > 1,3-CHDO ≈ 1,4-CHDO. These results substantiate comments previously made about the Bronsted basicity rankings of these epoxides, determined *via* infrared spectroscopy (*vide supra*) as follows: CHO > 1,3-CHDO > 1,4-CHDO. These results indicate that 1,3- and 1,4-CHDO are less able to displace the growing polymer chain than CHO prior to epoxide ring-opening. The assumption made is that the electronics of the respective polymeric carbonates are similar.

Table 18 Enthalpies and free energies (kcal/mol) for epoxide ligands to bind to the (salen)Cr(III)Cl and (salen)Co(III)Cl fragments.

	[Cr]-bound		[Co]-bound	
L	Enthalpy	Free energy	Enthalpy	Free energy
CHO	-19.5	-8.8	-18.8	-4.1
R-1,3-CHDO	-13.7	-1.9	-11.7	3.3
S-1,3-CHDO	-16.0	-5.5	-15.5	-1.4
1,4-CHDO	-15.3	-4.5	-13.0	2.0

The energy barriers for the elementary epoxide ring-opening reaction are presented in Table 19. The structures of the {[M]-epoxide + polymeric carbonate} van der Waals complexes have been assumed to be the same for the metal-catalyzed epoxide ring-opening reactions at the vinylic ("-1" and methylene ("-2") positions. The relative differences between these two epoxide ring-opening modes can thus be fairly compared. We should exercise caution when comparing the energy barriers between different epoxides or between different metal-catalyzed systems, because the {[M]-epoxide + polymeric carbonate} van der Waals complexes are poorly defined.

Even so, we find that attack at the vinylic carbon (“-1”) is consistently more favorable than at the methylene carbon in general. One might imagine that the vinylic p_π system will stabilize the pentacoordinate transition state for the reaction. Such interactions have been seen in the reaction where poly(styrene carbonate) undergoes the

metal-free carbonate backbiting reaction, but a careful review of the calculated molecular orbitals did not reveal such a simple answer for the metal-catalyzed system.[76]

Table 19 Energy barriers (kcal/mol) for the elementary epoxide ring-opening reaction, catalyzed by (salen)Cr(III)Cl and (salen)Co(III)Cl.

		[Cr]-bound		[Co]-bound
Epoxide	$\Delta H^{‡}$	$\Delta G^{‡}$	$\Delta H^{‡}$	$\Delta G^{‡}$
CHO[a]	9.5	11.4	9.4	10.5
1,3-CHDO-1[a]	3.6	4.3	5.4	6.1
1,3-CHDO-2[a]	7.5	10.2	7.9	9.7
1,4-CHDO[a]	8.8	9.9	9.1	11.0

[a]Cyclohexyl carbonate nucleophile.

Even though 1,3-cyclohexadiene oxide has a lower free energy barrier for epoxide ring-opening than cyclohexene oxide, this epoxide is less able to displace the polymeric carbonate from the metal center. The advantage that 1,3-cyclohexadiene oxide has is thus muted. The importance of considering the ligand exchange and the epoxide ring-opening steps are emphasized as a result.

Experimental Section

General information

All manipulations involving air- and/or water-sensitive compounds were carried out in a glove box under an argon atmosphere. 1,2-epoxy-3-cyclohexene (Sigma-Aldrich) was stirred over CaH_2 distilled, and stored in an argon-filled glovebox. Research grade 99.999% carbon dioxide supplied in a high-pressure cylinder and equipped with a liquid dip tube was purchased from Airgas. The CO_2 was further purified by passing through

two steel columns packed with 4 Å molecular sieves that had been dried under vacuum at $\geq$ 200 ^{o}C. The 15 mL high pressure stainless steel reactors used in the copolymerization and cycloaddition reactions were previous dried at 170 ^{o}C for 6 h prior to their use.

Measurements

Molecular weight determinations (M_n and M_w) were carried out with a Malvern Modular GPC apparatus equipped with ViscoGEL I-series columns (H+L) and Model 270 dual detector comprised of RI and light scattering detectors. Samples (~10 mg) were weighed into a 2 mL volumetric cylinder, dissolved in THF and filtered with 0.2 μm syringe filter before injection. Glass transition temperatures (T_g) were measured using a Mettler Toledo polymer DSC. Samples (~6 mg) were weighed into 40 μL aluminum pans and subjected to two heating cycles. The first cycle covered the range from 25 to 150 °C at 10 °C/min heating rate and was cooled down to 0 °C at −10 °C/min cooling rate. The second cycle ranged from 0 ^{o}C to 150 ^{o}C at 5 ^{o}C/min heating rate and was where T_g was measured.

Representative coupling reaction of 1,2-epoxy-3-cyclohexene and CO_2

(*S,S*)-(salen)CoDNP (4.5 mg, 5.7 μmol, 1 eq.), PPNDNP (4.1 mg, 5.7 μmol, 1 eq.) and 1,2-epoxy-3-cyclohexene (0.5 mL, 5.7 mmol, 1000 eq.) were charged in a 15 mL stainless steel autoclave reactor. The reactor was pressurized to slightly less than 2.0 MPa and heated to 40 ^{o}C in an oil bath with magnetic stirring. After 5 h, the reactor was

cooled to 0 ^{o}C, depressurized, and a ^{1}H NMR spectrum of the crude reaction mixture was taken immediately. The crude reaction mixture was dissolved in CH_2Cl_2 and added to about 1M HCl/methanol solution to quench the reaction and precipitate any copolymer formed. The supernatant HCl/methanol solution was removed and the polymer precipitate was re-dissolved in CH_2Cl_2 and reprecipitated from methanol. The resulting copolymer was obtained by removing the supernatant and subsequently drying *in vacuo* at 40 ^{o}C for further analysis by GPC and DSC. ^{1}H NMR (300 MHz, $CDCl_3$): δ 5.95 (br, 1H), 5.68 (br, 1H), 5.19 (d, J=18 Hz, 1H), 4.91 (br, 1H), 2.20 (s, 2H), 2.08 (s, 1H) and 1.87 (s, 1H) ppm. ^{13}C NMR (125 MHz, $CDCl_3$): δ 153.6, 132.4, 122.8, 72.8-75.06, 24.4 and 22.6 ppm. Infrared (CH_2Cl_2): 1749.4 cm^{-1}.

Synthesis of cis-1,3-cyclohexadiene carbonate

$ZnCl_2$ (5.7 mg, 0.042 mmol, 1 eq.), PPNI (107.5 mg, 0.162 mmol, 4 eq.) and 1,2-epoxy-3-cyclohexene (0.35 mL, 4.0 mmol, 100 eq.) were charged in a 15 mL stainless steel autoclave reactor. The reactor was pressurized to slightly less than 3.0 MPa and heated to 70 ^{o}C in an oil bath with magnetic stirring. After 43 h, the reactor was cooled to 0 ^{o}C, depressurized, and a ^{1}H NMR spectrum of the crude reaction mixture was taken immediately, which showed 100 % conversion to *cis*-cyclic carbonate product. Ether was added to reaction mixture in order to isolate the product. The ether solution was filtered through a celite pad to remove insoluble $ZnCl_2$ and PPNI and the filtrate was dried in vacuo to provide 0.463 g (3.30 mmol, 82.6 % isolated yield) of a yellow oil as desired product. Elemental analysis calculated for $C_7H_8O_3$ (found): C, 60.00 (60.20); H,

5.75 (5.68). ^{1}H NMR (300 MHz, $CDCl_3$): δ 6.22 (m, 1H), 5.78 (d, J=4.5 Hz, 1H), 5.01 (m, 1H), 4.90 (m, 1H) and 1.85-2.38 (m, 4H) ppm. ^{13}C NMR (75 MHz, $CDCl_3$): δ 154.9, 135.2, 121.3, 74.8, 72.1, 24.1 and 19.5 ppm. Infrared (CH_2Cl_2): 1799.5 cm^{-1}.

Synthesis of trans-1,3-cyclohexadiene carbonate

Poly(1,3-cyclohexadiene carbonate) (0.2033 g, 1.45 mmol repeating unit, 1 eq.), NaOH (0.1168 g, 2.92 mmol, 2 eq.) and 10 mL methanol were added to a 50 mL round bottom flask, and heated to 57 ^{o}C for 3h. The reaction mixture was neutralized by adding 0.6 mL 6M HCl and then dried with $MgSO_4$. After removing $MgSO_4$ by filtration, the solvent was evaporated under reduced pressure affording 0.162 g (1.42 mmol, 97.8 % yield) of a brown powder as the desired *trans*-diol product. Subsequently, *trans*-diol (0.162 g, 1.42 mmol, 1 eq.) was converted to *trans*-cyclic carbonate based on the literature procedure[105] using ethylchloroformate (0.3 mL, 3.15 mmol, 2.2 eq.) and triethylamine (0.4 mL, 2.87 mmol, 2 eq.) in THF. The crude reaction mixture was filtered and the solvent was removed under reduced pressure, followed by being redissolved in hexane/ethyl acetate (3/1) solvent and filtered through a silica pad to purify. The eluent was concentrated and dried to afford a yellow powder (84.5 mg, 0.603 mmol, 42.5% yield). Elemental analysis calculated for $C_7H_8O_3$ (found): C, 60.00 (60.83); H, 5.75 (6.08). ^{1}H NMR (300 MHz, $CDCl_3$): δ 6.07 (dd, J=3, 9 Hz, 1H), 5.69 (m, 1H), 4.75 (d, J=9 Hz, 1H), 4.31 (dd, J= 3, 9, 12 Hz, 1H), 2.30-2.51 (m, 3H) and 2.10-1.90 (m, 1H) ppm. ^{13}C NMR (75 MHz, $CDCl_3$): δ155.4, 129.6, 122.6, 81.3, 80.5, 25.2 and 23.8 ppm. Infrared (CH_2Cl_2): 1809.2, 1834.3 and 1867.0 cm^{-1}.

Ring-opening polymerization of trans-1,3-cyclohexadiene carbonate

Trans-1,3-cyclohexadiene carbonate (51.8 mg, 0.37 mmol, 50 eq.) was added to a round bottom flask which was charged with 0.10 mL of a stock solution of 73 mM TBD (7.3 μmol, 1 eq.) and 77 mM benzyl alcohol (7.7 μmol, 1 eq.) in toluene. Toluene (0.1 mL) was subsequently added to the above solution resulting in a *trans*-1,3-cyclohexadiene carbonate solution with a concentration of 1.85 M. After stirring the solution at 60 ^{o}C for 64 h, an NMR spectrum of the crude reaction mixture was taken to determine the monomer conversion (87.4%). The copolymer was isolated from methylene chloride upon addition of methanol. The molecular weight (M_n) of the copolymer was determined to be 2100 Da with a PDI of 1.12.

Thiol-ene click reaction of poly(1,3-cyclohexadiene carbonate) and thioglycolic acid

This was done in a similar manner as was previously reported in literature. Poly(1,3-cyclohexadiene carbonate) (M_n=10.0 kDa, 0.254 g, 1.81 mmol of C=C groups, 1 eq.) and thioglycolic acid (5.2 mL, 71.4 mmol, 40 eq.) were added to 10 mL THF solution of AIBN (0.098 g, 0.589 mmol, 0.33 eq.) in a 50 mL Schlenk flask under argon atmosphere. The reaction mixture was stirred for 24 h at 70 ^{o}C and subsequently concentrated under reduced pressure. The crude product was redissolved in THF and precipitated from diethyl ether three times in order to purify the material. After the first thiol-ene coupling, ^{1}H NMR spectrum of product showed non-reacted olefin, so the secondary thiol-ene coupling was conducted. After the second time thiol-ene coupling, no olefin was observed by ^{1}H NMR spectrum indicating 100 % conversion of olefin to

thioether. 0.182 g (0.783 mmol repeating unit, 43.3 % isolated yield) white product was obtained with M_n 15.7 kDa and a T_g value of 89 ^oC. The functionalized polymer dissolves in polar solvents like methanol, DMSO, acetone and THF, but not in acetonitrile, ethyl acetate, dichloromethane, or chloroform.

X-ray crystal structure analyses

Single crystals of *trans*-1,3-CHDC were obtained by slow evaporation of a diethyl ether solution at -18 ^oC. A Leica MZ7.5 stereomicroscope was used to identify suitable crystals of the same habit. Each crystal was coated in paratone, affixed to a Nylon loop and placed under streaming nitrogen (150K) in a SMART Apex CCD diffractometer (See details in .cif files). The space group was determined on the basis of systematic absences and intensity statistics. The structure was solved by direct methods and refined by full-matrix least squares on F^2. Anisotropic displacement parameters were determined for all non-hydrogen atoms. Hydrogen atoms were placed at idealized positions and refined with fixed isotropic displacement parameters. The following is a list of programs used: data collection and cell refinement, APEX2;[84a] data reductions, SAINTPLUS Version 6.63;[84b] absorption correction, SADABS;[84c] structural solutions, SHELXS-97;[84d] structural refinement, SHELXL-97;[84e] graphics and publication materials, Mercury version 3.0.[112]

Computational methods

All calculations were performed using the Gaussian 09 suite.[113] All local minima and saddle points were confirmed by their calculated vibrational frequencies (zero and one imaginary frequencies respectively). The saddle points found were confirmed to be the correct ones by visualizing the imaginary vibrational modes with AGUI[114] and Avogadro.[115]

Consistent with previous work,[76,107,116] gas phase enthalpies of polymerization were obtained by the CBS-4M composite method (1-mer to 2-mer).[117,118] In the same way, changes in energy for the exchange and epoxide ring-opening reactions (representing the slow step in the enchainment reaction) were calculated using the M06[119] and M06L functionals,[120] in conjunction with the BS2 and BS2+ basis sets.[107] These basis sets comprise the Stuttgart/Dresden effective core potential and basis sets (SDD)[121] for the cobalt and chromium atoms, and the all-electron 6-31G(d',p') of Petersson and coworkers were used for remaining atoms.[122,123] Basis set BS2+ was similar to BS2, except that diffuse functions were added (i.e. 6-31+G(d',p') instead of 6-31G(d',p')). Free energies of carbonate and alkoxide back-biting reactions were calculated using the CBS-QB3[113] and CBS-QB3(+)[124,125] composite methods respectively.

Except for determining enthalpies of polymerization and cyclic carbonate formation, solvation was applied. Tetrahydrofuran was the prototypical solvent, and the Integral Equation Formalism Polarization Continuum Model (IEFPCM) calculation with

radii and non-electrostatic terms for Truhlar and coworkers' SMD solvation model was used.[126]

Conclusion

The copolymerization reaction of 1,3-cyclohexadiene oxide and carbon dioxide differ strikingly from the corresponding processes involving its symmetrical or saturated analogs, 1,4-cyclohexadiene oxide and cyclohexene oxide, respectively. Notably, it is the most reactive of the three epoxides, in general being slightly more reactive than cyclohexene oxide, with the 1,4-isomer being by far the least reactive. Computational studies support these experimental observations, i.e., the free energy barriers for epoxide ring-opening increase in the order: 1,3-CHDO < CHO < 1,4-CHDO. This reactivity order is especially evident in terpolymerization reactions of 1,3-cyclohexadiene oxide with propylene oxide and CO_2, where the reactivity ratios were determined to be r_{PO} = 0.553 and $r_{1,3\text{-CHDO}}$ = 0.846 at ambient temperature from a Fineman-Ross analysis. For reaction processes catalyzed by (salen)CrX in the presence of onium salts, unlike the other epoxides, the 1,3-cycloheadiene oxide and CO_2 produce *no trans*-cyclic carbonate. This is ascribed, based on computational studies to the *trans*-1,3-cyclohexadiene carbonate being thermodynamically less stable than its polymeric form. This is further demonstrated when the isolated, pure copolymers is deprotonated by a strong base, no depolymerization takes place with formation of *trans*-1,3-cyclohexadiene carbonate. That is, contrary to the other two closely related polycarbonates, poly(1,3-cyclohexadiene carbonate) does not degrade to cyclic carbonate in the presence of base.

Currently, we are exploring the ring-opening polymerization of *trans*-cyclohexadiene carbonate to afford the corresponding copolymer, for preliminary observations suggest the copolymer produced *via* this route has a different microstructure from that obtained by the copolymerization reaction of the epoxide and CO_2.

CHAPTER VII

SEQUESTERING CO_2 FOR SHORT-TERM STORAGE IN MOFS: COPOLYMER SYNTHESIS WITH OXIRANES*

Introduction

One of the major challenges of the next few decades will be redesigning our present chemical industry to accommodate the widespread use of renewable resources. A viable contribution to this matter will be to convert some of the carbon dioxide emissions into important chemicals and materials needed by the chemical industry. Indeed, carbon capture and utilization used in conjunction with carbon storage can not only provide an alternative and renewable feedstock for the chemical industry, but can generate revenue to offset the cost of carbon capture and storage.

Much current research is being directed worldwide towards the development of processes which use carbon dioxide as a feedstock for producing useful chemicals.[1,127] One of the processes which has proven to be viable, having been commercialized, is the production of polymers derived from CO_2 and propylene oxide.[66] Indeed, presently there are several oxiranes which undergo copolymerization with CO_2 to afford completely alternating copolymers (eq. 25).[2] In addition, this coupling reaction can as well be made selective for producing cyclic carbonates from the cycloaddition of CO_2 and oxiranes

*Reproduced in part with permission from: "Sequestering CO_2 for Short-Term Storage in MOFs: Copolymer Synthesis with Oxiranes." Darensbourg, D. J.; Chung, W.-C.; Wang, K.; Zhou, H.-C. *ACS Catal.* **2014**, *4*, 1511.Copyright 2015. American Chemical Society.

(eq. 26).[67] Although for both of these processes there are several catalytic systems which operate at one atmosphere of CO_2 pressure, in general these processes are enhanced in rate in the presence of higher pressures of CO_2.[128]

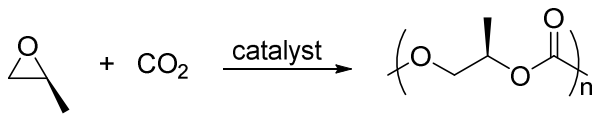

(eq. 25)

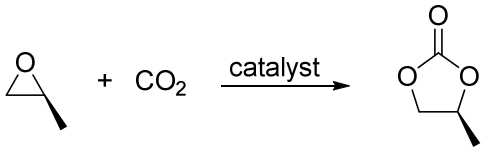

(eq. 26)

Hence, for processes utilizing CO_2 from stationary point sources at or below atmospheric pressure, such as coal-based power generating plants or natural gas production facilities, it would be necessary to first mechanically compress the carbon dioxide in order to enhance the rates of these chemical reactions. Since much progress has been made in the synthesis of metal-organic framework materials (MOFs) for the selective adsorption of CO_2, an alternative approach would be to first sequester the CO_2 employing a solid porous adsorbent material or a metal-organic framework material.[129] *This captured CO_2 could subsequently be released at higher pressures from such origins using heat generated elsewhere in the plant or from solar heat sources.*[75]

Herein, we describe the use of a commercially available metal-organic framework (MOF) material, $[Cu_3(btc)_2(H_2O)_3]$ (btc = benzene-1,3,5-tricarboxylate) otherwise referred to as HKUST-1, for the short term capture and storage of CO_2 and its utilization in the copolymerization with propylene oxide to afford poly(propylene

carbonate).[130] The aim of this study is to examine whether CO_2 collected continuously over a MOF material at atmospheric pressure under aerobic conditions can be effectively copolymerized with epoxides to provide polycarbonates. Comparative studies employing CO_2 from compression storage under anaerobic conditions are also reported. These findings are ultimately necessary as baseline studies for comparable reactions carried out using CO_2 from point source of emission.[75]

Result and Discussion

The MOF material chosen for these studies is the commercially available, highly porous $[Cu_3(btc)_2(H_2O)_3]$ (btc = benzene-1,3,5-tricarboxylate) referred to as HKUST-1.[130,131] The material used herein was synthesized following a slightly modified procedure to that reported by Rowsell and Yaghi.[132] The adsorption properties we determined for this metal organic framework are shown in Figure 42 and Table 20.

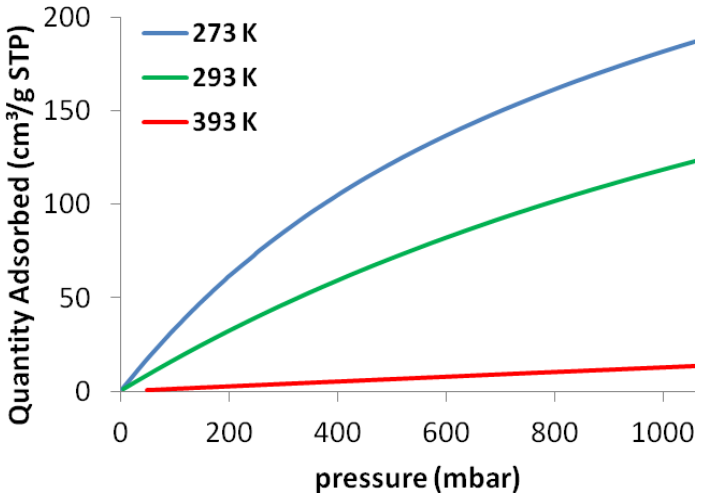

Figure 42 Adsorption properties of our sample of HKUST-1 determined as a function of temperature and pressure.

Table 20 Quantities of CO_2 adsorbed on our sample of HKUST-1 at atmospheric pressure.

	273 K	293K	393K
cm^3 CO_2 (STP) / g MOF	182	118	14
mole CO_2 / g MOF	0.008109	0.005292	0.000639
Total g CO_2 adsorbed (8 g MOF)	2.85	1.86	0.22

The reaction initially examined was the copolymerization of propylene oxide and carbon dioxide (eq. 25), a process well-studied and known to selectively afford completely alternating copolymers of narrow polydispersity. Two types of experiments were performed. The first was designed to test the reproducibility of the process. This was done by carrying out a series of reactions where the MOF vessel was refilled with CO_2 before each run, and the copolymerization process was repeated in a similar manner.

The MOF captured CO_2 was thermally released into a reaction vessel which contained propylene oxide in the presence of a binary catalyst system, (salen)CoDNP/PPNDNP, where DNP = deprotonated 2,4-dinitrophenol. The schematic of the process is depicted in Figure 43 and Figure 44. Pretreatment of the MOF material was accomplished by drying under vacuum at 130 ^{o}C. Subsequently, no care was taken to exclude moist air during refilling cycles of the MOF vessel with CO_2.

(a) **(b)**

Figure 43 (a) 10 mL stainless steel vessel filled with 6.1 g of HKUST-1 and 1.2 g of CO_2. (b) 10 mL stainless steel reactor containing 1.0 mL (14.3 mmol) of propylene oxide and 5.6 mg (7.1 μmoles) of catalyst with 1 equivalent of PPNDNP.

Figure 44 indicates the pressure swings in the MOF vessel during each refilling cycle, where after maximum CO_2 uptake, excess pressure is released leading to vessel **a** being at atmospheric pressure at ambient temperature. *A note of importance, the process described in Figure 44 could as well be achieved adsorbing CO_2 at atmospheric pressure. The employment of higher pressure CO_2 uptake with subsequent release to*

atmospheric pressure is utilized as a matter of convenience for saving time. The graph in Figure 45 represents the time-dependent CO_2 pressure increases upon heating the MOF vessel **a** at 120 ^oC, i.e., prior to injecting CO_2 into the reactor **b**.

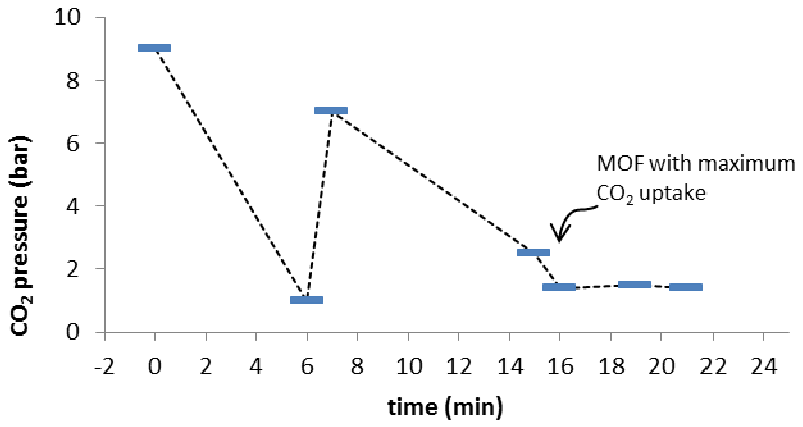

Figure 44 Illustration of CO_2 adsorption process at ambient temperature by HKUST-1, where vessel a was pressurized at 9 and 7 bar to reach maximum CO_2 uptake.

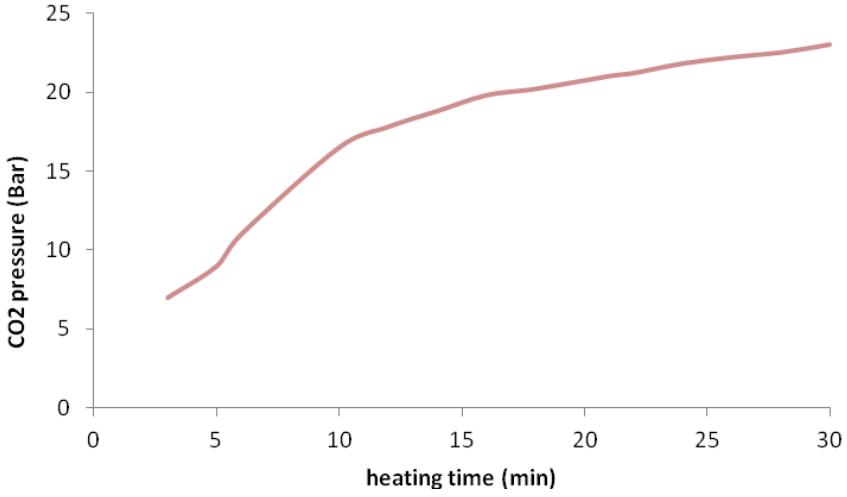

Figure 45 CO_2 released by MOF in vessel a upon heating at 120 ^oC.

The copolymerization results obtained for *ten* reaction cycles of propylene/CO_2 employing the same MOF sample are illustrated in Figure 46 and listed in Table 21. All reactions were carried out under the same conditions as indicated in Figure 43, and the conversions to copolymer are based on spectroscopic (^{1}H NMR) yields. Since these processes are carried out in the absence of added solvent, the copolymerization reactions were terminated < 60% conversion. Otherwise, the reaction mixture becomes too viscous. The CO_2 pressure in the reaction vessel **b** upon opening vessel **a** at 120 ^oC was consistently around 11.0 bar. As indicated in Figure 47 and Table 22, in the CO_2 pressure range between 9 – 15 bar, the rate of the copolymerization reaction is independent of the pressure of CO_2.

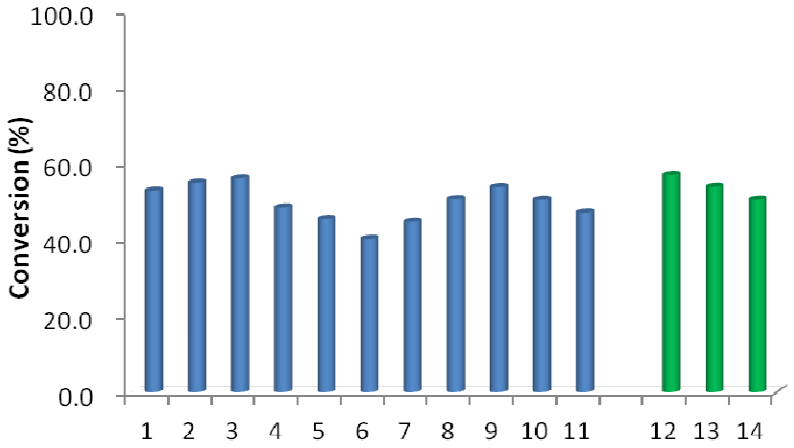

Figure 46 Conversion of propylene oxide/CO_2 to copolymer for reactions carried out for 5 hours at ambient temperature.

Table 21 Copolymerization Reactions of Propylene Oxide/CO_2.

Run	Conv (%)	TOF (h^{-1})	M_n (kDa)	PDI
1	53.0	212.0	8.87	1.06
2	55.0	220.1	8.90	1.05
3	56.1	224.5	9.14	1.05
4	48.6	194.2	7.93	1.05
5	45.6	182.3	7.01	1.06
6	40.4	161.6	7.40	1.05
7	44.8	179.2	6.76	1.06
8	50.7	202.9	8.60	1.06
9	53.9	215.6	9.81	1.07
10	50.5	202.1	8.65	1.06
11[a]	47.3	189.0	9.79	1.12
12[b]	57.1	228.2	12.73	1.06
13[b]	54.0	215.9	13.04	1.08
14[b]	50.6	202.3	12.72	1.08

[a] MOF was exposed in 1 atm CO_2 for 18 h instead of pressurizing to 9 bar in CO_2 adsorption process. [b] Reactions carried out with CO_2 obtained directly from high pressure tank.

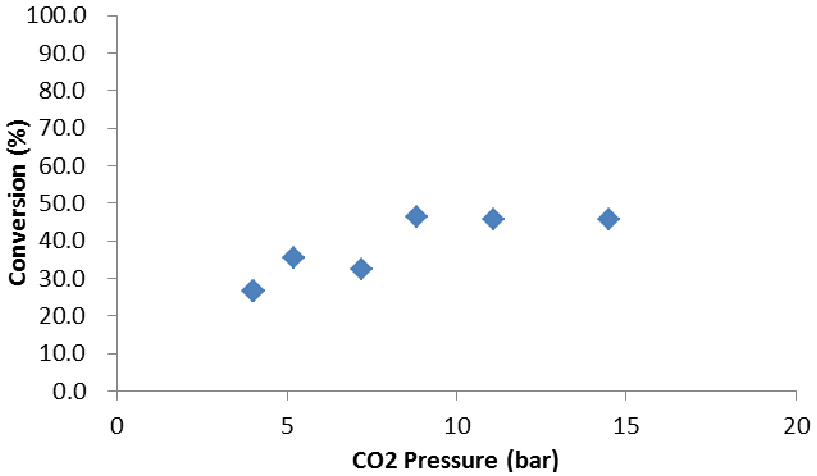

Figure 47 Copolymerization runs as a function of CO_2 pressure. Reaction conditions as in Figure 46.

Table 22 Copolymerization data as a function of CO_2 pressure.

Entry	CO_2 pressure (bar)	Conv (%)	TOF (h^{-1})	M_n (kDa)	PDI
1	14.5	45.5	182.0	8.62	1.06
2	11.1	45.8	183.2	9.32	1.06
3	8.8	46.4	185.7	8.44	1.05
4	7.2	32.4	129.5	5.96	1.07
5	5.2	35.5	142.1	6.58	1.06
6	4.0	26.5	106.0	4.99	1.06

Despite some random variations in the quantity of copolymer produced, the MOF material held up well to continued filling under aerobic conditions and thermally releasing of CO_2. The average propylene oxide/CO_2 conversion to poly(propylene carbonate) over the ten runs was 49.9%. This was only slightly lower than that observed

for three identical processes (Table 21, entries 11-13) carried out under anaerobic conditions with CO_2 taken directly from a pressurized cylinder of 53.9%. Furthermore, the polymeric material afforded from the two different pathways possessed similar T_gs, molecular weights, and polydispersities (see Figure 48). The slight increase in molecular weights of the copolymers produced using CO_2 directly from the CO_2 cylinder are likely due to an increased trace of water in the MOF captured CO_2 reactions. This is seen in the bimodal molecular weight distributions in the GPC traces in Figure 49 for the two different processes.

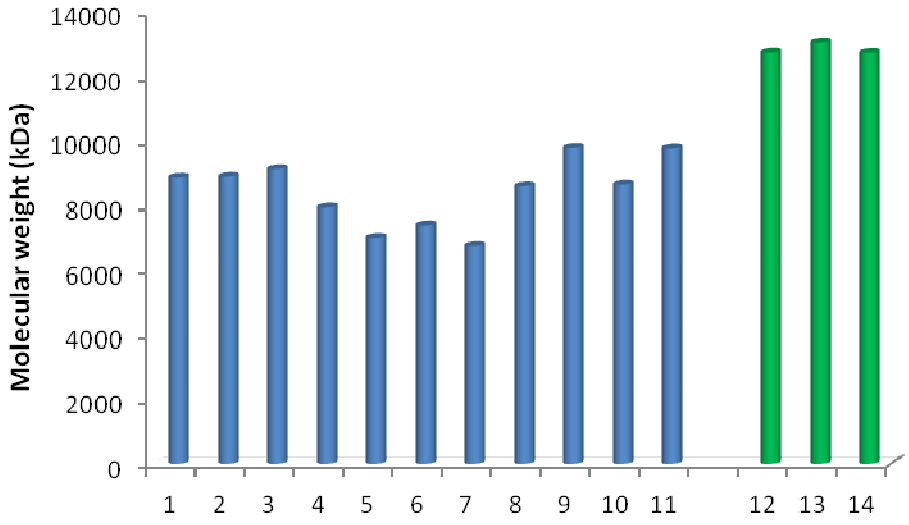

Figure 48 Molecular weight results from ten consecutive runs and the three runs without HKUST-1 (Table 21, entries 11-13). The T_gs of entries 4 and 12 were 34.2 ^oC and 38.6 ^oC, respectively.

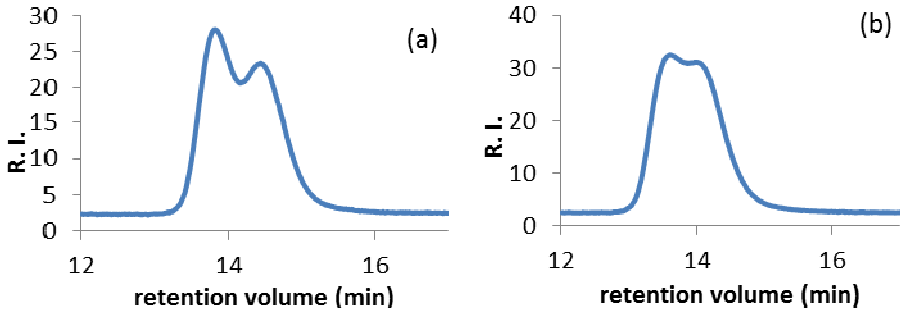

Figure 49 GPC traces for polymer from Table 21 entry 1 (a) and entry 11 (b).

The second set of experiments performed involved the use of a MOF filled vessel which was loaded with CO_2 at 0 ^oC as described previously (Figure 44). This vessel then served as a gas storage unit for carrying out a series of propylene oxide/CO_2 copolymerization reactions. These data are represented in Table 22, where over the series of copolymerization reactions, the pressure decreased from 14.5 bar to 4.0 bar with a concomitant decrease in reactivity occurring below a CO_2 pressure of about 9 bar. Over the course of the six polymerization cycles, 72% of the CO_2 adsorbed on the MOF was converted to poly(propylene carbonate). Also apparent from the data in Table 3, there is a linear relationship between M_n and % conversion (Figure 50). This, coupled with the narrow molecular weight distribution clearly illustrates these processes to be well-controlled.

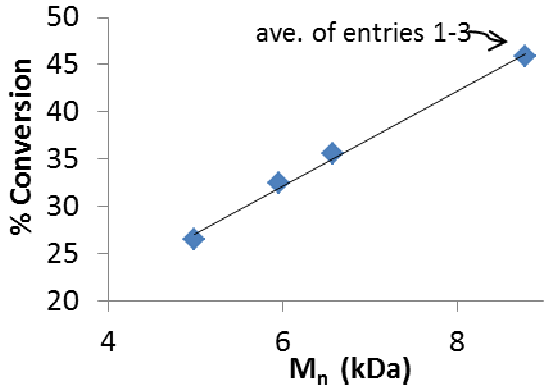

Figure 50 Linear relationship between M_n and % conversion for the copolymerization of propylene oxide and CO_2. Data are found in Table 22. %conversion = 5.03 M_n + 2.01. R^2 = 0.996.

A much less reactive epoxide, *cis*-2-butylene oxide, was examined for its copolymerization characteristics employing CO_2 from the two sources. Employing the bifunctional Cr catalyst (**15**) at 70 ^oC, *cis*-2-butylene oxide and CO_2 produced copolymers with a selectivity of 79% when using pressurized CO_2 directly or CO_2 released following storage over HKUST-1. Poly(butylene carbonate) with a narrow PDI was isolated in both instances with a T_g of 65.3 ^oC.

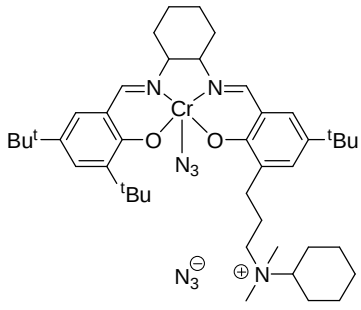

15

Experiental Section

General information

All manipulations involving air- and/or water-sensitive compounds were carried out in a glove box under an argon atmosphere. 1, 3, 5-benzene-tricarboxylate (btc) and copper (II) nitrate hemipentahydrate were purchased from VWR International, LLC, and used as received. Propylene oxide (Alfa Aesar) and *cis*-2-butylene oxide (Alfa Aesar) were stirred over CaH_2, distilled, and stored in an argon-filled glovebox prior to use. Research Grade 99.999% carbon dioxide supplied in a high-pressure cylinder and equipped with a liquid dip tube was purchased from Airgas. The CO_2 was further purified by passing through two steel columns packed with 4 Å molecular sieves that had been dried under vacuum at ≥ 200 ^oC. Powder X-ray diffraction (PXRD) was carried out with a BRUKER D8-Focus Bragg−Brentano X-ray powder diffractometer equipped with a Cu sealed tube (λ = 1.541 78) at 40 kV and 40 mA. Gas adsorption measurements were conducted using a Micrometritics ASAP 2420 system at various temperatures. High pressure stainless steel reactors were dried at 170 ^oC for 6 h before use.

Synthesis

HKUST-1. We modified the approach reported by Roswell and Yaghi[132]: $Cu(NO_3)_2 \cdot 2.5H_2O$ (600 mg), BTC (300 mg) in 15 mL of solvent (DMF: deionized H_2O: EtOH=1:1:1) were ultrasonically dissolved in a Pyrex vial, followed by the addition of 0.7 ml of nitric acid. The mixture was heated at 85 °C in an oven overnight. After cooling down to room temperature, cubic dark blue crystals were harvested by filtration.

The product was soaked in anhydrous methanol and dichloromethane for three days respectively, during which the solvent was decanted and replenished several times. Finally, the solvent was removed under vacuum at 150 °C for 12 h.

Salen cobalt catalyst. This complex was synthesized following the literature procedure.[14] (*S,S*)-*N,N*'-bis(3,5-di-tert-butylsalicylidine)-1,2-cyclohexanediaminocobalt (II) (0.500 g, 0.828 mmol, 1 eq) and 2,4-dinitrophenol (0.152 g, 0.828 mmol, 1 eq) were dissolved in dichloromethane. After bubbling oxygen for one day, the solvent was reduced *in vacuo* followed by recrystallization with hexane. The resulting solid was dried *in vacuo* overnight. The yield was 0.596 g (0.757 mmol) or 91.4%. MS for M-(2,4-dinitrophenoxide): m/z = 603.3338.

Procedure

Representative HKUST-1 CO_2 adsorbing process. A 14 mL high pressure reactor was filled with HKUST-1 (6.1 g) to the top, and was pressurized to 9 bar. After 7 minutes, the pressure decreased to lower than 2 bar and the reactor was pressurized again to 7 bar. After 9 minutes the pressure decreased again and it was released until being stabilized at 1.4 bar.

Copolymerization of propylene oxide and CO_2 from HKUST-1. The HKUST-1 (with CO_2) reactor was heated to 120 ^oC for 30 minutes. And it was subsequently connected to the 14 mL reaction reactor which contained salen cobalt catalyst (5.6 mg, 7.1 µmol, 1 eq), PPNDNP cocatalyst (5.2 mg, 7.1 µmol, 1 eq) and propylene oxide (1.00 mL, 14.3 mmol, 2000 eq). The connector was open for 20 seconds to let CO_2 transfer

from HKUST-1 to reaction, and the remaining CO_2 in the HKUST-1 vessel was released to the atmosphere. After being stirred at ambient temperature for 5 h, the copolymer reactor was put in an ice bath for ten minutes and opened to air, and the NMR spectrum of the crude mixture was taken. The crude reaction mixture was dissolved in CH_2Cl_2 and added to about 1 M HCl/methanol solution to quench the reaction and precipitate the copolymer. The supernatant HCl/methanol solution was removed and the polymer precipitate was re-dissolved in dichloromethane and reprecipitated from methanol. The resulting copolymer was obtained by removing the supernatant and subsequently dried *in vacuo* at 40 ^{o}C for further analysis by GPC and DSC. The whole CO_2 adsorbing-releasing and copolymerization process was repeated ten times to test the sustainability of HKUST-1 of undergoing CO_2 adsorbing-desorbing cycles.

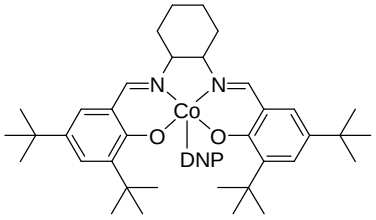

Salen cobalt catalyst

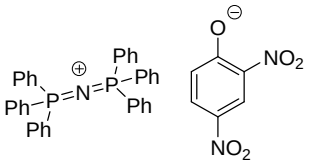

PPNDNP

Copolymerization of propylene oxide and CO_2 without HKUST. The whole process of copolymerization of propylene oxide and CO_2 was repeated except pressurizing an empty high pressure reactor without HKUST-1 to 24 bar thirty minutes before transferring.

Copolymerization of *cis*-2-butylene oxide and CO_2 from HKUST-1. The CO_2 adsorbing process and copolymerization of propylene oxide and CO_2 were repeated

except using a bifunctional salen chromium catalyst (4.9 mg, 5.7 μmol, 1 eq) and *cis*-2-butylene oxide (0.50 mL, 5.7 mmol, 1000 eq).

Copolymerization of propylene oxide and CO_2 without refilling HKUST-1 with CO_2. The same process as mentioned before was repeated six times, except only carrying out CO_2 adsorbing process once at the beginning.

Conclusion

In conclusion, a process for the synthesis of polycarbonates from the metal-catalyzed copolymerization of propylene oxide and CO_2 has been reported, where the CO_2 utilized was collected over the MOF material, HKUST-1, under aerobic conditions and thermally released at the optimal pressure for efficient synthesis. These studies have focused on the *practical*, incorporating our fundamental understanding of CO_2/epoxide coupling reactions, in an effort to begin the long term challenge of utilizing the abundant and renewable CO_2 source for the production of chemicals and fuels. It should be noted that there are reports where active (salen)cobalt or (porphyrin)cobalt catalysts are parts of the coordinated conjugated microporous polymer or metal organic framework structures which have been employed as catalysts for CO_2/epoxide coupling to produce cyclic carbonates.[133,134] However, synthesizing the alternative copolymer products utilizing these catalysts is not possible.

CHAPTER VIII

CONCLUSION

Metal complex catalyzed copolymerization of epoxides and CO_2 presents a route for the production of polycarbonates using a renewable resource. This process was shown to be promising for a variety of epoxides and thus be able to provide a wide range of polycarbonates. Electronics, sterics and structure of epoxide play important roles in CO_2/epoxide copolymerization. Postpolymerization functionalization provides a way to attach functional groups to polycarbonates without interfering with the copolymerization process. With that, a hydrophilic polycarbonate can be made for applications in the biomedical field.

In the copolymerization, coordination of epoxide to the metal center which activates the epoxide is a crucial step. Epoxide coordinating ability was measured by infrared spectroscopy, based on the O-D vibration band shifts of CH_3OD in epoxides versus that observed in benzene. The relationship between the O-D vibration band shifts and the pK_b of bases was determined by a calibration curve from a series of amines. This relationship was then utilized to calculate epoxides' pK_bs. The relative epoxide basicity was observed to be affected by the electronics of the substituent groups.

In the terpolymerization of propylene oxide and styrene oxide with CO_2, each epoxide's reactivity ratio, the ratio of self- and cross-propagation rate, was measured by Fineman-Ross analysis. Reactivity ratio of propylene oxide was found to be larger than one, whereas that of styrene oxide be smaller than one, indicating propylene oxide is

more reactive than styrene oxide. This is due to higher coordinating ability of propylene oxide with a electron-donating methyl group on the epoxide carbon. However, when epoxide coordination factor was taken out from reactivity ratios based on their relative basicities, we found that styrene oxide ring-opens faster than propylene oxide.

On the other hand, steric effects of epoxides are also important in the copolymerization. In order to study the steric effect, I investigated copolymerization of CO_2 with a series of butene oxides with methyl substituent groups at different positions. Among *cis*- and *trans*-2-butene oxide, isobutene oxide and 2-methylbutene oxide, only *cis*-2-butene oxide provided polycarbonate. Coupling reaction of CO_2 with either *trans*-2-butene oxide or isobutene oxide at higher temperature resulted in corresponding cyclic carbonates. The tri-substituted 2-methyl-2-butene oxide did not react with CO_2 at tested temperature. The glass transition temperature (T_g) of polymer heavily depends on the monomer structure. The T_g of poly(2-butene carbonate) derived from copolymerization of CO_2 and *cis*-2-butene oxide was measured to be 68 °C, which is 30 °C higher than poly(propylene carbonate) and 60 °C higher than its isomer poly(1-butene carbonate).

Besides, monomer structure also affects the copolymerization process. For example, cyclohexene oxide easily copolymerizes with CO_2 by conventional cobalt or chromium salen catalysts with onium salt cocatalysts, but cyclopentene oxide does not. Cyclopentene oxide is of interest due to the recyclability of the corresponding polycarbonate to cyclopentene oxide. Bifunctional salen metal complexes bearing tethered cocatalyst, which have been reported to have high activity and polymer selectivity over cyclic product, were shown to be good catalysts for cyclopentene oxide.

Derived from a renewable resource 1,4-cyclohexadiene, 1,4-cyclohexadiene oxide was studied for postpolymerization functionalization from the double bond. Copolymerization of 1,4-cyclohexadiene oxide and CO_2 was much slower than saturated cyclohexene oxide. However, 1,3-cyclohexadiene oxide, having the double bond next to epoxide carbon, showed similar reactivity as cyclohexene oxide. The T_g of poly(1,3-cyclohexadiene carbonate) is 15 ^oC lower than its 1,4-isomer due to the break of monomer symmetry. Furthermore, poly(1,4-cyclohexadiene carbonate) degrades to cyclic carbonate in the presence of a base at high temperature, but the 1,3-isomer does not because of the high free energy of the corresponding cyclic carbonate. Postpolymerizatoin modification of generally hydrophobic polycarbonates can make them more hydrophilic thus provides them wider application in biomedical field. An acetic acid group was built onto the poly(cyclohexadiene carbonate) via thiol-ene click reaction. Further deprotonation turned the polymer water-soluble.

Lastly, a method to use MOF as CO_2 storage for copolymerization was developed. By heating the CO_2 filled MOF, CO_2 was released and thus optimum pressure was created for its copolymerization with propylene oxide. The CO_2 uptake-release-copolymerization cycle was repeated ten times. The propylene oxide conversions and polymer molecular weights from these ten cycles were in the same range and comparable to direct CO_2 utilization without MOF. These studies showed the possibility of practically converting the abundant and renewable CO_2 from point source to the production of useful chemicals.

Overall, this dissertation displayed the copolymerization of CO_2 with various epoxides to make polycarbonates with different thermal and chemical properties. Reactivity, polymer selectivity, glass transition temperature and degradability of a polycarbonate are substantially affected by the nature of the epoxide reagent. The feasibility of conversion of the "wasteful" CO_2 to useful material was demonstrated. Using the epoxides derived from the renewable resource and application of MOF in CO_2 capture from its source will be the future focus of this topic in response to the energy reduction issue for this process.

REFERENCES

1. Aresta, M. *Carbon Dioxide as a Chemical Feedstock*; Aresta, M., Ed., Wiley-VCH: Weinheim, Germany, **2010**.
2. For comprehensive reviews in this area, see: (a) Darensbourg, D. J.; Holtcamp, M. W. *Coord. Chem. Rev.* **1996**, *153*, 155. (b) Coates, G. W.; Moore, D. R. *Angew. Chem., Int. Ed.* **2004**, *43*, 6618. (c) Sugimoto, H.; Inoue, S. *J. Polym. Sci., Part A: Polym. Chem.* **2004**, *42*, 5561. (d) Darensbourg, D. J.; Mackiewicz, R. M.; Phelps, A. L.; Billodeaux, D. R. *Acc. Chem. Res.* **2004**, *37*, 836. (e) Chisholm, M. H.; Zhou, Z. *J. Mater. Chem.* **2004**, *14*, 3081. (f) Darensbourg, D. J. *Chem. Rev.* **2007**, *107*, 2388. (g) Klaus, S.; Lehnmeier, M. W.; Anderson, C. E.; Rieger, B. *Coord. Chem. Rev.* **2011**, *255*, 1460. (h) Kember, M. R.; Buchard, A.; Williams, C. K. *Chem. Commun.* **2011**, *47*, 141. (i) Lu, X.-B.; Darensbourg, D. J. *Chem. Soc. Rev.* **2012**, *41*, 1462. (j) Darensbourg, D. J.; Wilson, S. J. *Green Chem.* **2012**, *45*, 6781. (k) Lu, X.-B.; Ren, W.-M.; Wu, G.-P. *Acc. Chem. Res.* **2012**, *45*, 1721−1735. (l) Paul, S.; Zhu, Y.; Romain, C.; Brooks, R.; Saini, P. K.; Williams, C. K. *Chem. Commun.*, **2015**, *51*, 6459.
3. Fukuoka, S.; Fukawa, I.; Kawamura, M.; Komiya, K.; Tojo, M.; Hachiya, H.; Hasagawad, K.; Aminaka, M.; Okamoto, H.; Konno, S. *Green Chemistry*, **2003**, *5*, 497.
4. Inoue, S.; Koinuma, H.; Tsuruta, T. *J. Polym. Sci., Part B: Polym. Lett.* **1969**, *7*, 287.
5. Darensbourg, D. J.; Yarbrough, J. C. *J. Am. Chem. Soc.* **2002**, *124*, 6335.

6. Qin, z.; Thomas, C. M.; Lee, S.; Coates, G. W. *Angew. Chem. Int. Ed.* **2003**, *42*, 5484.
7. Lu, X.-B.; Wang, Y. *Angew. Chem. Int. Ed.* **2004**, *43*, 3574.
8. Nakano, K.; Kamada, T.; Nozaki, K. *Angew. Chem., Int. Ed.* **2006**, *45*, 7274.
9. Noh, E. K.; Na, S. J.; S, S.; Kim, S.-W.; Lee, B. Y. *J. Am. Chem. Soc.* **2007**, *129*, 8082.
10. S, S.; Min, J. K.; Seong, J. E.; Na, S. J.; Lee, B. Y. *Angew. Chem. Int. Ed.* **2008**, *47*, 7306 .
11. Na, S. J.; S, S.; Cyriac, A.; Kim, B. E.; Yoo, J.; Kang, Y. K.; Han, S. J.; Lee, C.; Lee, B. Y. *Inorg. Chem.* **2009**, *48*, 10455.
12. Ren, W.-M.; Liu, Z.-W.; Wen, Y.-Q.; Zhang, R.; Lu, X.-B. *J. Am. Chem. Soc.* **2009**, *131*, 11509.
13. Liu, J.; Ren, W.-M.; Liu, Y.; Lu, X.-B. *Macromolecules*, **2013**, *46*, 1343.
14. Lu, X.-B.; Shi, L.; Wang, Y.-M.; Zhang, R.; Zhang, Y.-J.; Peng, X.-J.; Zhang, Z.-C.; Li, B. *J. Am. Chem. Soc.* **2006**, *128*, 1664.
15. Ren, W.-M.; Liu, Y.; Wu, G.-P.; Liu, J.; Lu, X.-B. *J. Polym. Sci. Part A: Polym. Chem*. **2011**, *49*, 4894.
16. Seong, E. J.; Na, S. J.; Cyriac, A.; Kim, B.-W.; Lee, B. Y. *Macromolecules* **2010**, *43*, 903.
17. Ren, W.-M.; Zhang, X.; Liu, Y.; Li, J.-F.; Wang, H.; Lu, X.-B. *Macromolecules* **2010**, *43*, 1396.

18. Wu, G.-P.; Wei, S.-H.; Ren, W.-M.; Lu, X.-B.; Xu, T.-Q.; Darensbourg, D. J. *J. Am. Chem. Soc*. **2011**, *133*, 15191.

19. Wu, G.-P.; Xu, P.-X.; Lu, X.-B.; Zu, Y.-P.; Wei, S.-H.; Ren, W.-M.; Darensbourg, D. J. *Macromolecules* **2013**, *46*, 2128.

20. (a) Wu, G.-P.; Wei, S.-H.; Lu, X.-B.; Ren, W.-M.; Darensbourg, D. J.; *Macromolecules*, **2010**, *43*, 9202. (b) Wu, G.-P.; Wei, S.-H.; Ren, W.-M.; Lu, X.-B.; Li, B.; Zu, Y.-P.; Darensbourg, D. J. *Energy Environ. Sci*. **2011**, *4*, 5084.

21. Darensbourg, D. J.; Tsai, F.-T. *Macromolecules* **2014**, *47*, 3806.

22. Ren, W.-M.; Liang, M.-W.; Xu, Y.-C.; Lu, X.-B. *Polym. Chem*., **2013**, *4*, 4425.

23. (a) Zhou, Q.; Gu, L.; Gao, Y.; Qin, Y.; Wang, X.; Wang, F *J. Polym. Sci. Part A: Polym. Chem*. **2013**, *51*, 1893. (b) Gu, L.; Qin, Y.; Gao, Y.; Wang, X.; Wang, F. *J. Polym. Sci. Part A: Polym. Chem*. **2013**, *51*, 2834.

24. Zhang, H.; Grinstaff, M. W. *J. Am. Chem. Soc.* **2013**, *135*, 6806.

25. Zhang, H.; Grinstaff, M. W. *J. Appl. Polym. Sci.* **2014**, DOI: 10.1002/app.39893.

26. Konieczynska, M. D.; Lin, X.; Zhang, H.; Grinstaff, M. W. *ACS Macro Lett.* **2015**, *4*, 533.

27. Darensbourg, D. J.; Wang, Y. *Polym. Chem.*, **2015**, *6*, 1768.

28. Hilf, J.; Scharfenberg, M.; Poon, J.; Moers, C.; Frey, H. *Macromol. Rapid Commun*. **2015**, *36*, 174.

29. Darensbourg, D. J.; Yarbrough, J. C.; Ortiz, C.; Fang, C. C. *J. Am. Chem. Soc.* **2003**, *125*, 7586.

30. Cohen, C. T.; Thomas, C. M.; Peretti, K. L.; Lobkovsky, E. B.; Coates¸G. W. *Dalton Trans*., **2006**, 237.

31. Shi, L.; Lu, X.-B.; Zhang, R.; Peng, X.-J.; Zhang, C.-Q.; Li, J.-F.; Peng, X.-M. *Macromolecules* **2006**, *39*, 5679.

32. Darensbourg, D. J.; Rodgers, J. L.; Fang, C. C. *Inorg. Chem.* **2003**, *42*, 4498.

33. Cherian, A. E.; Sun, F. C.; Sheiko, S. S.; Coates, G. W. *J. Am. Chem. Soc.* **2007**, *129*, 11350.

34. Liu, Y.; Ren, W.-M.; Liu, J.; Lu, X.-B. *Angew. Chem. Int. Ed*. **2013**, *52*, 11594.

35. Darensbourg, D. J.; Wilson, S. J. *J. Am. Chem. Soc.* **2011**, *133*, 18610.

36. Darensbourg, D. J.; Wilson, S. J. *Macromolecules* **2013**, *46*, 5929.

37. Darensbourg, D. J.; Fang, C. C.; Rodgers, J. L. *Organometallics* **2004**, *23*, 924.

38. Liu, Y.; Ren, W.-M.; He, K.-K.; Lu, X-B. *Nat. Commun.* **2014**, DOI: 10.1038/ncomms6687.

39. Darensbourg, D. J.; Chung, W.-C.; Wilson, S. J. *ACS Catal.* **2013**, *3*, 3050.

40. Liu, Y.; Wang, M.; Ren, W.-M.; He, K.-K.; Xu, Y.-C.; Liu, J.; Lu, X.-B. *Macromolecules* **2014**, *47*, 1269.

41. Darensbourg, D. J.; Ulusoy, M.; Karroonnirum, O.; Poland, R. R.; Reibenspies, J. H.; Çetinkaya, B. *Macromolecules* **2009**, *42*, 6992.

42. Fox, T. G.; Loshaek, S. *J. Polym. Sci.* **1955**, *15*, 371.

43. Fineman, M.; Ross, S. D. *J. Polym. Sci.* **1950**, *5*, 259.

44. Darensbourg, D. J.; Poland, R. R.; Strickland, A. L. *J. Polym. Sci., Part A: Polym. Chem.* **2012**, *50*, 127.

45. Wu, G.-P.; Xu, P.-X.; Zu, Y.-P.; Ren, W.-M.; Lu, X.-B. *J. Polym. Sci., Part A: Polym. Chem.* **2013**, *51*, 874.

46. X. Wu , H. Zhao , B. Nörnberg , P. Theato , G. A. Luinstra , *Macromolecules* **2014** , *47* , 492 .

47. (a) Geschwind , J; Frey, H. *Macromolecules* **2013**, *46*, 3280. (b) Geschwind , J; Frey, H. *Macromol. Rapid Commun.* **2013**, *34*, 150. (c) Hilf, J.; Phillips, A.; Frey, H. *Polym. Chem.* **2014**, *5*, 814.

48. Geschwind , J; Frederik, W.; Frey, H. *Macromol. Chem. Phys.* **2013**, *214*, 892.

49. (a) Kim, J. G.; Cowman, C. D.; LaPointe, A, M.; Wiesner, U.; Coates, G. W. *Macromolecules* **2011**, *44*, 1110. (b) Kim, J. G.; Coates, G. W. *Macromolecules* **2012**, *45*, 7878.

50. (a) Wu, G.-P; Darensbourg, D. J.; Lu, X.-B. *J. Am. Chem. Soc.* **2012**, *134*, 17739. (b) Wu, G.-P; Darensbourg, D. J. *Angew. Chem. Int. Ed.* **2013**, *52*, 10602.

51. Sakakura, T.; Choi, J.-C.; Yasuda, H. *Chem. Rev.* **2007**, *107*, 2365.

52. Yamashita, Y.; Tsuda, T.; Okada, M.; Iwatsuki, S. *J. Polym. Sci.. A-1* **1966**, *4*, 2121.

53. (a) Gordy, W. *J. Chem. Phys.* **1939**, *7*, 93. (b) Gordy, W. *J. Chem. Phys.*. **1940**, *8*, 170. (c) Gordy, W.; Stanford, S. C. *J. Chem. Phys.*. **1941**, *9*, 204. (d) Gordy, W. *J. Chem. Phys.* **1941**, *9*, 215.

54. (a) Hall, H. K. Jr., *J. Am. Chem. Soc.* **1957**, *79*, 5441. (b) Hall, N. F. *J. Am. Chem. Soc.* **1930**, *52*, 5115. (c) Hall, N. F.; Sprinkle, M. R.; *J. Am. Chem. Soc.* **1932**, *54*, 3469. (d) Zevatskii, Y. ; Lysora, S. *Russ. J. Org. Chem.* **2009**, *45*, 825. (e) Pearson, R.

G.; Williams, F. V. *J. Am. Chem. Soc*. **1953**, *75*, 3073. (f) Fujii, T.; Nishida, H.; Abiru, Y.; Yamamoto, M.; Kise, M. *Chem. Pharm. Bull*. **1995**, *43*, 1872.

55. Strong, J. *Rev. Sci. Instrum.* **1931**, *2*, 585.
56. Arnett, E. M.; Wu, C. Y. *J. Am. Chem. Soc.* **1962**, *84*, 1684.
57. Gorshkova, G. N.; Barinova, Z. B.; Aleksanyan, V. T.; Ponomarenko, V. A. *Russian Chemical Bulletin* **1968**, *17*, 303.
58. Jacobsen, E. N. *Acc. Chem. Res*. **2000**, *33*, 421.
59. Darensbourg, D. J.; Niezgoda, S. A.; Holtcamp, M. W.; Draper, J. D.; Reibenspies, J. H. *Inorg.Chem*.**1997**, *36*, 2426.
60. Darensbourg, D. J.; Billodeaux, D. R.; Perez, L. M. *Organometallics* **2004**, *23*, 5286.
61. Darensbourg, D. J.; Holtcamp, M. W.; Khandelwal, B.; Klausmeyer, K. K.; Reibenspies, J. H. *J. Am. Chem. Soc*. **1995**, *117*, 538.
62. Darensbourg, D. J.; Moncada, A. I.; Choi, W.; Reibenspies, J. H. J. Am. Chem. Soc. **2008**, *130*, 6523.
63. Darensbourg, D. J.; Moncada, A. I. *Inorg. Chem*. **2008**, *47*, 10000.
64. For a brief review of the life of Walter Gordy, see: J. Mol. Struct. **1988**, *190*, 1.
65. Omae, I. *Coord. Chem. Rev.* **2012**, *256*, 1384
66. (a) Novomer: Carbon Dioxide, http://www.novomer.com/?action=CO2, accessed 17 July 2015. (b) Empower Materials: Home, www.empowermaterials.com, accessed 17 July 2015. (c) Ok, M.-A.; Jeon, M. *Properties of poly(propylene carbonate) produced via SK Energy's Greenpol™ Technology*, ANTEC 2011 Plastics: Annual Technical Conference Proceedings. Society of Plastics Engineers. **2011**. (d) Lee, B.

Y.; Cyriac, A. *Nat. Chem.* **2011**, *3*, 505. (e) Aschenbrenner, N.; Kunze, K., Green Polymer Made of CO_2 from Exhaust Gases, http://w1.siemens.com.cn/news_en/frontier_technology_en/2292.aspx, accessed 17 July 2015. Econic Technologies: Polymers from CO_2, http://www.econic-technologies.com/, accessed 17 July 2015.

67. (a) North, M.; Pasquale, R.; Young, C. *Green Chem.* **2010**, *12*, 1514. (b) DeCortes, A.; Castilla, A. M.; Kleij, A. W. *Angew. Chem. Int. Ed.* **2010**, *49*, 9822.
68. Yoo, J.; Na, S. J.; Park, H. C.; Cyriac, A.; Lee, B. Y. *Dalton Trans.* **2010**, *39*, 2622.
69. Nozaki, K.; Nakano, K.; Hiyama, T. *J. Am. Chem. Soc.* **1999**, *121*, 11008.
70. Acemoglu, M.; Nimmerfall, F.; Bantle, S.; Stoll, G. H. *J. Control. Release* **1997**, *49*, 263.
71. Cyriac, A.; Lee, S. H.; Varghese, J. K.; Park, E. S.; Park, J. H.; Lee, B. Y. *Macromolecules* **2010**, *43*, 7398.
72. Whiteoak, C. J.; Martin, E.; Escudero-Adán, E.; Kleij, A. W. *Adv. Synth. Catal.* **2013**, *355*, 2233.
73. Byrne, C. M.; Allen, S. D.; Lobkovsky, E. B.; Coates, G. W. *J. Am. Chem. Soc.* **2004**, *126*, 11404.
74. Unpublished preliminary results from our laboratory by Mireya Luna.
75. von der Assen, N.; Jung, J.; Bardow, A. *Energy Environ. Sci.* **2013**, *6*, 2721.
76. Darensbourg, D. J.; Yeung, A. D. *Macromolecules* **2013**, *46*, 83.
77. Darensbourg, D. J.; Yeung, A. D.; Wei, S.-H. *Green Chem.* **2013**, *15*, 1578.

78. Darensbourg, D. J.; Wei, S.-H.; Yeung, A. D.; Ellis, W. C. *Macromolecules* **2013**, *46*, 5850.

79. Cheng, M.; Darling, N. A.; Lobkovsky, E. B.; Coates, G. W. *Chem. Commun.* **2000**, 2007.

80. A copolymer of CPO/CO_2 has been reported to be produced from a reaction catalyzed by a DMC complex derived from $K_3Co(CN)_6$ and ZnX_2 (X = F, Cl, Br, I) with greatly reduced CO_2 content (33 – 37%). Kim, I.; Yi, M. J.; Lee, K. J.; Park, D.-W.; Ki, B. U.; Ha, C.-S., *Catal. Today*, 2006, **111**, 292.

81. Darensbourg, D. J.; Wilson, S. J.; Yeung, A. D. *Macromolecules* **2013**, *46*, 8102.

82. Iqbal, S. M.; Owen, L. N. *J. Chem. Soc.* **1960**, 1030.

83. Koning, C.; Wildeson, J.; Parton, R.; Plum, B.; Steeman, P.; Darensbourg, D. J. *Polymer* **2001**, *42*, 3995.

84. (a) *APEX2*, 2009.7-0; Bruker AXS Inc.: Madison, WI, **2007**. (b) *SAINTPLUS: Program for Reduction of Area Detector Data*, 6.63; Bruker AXS Inc.: Madison, WI, **2007**. (c) Sheldrick, G.M. *SADABS: Program for Absorption Correction of Area Detector Frames*, Bruker AXS Inc.: Madison, WI, **2001**. (d) Sheldrick, G.M. *SHELXS-97: Program for Crystal Structure Solution*, Universitat Gottingen: Gottingen, Germany, **1997**. (e) Sheldrick, G.M. *SHELXL-97: Program for Crystal Structure Refinement.* Universitat Gottingen: Gottingen, Germany, **1997**.

85. Darensbourg, D. J.; Mackiewicz, R. M.; Rodgers, J. L.; Fang, C. C.; Billodeaux, D. R.; Reibenspies, J. H. *Inorg. Chem.* **2004**, *43*, 6024.

86. Darensbourg, D. J.; Yeung, A. D. *Polymer Chemistry* **2014**, *5*, 3949.

87. Winkler, M.; Romain, C.; Meier, M. A. R.; Williams, C. K. *Green Chem.* **2015**, *17*, 300.

88. Dondoni, A. *Angew. Chem., Int. Ed.* **2008**, *47*, 8995.

89. Zhang, J.-F.; Ren, W.-M.; Sun, X.-K.; Meng, Y.; Du, B.-Y.; Zhang, X.-H. *Macromolecules* **2011**, *44*, 9882.

90. Hilf, J.; Frey, H. *Macromol. Rapid. Commun.* **2013**, *34*, 1395.

91. (a) Mathers, R. T.; Shreve, M. J.; Meyler, E.; Damodaran, K.; Iwig, D. F.; Kelley, D. J. *Macromol. Rapid Commun.* **2011**, *32*, 1338. (b) Mutlu, H.; Hafsa, R.; Montenegro, R. E.; Meier, M. A. R. *RSC Adv.* **2013**, *3*, 4927. (c) Mmongoyo, J. A.; Mgani, Q. A.; Mdachi, S. J. M.; Pogorzelec, P. J.; Cole-Hamilton, D. J. *Eur. J. Lipid Sci. Technol.* **2012**, *114*, 1183.

92. Zhang, H.; Liu, H.-B.; Yue, J.-M. *Chem. Rev.* **2014**, *114*, 883.

93. Line, K.; Isupov, M. N.; Littlechild, J. A. *J. Mol. Biol.* **2004**, *338*, 519.

94. Connelly, S.; Line, K.; Isupov, M. N.; Littlechild, J. A. *Org. Biomol. Chem.* **2005**, *3*, 3260.

95. Marco-Contalles, J.; Molina, M. T.; Anjum, S. *Chem. Rev.* **2004**, *104*, 2857.

96. (a) Tan, Q.; Hayashi, M. *Org. Lett.* **2009**, *11*, 3314. (b) Burns, D. J.; Hachisu, S.; O'Brien, P.; Taylor, R. J. K. *Org. Biomol. Chem.* **2012**, *10*, 7666.

97. (a) O'Brien, P.; Poumellee, P. *J. Chem. Soc., Perkin Trans.* **1998**, *1*, 2435. (b) deSousa, S. E.; O'Brien, P.; Pilgram, C. D. *Tetrahedron* **2002**, *58*, 4643.

98. Burk, R. M.; Roof, M. B. *Tetrahedron Lett.* **1993**, *34*, 395.

99. Darensbourg, D. J.; Kyran, S. J.; Arp, C. J., unpublished results.

100. Dümler, W.; Kisch, H. *Chem. Ber.* **1990**, *123*, 277.

101. Darensbourg, D. J.; Wei, S.-H. *Macromolecules* **2012**, *45*, 5916.

102. Honda, S.; Mori, T.; Goto, H.; Sugimoto, H. *Polymer* **2014**, 55, 4832.

103. Michaud, S.; Viala, J. *Tetrahedron* **1999**, *55*, 3019.

104. Darensbourg, D. J.; Moncada, A. I.; Wei, S.-H. *Macromolecules* **2011**, *44*, 2568.

105. Darensbourg, D. J.; Chung, W.-C.; Arp, C. J.; Tsai, F.-T.; Kyran, S. J. *Macromolecules* **2014**, *47*, 7347.

106. Darensbourg, D. J.; Chung, W.-C. *Polyhedron*, **2013**, *58*, 139.

107. Darensbourg, D. J.; Yeung, A. Y. *Polym. Chem.* **2015**, *6*, 1103.

108. An alternate synthesis of this epoxide is reported in the literature. Crandall, J. K.; Banks, D. B.; Colyer, R. A.; Watkins, R. J.; Arrington, J. P. *J. Org. Chem.* **1968**, *33*, 423.

109. Diallo, A. K.; Kirillov, E.; Slawinski, M.; Brusson, J.-M.; Guillaumea, S. M.; Carpentier, J.-F. *Polym. Chem.* **2015**, *6*, 1961.

110. (a) Inoue, S.; Koinuma, H.; Yokoo, Y.; Tsuruta, T. *Makromol. Chem.* **1971**, *143*, 97. (b) Darensbourg, D. J.; Holtcamp, M. W.; Strack, G. E.; Zimmer, M. S.; Niezgoda, S. A.; Rainey, P.; Robertson, J. B.; Draper, J. D.; Reibenspies, J. H. *J. Am. Chem. Soc.* **1999**, *121*, 107.

111. Darensbourg, D. J.; Lewis, S. J.; Rodgers, J. L.; Yarbrough, J. C. *Inorg. Chem.* **2003**, *42*, 581.

112. Macrae, C. F.; Edgington, P. R.; McCabe, P.; Pidcock, E.; Shields, G. P.; Taylor, R.; Towler, M.; van de Streek, J. *J. Appl. Cryt.* **2006**, *39*, 453.

113. Gaussian 09. Frisch, M. J.; Trucks, G. W.; Schlegel, H. B.; Scuseria, G. E.; Robb, M. A.; Cheeseman, J. R.; Scalmani, G.; Barone, V.; Mennucci, B.; Petersson, G. A.; Nakatsuji, H.; Caricato, M.; Li, X.; Hratchian, H. P.; Izmaylov, A. F.; Bloino, J.; Zheng, G.; Sonnenberg, J. L.; Hada, M.; Ehara, M.; Toyota, K.; Fukuda, R.; Hasegawa, J.; Ishida, M.; Nakajima, T.; Honda, Y.; Kitao, O.; Nakai, H.; Vreven, T.; Montgomery, J. A., Jr.; Peralta, J. E.; Ogliaro, F.; Bearpark, M.; Heyd, J. J.; Brothers, E.; Kudin, K. N.; Staroverov, V. N.; Kobayashi, R.; Normand, J.; Raghavachari, K.; Rendell, A.; Burant, J. C.; Iyengar, S. S.; Tomasi, J.; Cossi, M.; Rega, N.; Millam, J. M.; Klene, M.; Knox, J. E.; Cross, J. B.; Bakken, V.; Adamo, C.; Jaramillo, J.; Gomperts, R.; Stratmann, R. E.; Yazyev, O.; Austin, A. J.; Cammi, R.; Pomelli, C.; Ochterski, J. W.; Martin, R. L.; Morokuma, K.; Zakrzewski, V. G.; Voth, G. A.; Salvador, P.; Dannenberg, J. J.; Dapprich, S.; Daniels, A. D.; Farkas, Ö.; Foresman, J. B.; Ortiz, J. V.; Cioslowski, J.; Fox, D. J. Gaussian Inc., Wallingford CT, **2009**.

114. Ampac GUI 9. Semichem, Inc., **2008**.

115. Hanwell, M. D.; Curtis, D. E.; Lonie, D. C.; Vandermeersch, T.; Zurek, E.; Hutchison, G. R. *J. Cheminf.* **2012**, *4*, 17.

116. Darensbourg, D. J.; Yeung, A. D. *Green Chem.* **2014**, *16*, 247.

117. Montgomery, J. A.; Frisch, M. J.; Ochterski, J. W.; Petersson, G. A. *J. Chem. Phys.* **1999**, *110*, 2822.

118. Ochterski, J. W.; Petersson, G. A.; Montgomery, J. A. *J. Chem. Phys.* **1996**, *104*, 2598.

119. Zhao, Y.; Truhlar, D. G. *Theor. Chem. Acc.* **2008**, *120*, 215.

120. Zhao, Y.; Truhlar, D. G. *J. Chem. Phys.* **2006**, *125*, 194101/1.

121. Dolg, M.; Wedig, U.; Stoll, H.; Preuss, H. *J. Chem. Phys.* **1987**, *86*, 866.

122. Petersson, G. A.; Bennett, A.; Tensfeldt, T. G.; Al-Laham, M. A.; Shirley, W. A.; Mantzaris, J. *J. Chem. Phys.* **1988**, *89*, 2193.

123. Petersson, G. A.; Al-Laham, M. A. *J. Chem. Phys.* **1991**, *94*, 6081.

124. Montgomery, J. A.; Frisch, M. J.; Ochterski, J. W.; Petersson, G. A. *J. Chem. Phys.* **2000**, *112*, 6532.

125. Parthiban, S.; de Oliveira, G.; Martin, J. M. L. *J. Phys. Chem. A* **2001**, *105*, 895.

126. Marenich, A. V.; Cramer, C. J.; Truhlar, D. G. *J. Phys. Chem. B* **2009**, *113*, 6378.

127. (a) Sakakura, T.; Choi, J.-C.; Yasuda, H. *Chem. Rev.* **2007**, *107*, 2364. (b) Riduan, S. N.; Zhang, Y. *Dalton Trans.* **2010**, *39*, 3347. (c) Cokaja, M.; Bruckweier, C.; Rieger, B.; Herrmann, W. A.; Kühn, F. E. *Angew. Chem., Int. Ed.* **2011**, *50*, 8510.

128. Exceptions to that statement can be found: (a)Qutz, F.; Buchard, A.; Kember, M. R.; Fredrichson, S. B.; Williams, C. K. *J. Am. Chem. Soc.* **2011**, *133*, 17395. (b) Buchard, A.; Qut, F.; Kember, M. R.; White, A. J. P.; Rzepa, H. S.; Williams, C. K. *Macromolecules*, **2012**, *45*, 6781.

129. (a) Sumida, K.; Rogow, D. L.; Mason, J. A.; McDonald, T. M.; Bloch, E. D.; Herm, Z. R.; Bae, T.-H.; Long, J. R. *Chem. Rev.* **2012**, *112*, 724. (b) MacDowell, N.; Florin, N.; Buchard, A.; Hallett, J.; Galindo, A.; Jackson, G.; Adjiman, C. S.; Williams, C. K.; Shah, N.; Fennell, P. *Energy Environ. Sci.* **2010**, *3*, 1645.

130. Chui, S. S.-Y.; Lo, S. M.-F.; Charmant, J. P. H.; Orpen, A. G.; Williams, I. D. *Science* **1999**, *283*, 1148.

131. Jacoby, M. *C&EN* **2013**, *91*, Issue 51, 34.

132. Rowsell, J. L. C.; Yaghi, O. M. *J. Am. Chem. Soc.* **2006**, *128*, 1304.

133. Xie, Y.; Wang, T.-T.; Liu, X.-H.; Zou, K.; Deng, W.-Q. *Nat. Commun.* **2013**, *4*, DOI: 10.1038/ncomms2960.

134. Feng, D.; Chung, W.-C.; Wei, Z.-W.; Gu, Z. Y.; Jiang, H. L.; Darensbourg, D. J.; Zhou, H.-C. *J. Am. Chem. Soc.* **2013**, *135*, 17105.

APPENDIX

Crystallographic Data for trans-1,3-CHDC

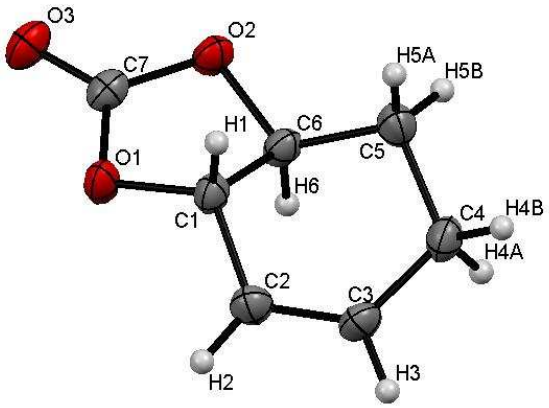

Table A1 Crystal data and structure refinement for 13CHDC.

Identification code	orthop212121	
Empirical formula	C7 H8 O3	
Formula weight	140.13	
Temperature	150(2) K	
Wavelength	0.71073 Å	
Crystal system	Orthorhombic	
Space group	P2(1)2(1)2(1)	
Unit cell dimensions	a = 6.871(5) Å	= 90°.
	b = 9.094(7) Å	= 90°.
	c = 10.694(8) Å	= 90°.
Volume	668.3(9) $Å^3$	
Z	4	
Density (calculated)	1.393 Mg/m^3	
Absorption coefficient	0.110 mm^{-1}	
F(000)	296	

Table A1 Continued

Crystal size	0.60 x 0.20 x 0.15 mm^3
Theta range for data collection	2.94 to 28.47°.
Index ranges	-9<=h<=9, -12<=k<=12, -14<=l<=14
Reflections collected	8032
Independent reflections	1658 [R(int) = 0.0612]
Completeness to theta = 28.47°	98.3 %
Absorption correction	None
Max. and min. transmission	0.9838 and 0.9372
Refinement method	Full-matrix least-squares on F^2
Data / restraints / parameters	1658 / 0 / 91
Goodness-of-fit on F^2	1.017
Final R indices [I>2sigma(I)]	R1 = 0.0406, wR2 = 0.0910
R indices (all data)	R1 = 0.0485, wR2 = 0.0950
Absolute structure parameter	-0.5(12)
Largest diff. peak and hole	0.144 and -0.179 e.$Å^{-3}$

Table A2 Atomic coordinates (x 10^4) and equivalent isotropic displacement parameters ($Å^2$x 10^3) for 13CHDC. U(eq) is defined as one third of the trace of the orthogonalized U^{ij} tensor.

	x	y	z	U(eq)
O(3)	1317(2)	9405(1)	5951(1)	34(1)
O(2)	2885(2)	7477(1)	6817(1)	28(1)
O(1)	171(2)	7104(1)	5694(1)	28(1)
C(2)	159(3)	4311(2)	5769(2)	28(1)
C(3)	1308(3)	3192(2)	6073(2)	29(1)
C(4)	3094(3)	3291(2)	6902(2)	29(1)
C(6)	2749(2)	5905(2)	6546(2)	25(1)
C(7)	1450(3)	8108(2)	6139(2)	25(1)
C(1)	604(2)	5744(2)	6370(2)	24(1)
C(5)	3470(3)	4819(2)	7487(2)	31(1)

Table A3 Bond lengths [Å] and angles [°] for 13CHDC.

O(3)-C(7)	1.199(2)
O(2)-C(7)	1.352(2)
O(2)-C(6)	1.462(2)
O(1)-C(7)	1.354(2)
O(1)-C(1)	1.464(2)
C(2)-C(3)	1.328(2)
C(2)-C(1)	1.484(2)
C(3)-C(4)	1.517(3)
C(4)-C(5)	1.546(3)
C(6)-C(1)	1.493(3)
C(6)-C(5)	1.495(2)
C(7)-O(2)-C(6)	105.21(12)
C(7)-O(1)-C(1)	105.36(13)
C(3)-C(2)-C(1)	116.36(16)
C(2)-C(3)-C(4)	125.33(16)
C(3)-C(4)-C(5)	115.16(14)
O(2)-C(6)-C(1)	100.61(12)
O(2)-C(6)-C(5)	119.46(14)
C(1)-C(6)-C(5)	110.31(15)
O(3)-C(7)-O(2)	124.23(16)
O(3)-C(7)-O(1)	123.71(17)
O(2)-C(7)-O(1)	112.05(14)
O(1)-C(1)-C(2)	119.08(14)
O(1)-C(1)-C(6)	100.36(13)
C(2)-C(1)-C(6)	110.13(14)
C(6)-C(5)-C(4)	105.43(14)

Table A4 Anisotropic displacement parameters ($Å^2 x\ 10^3$) for 13CHDC. The anisotropic displacement factor exponent takes the form: $-2\ ^2[\ h^2\ a^{*2}U^{11} + ... + 2\ h\ k\ a^*\ b^*\ U^{12}\ ]$

	U^{11}	U^{22}	U^{33}	U^{23}	U^{13}	U^{12}
O(3)	40(1)	19(1)	43(1)	2(1)	5(1)	1(1)
O(2)	29(1)	18(1)	36(1)	-3(1)	-4(1)	-2(1)
O(1)	31(1)	18(1)	36(1)	4(1)	-8(1)	1(1)
C(2)	31(1)	24(1)	30(1)	-1(1)	-5(1)	-3(1)
C(3)	36(1)	18(1)	32(1)	-3(1)	-3(1)	-2(1)
C(4)	30(1)	21(1)	36(1)	3(1)	-2(1)	4(1)
C(6)	26(1)	17(1)	31(1)	-2(1)	-1(1)	-1(1)
C(7)	27(1)	20(1)	28(1)	-1(1)	5(1)	0(1)
C(1)	26(1)	18(1)	28(1)	3(1)	-3(1)	2(1)
C(5)	30(1)	27(1)	35(1)	1(1)	-10(1)	2(1)

Table A5 Hydrogen coordinates ($x\ 10^4$) and isotropic displacement parameters ($Å^2 x\ 10^3$) for 13CHDC.

	x	y	z	U(eq)
H(2)	-890	4201	5198	34
H(3)	985	2253	5744	34
H(4A)	4249	3010	6402	35
H(4B)	2961	2564	7585	35
H(6)	3408	5708	5730	29
H(1)	-44	5779	7207	29
H(5A)	2754	4923	8286	37
H(5B)	4876	4964	7648	37

Table A6 Torsion angles [°] for 13CHDC.

C(1)-C(2)-C(3)-C(4)	-4.5(3)
C(2)-C(3)-C(4)-C(5)	4.2(3)
C(7)-O(2)-C(6)-C(1)	-33.15(16)
C(7)-O(2)-C(6)-C(5)	-153.91(16)
C(6)-O(2)-C(7)-O(3)	-166.56(16)
C(6)-O(2)-C(7)-O(1)	13.56(17)
C(1)-O(1)-C(7)-O(3)	-167.13(16)
C(1)-O(1)-C(7)-O(2)	12.75(17)
C(7)-O(1)-C(1)-C(2)	-152.73(15)
C(7)-O(1)-C(1)-C(6)	-32.60(16)
C(3)-C(2)-C(1)-O(1)	149.32(15)
C(3)-C(2)-C(1)-C(6)	34.3(2)
O(2)-C(6)-C(1)-O(1)	39.21(16)
C(5)-C(6)-C(1)-O(1)	166.29(12)
O(2)-C(6)-C(1)-C(2)	165.60(12)
C(5)-C(6)-C(1)-C(2)	-67.32(19)
O(2)-C(6)-C(5)-C(4)	179.75(14)
C(1)-C(6)-C(5)-C(4)	63.99(18)
C(3)-C(4)-C(5)-C(6)	-32.5(2)